UNIVERSITÀ DEGLI STUDI DI PADOVA

UNIVERSITÁ DEGLI STUDI DI PADOVA

Dipartimento di Ingegneria Industriale DII

Corso di Laurea Magistrale in Ingegneria Aerospaziale

NUMERICAL AND EXPERIMENTAL INVESTIGATION OF CARBON STEEL WIRES PROPERTIES AND THEIR AEROSPACE APPLICATION

Candidate:

Antonio Comazzetto

Advisor:

Prof. Manuele Dabalá

Co-Advisor:

Prof. Marina Polyakova

Academic Year 2018-2019

Contents

Abstract

Object of this work of thesis, written during six months spent at Nosov Magnitogorsk State Technical University, is the continuous process of combined deformational processing by drawing with bending and torsion. The necessity to implement innovative manufacturing processes, in order to answer to an always higher demand from the market of metallic products, maintaining a high quality of mechanical properties, is nowadays a very important aspect. Combination of different operations is a new tendency in manufacturing processes in general, so also for wire manufacturing. Requirements of industry to drawn products are to increase their quantity and improve their quality.

The present research focuses the interest on a continuous process where drawing of carbon steel wire, together with bending and torsion of the wire itself in a four-rolls system, allows to vary mechanical properties of wires in wide range. After a first numerical study, where was possible, for example, to gain information about drawing force, it followed the experimental part. Carbon steel wires with 0.50% and 0.70% of carbon content were analyzed, and different torsion rates were implemented in the rolls system. Results demonstrated the variability of mechanical properties of the wires varying the torsion rate of the system.

Sommario

L'oggetto di questo lavoro di tesi, svolto nell'arco di sei mesi presso l'Universitá Tecnica Statale Nosov di Magnitogorsk, é il processo continuo di deformazione combinata con trafilatura, flessione e torsione. La necessitá di implementare processi manifatturieri innovativi, nell'ottica di rispondere ad un'esigenza sempre maggiore da parte del mercato di prodotti metallici, mantenendo un alto livello delle proprietá meccaniche, é attualmente un aspetto molto importante.
La combinazione di operazioni differenti é una nuova tendenza nei processi manufatturieri in generale, quindi anche nella lavorazione dei fili. I requisiti dell'industria nei confronti dei prodotti trafilati sono l'aumento della produzione e il miglioramento della qualitá degli stessi.
La presente ricerca focalizza l'interesse su un processo continuo dove la trafilatura di fili in acciaio al carbonio, unitamente alla flessione e torsione degli stessi in un sistema costituito da quattro rulli, permette di variare entro un ampio range le proprietá meccaniche dei fili. Ad un primo studio numerico, dove é stato possibile, ad esempio, ottenere informazioni riguardanti la forza di trafilatura, é seguita la parte sperimentale. Sono stati analizzati fili in acciaio con contenuti di carbonio pari a 0.50% e 0.70%, e sono stati effettuati diversi regimi di torsione del sistema di rulli. I risultati dimostrano la variabilitá delle proprietá meccaniche dei fili al variare della velocitá torsionale del sistema.

Introduction

The choice of materials is based on two main factors, the customer demands and the exploitation conditions of the final product.
The rapid changings in market conditions and the increasing demand of customers to metal ware properties makes necessary the development of new ideas, in order to react properly to these changings. Keep high quality of the products and be able to control their properties and quality characteristics for all stages of production are important aspects in modern metallurgy, and companies should be able to preserve production efficiency trying to adapt to external impact.
Basic operations for metal ware production are based on different kinds of plastic deformation. It is necessary change the shape of the workpiece but also its dimensions. Basic operations like rolling, drawing, extrusion, are limited in performance, productivity, and energy consumption. Moreover, nowadays more flexibility and variability in metal processing is required. This is why other approaches in metal manufacturing processes are essential to improve the performances and properties of the finished products.
Wires are one kind of metal-ware products, and steel wires in particular can be used as final product or as semiproduct (for example for rods, cable, ropes, etc.). Drawing process is the basic operation in wire manufacturing. One of the main problems of the drawing process is the high level of residual stresses in the drawn wire. Requirements of industry are to increase the quantity and improve the quality of drawn products. This lead to the investigation of new approaches for the process, and to improve the level of mechanical properties of the wire. Combination of different operations in metal ware production is a technological method that is used for wires and, more generally, long-length semi-finished products, processing. The main idea of combined deformational processing is the integration of different metal manufacturing

processes inducing different kinds of deformations with two or more basic processes. Existing applications of combination of different processes are, for example, the process of combined rolling-extruding, and the method of combined casting and rolling-extruding. Other examples are rolling-drawing integration to obtain complicated shapes of the cross-section of long-length products, rolling-forging method for crankshaft production. An important advantage that comes out using this kind of approach instead of direct metal processing is low energy and material consumption, so also lower costs. But another important reason why combined deformational processing with different kinds of deformation in metal ware production is used, is a technological one. Using specific process parameters and tools, this solution can improve the material properties of the processed workpiece, eliminate defects of it, and reduce the defects induced by a specific process thanks to the influence of the others.

Aim of this work of thesis is the study of a continuous method of combined deformational processing by drawing with bending and torsion to carbon steel wires. In the first chapter, the influence of drawing and other different kinds of deformation and combined deformations on the mechanical properties of carbon steel wires is described. From several years drawing, together with other kinds of deformations like torsion and bending, is applied to carbon steel wires, and experimental investigation is made at Nosov Magnitogorsk State Technical University. This method is presented, such as how the laboratory setup is implemented.

After the introductory chapter, a theoretical part based on dimensional analysis, will be outlined, especially the use of this technique not only to find dimensionless groups, but also to reduce the number of experiments, save time and costs. Application of FEM (Finite Element Method) to the process, carried out using software DEFORM 3D, is the main topic of Chapter 3. The main results of the simulations are presented. Experimental part is then described, such as the equipment used for the analysis, while in the following chapter results are discussed. The last chapter gives an overview of some applications of steels and carbon steel wires to aerospace.

Chapter 1

Influence of different kinds of deformation on carbon steel wire

At recent time the attention of engineers is focused to combined processes for wire manufacturing. It was shown that combination of drawing with different kinds of deformation (twisting, tension, compression, bending) makes it possible to increase the efficiency of the drawing process, to decrease consumption of material equipment and change significantly the stress-strain state to such scheme that ensures high level of mechanical properties and higher plasticity of the processed wire.

1.1 Carbon steels: classification and composition

Fe and C, with small content of Mn, is the essential composition of carbon steels, also called plain carbon steels. Variation of mechanical properties is possible thanks to specific heat treatments and with slightly changings in the composition. Usually three main groups are used to classify plain carbon steels [1]:

- Low-carbon steels (e.g., AISI-SAE grades 1005 to 1030), or mild steels, where carbon content upper limit is 0.30 wt.%C, and where steel is characterized by high ductility and low Ultimate Tensile Strength (UTS). It is impossible to harden this carbon steel by heat treatment, except for surface hardening processes.

- Medium-carbon steels (e.g., AISI-SAE grades 1030 to 1055), where carbon content is between 0.31 wt.%C and 0.55 wt.%C. Ductility and strength are well

balanced in this carbon steel. Heat treatment can be used to harden this steel, but only to thin sections or to the thin outer layer on thick parts.

- High-carbon steels (e.g., AISI-SAE grades 1060 to 1095) have a carbon content from 0.56 wt.%C to 1.0 wt.%C. They are characterized by high strength, they are hardanable and useful for high-strength and wear resistant parts.

Low-carbon steels

1006, 1008, 1010, and 1015 are the four AISI-SAE grades in the group of low carbon steels. Each of them is composed of pure iron, and carbon content is less than 0.30 wt.%C with a ferritic structure. It is the lowest carbon content considering the whole group of plain carbon steels. Because of the low UTS value, these steels are not suitable for mechanically demanding applications. Hardness and UTS increase when cold work or carbon content (or both) are increased, but the effect is a decrease of ductility and of the ability to withstand cold deformation. So low-carbon steels are the best solution when cold formability is required. If carbon content is less than 0.15 wt.%C, serious grain growth can occur causing brittleness, because of the combination of critical strain from cold work followed by heating with high temperatures. Machinability of products like bars, rods, wires is improved by cold drawing.

Medium-carbon steels

The sixteen AISI-SAE grades of this group are 1030, 1033, 1034, 1035, 1036, 1038, 1039, 1040, 1041, 1042, 1043, 1045, 1046, 1049, 1050, and 1052. Carbon content is between 0.31 wt.%C and 0.55 wt.%C. They are characterized by high mechanical properties, and often they are further hardened and strengthened by heat treatment or by cold work. They are especially suitable for automotive applications. In particular, AISI 1030 is used for shift and brake levers while AISI 1034 and 1035 are used in the form of wire and rod for cold upsetting such as bolts, and AISI 1038 for bolts and studs. These steels, after cold-forming and before use, are usually heat-treated. Higher carbon steels are often cold drawn to specific physical properties, without heat treatment and for applications like cylinder head studs. AISI 1030 and 1035 are used where

moderate properties are desired, while AISI 1036 is used for more critical parts where high strength and uniformity are important. From AISI 1038 to AISI 1045 are made forgings such as connecting rods, steering arms, truck front axles, while larger forgings at similar strength levels need more carbon content and perhaps more manganese. These last steels are also used for small forgings.

High-carbon steels

Fourteen AISI-SAE grades are in this group: 1055, 1060, 1062, 1064, 1065, 1066, 1070, 1074, 1078, 1080, 1085, 1086, 1090, and 1095. The carbon content of these steels is more than that is required to obtain maximum "as quenched" hardness. Springs and cutting edges, where wear resistance is important, are the main applications of these steels. Cold forming can not be used with these materials, forming is limited to springs coiled from small-diameter wires and flat stampings. Heat treatment is always applied before use. The application of AISI 1065 concerns pretempered wires, AISI 1066 cushion springs of hard-drawn wires. AISI 1064 can be used for thin stamped parts and small washers, while AISI 1074, 1080 and 1085 are used for flat products. Other special products are for example music wires and valve spring wires.

1.2 Peculiarities of different kinds of plastic deformation: drawing, bending, torsion

1.2.1 Basics of drawing process

Steel-based materials are semi-products suitable for cold-drawing processes. Drawing is one of the most used wire manufacturing process in the industrial field. The cross section of a rod or a wire is reduced (or its shape is changed), pulling the material through a conical die (called drawing die). A simple representation of the process is given in Figure 1.1 [2].

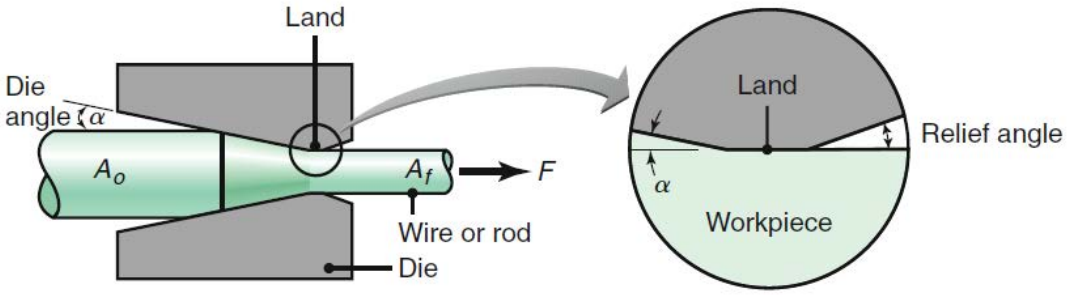

Figure 1.1. *Scheme of drawing process*

Materials that are usually drawn are aluminum, copper alloys and steel. Usually the process is conducted at room temperature.
Important variables of wire drawing are the semi-angle of the die α, reduction ratio r, friction coefficient μ and drawing velocity. Due to the great number of process parameters, the selection of each of them is very important, also cause of the complexity of the problem. Different methods were used to study the problem numerically, theoretically, and with experiments.
The stress-strain scheme after drawing is shown in Figure 1.2 [3].

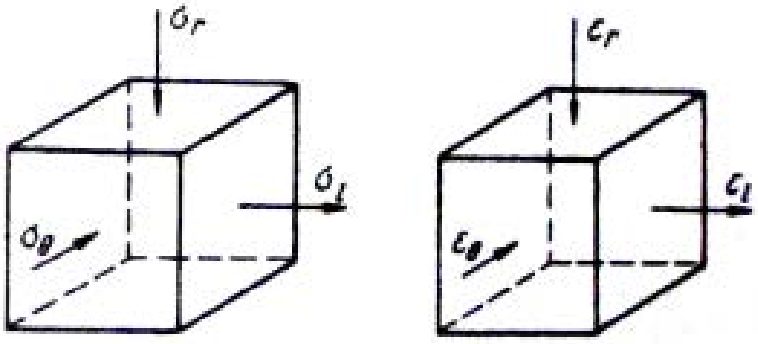

Figure 1.2. *Stress-strain scheme after drawing*

The stress state in drawing, characterized by one tension and two compression main stresses, makes conditions which decreases plasticity of the stretched metal to higher extent as compared with other metal processing methods excluding tension. Such deformation scheme causes special microstructure formation in metal denoted as texture. Grains elongate towards drawing direction without changing in

size [4]. The effects of reduction ratio and drawing velocity on tensile properties of low carbon steel wires was object of several studies. Cetinarslan and Guzey conducted experiments, and showed that yield strength and ultimate tensile strength increase when reduction ratio is increased. Also drawing velocity influences these parameters, and when drawing velocity is increased, yield strength and ultimate tensile strength decrease, but the effect is less than the reduction ratio of the drawing die. Drawing speed is also important because of the increase in the customer demand, and industrial rates of production.

Some of the results obtained by Cetinarslan and Guzey [5] are shown in Figure 1.3 and Figure 1.4.

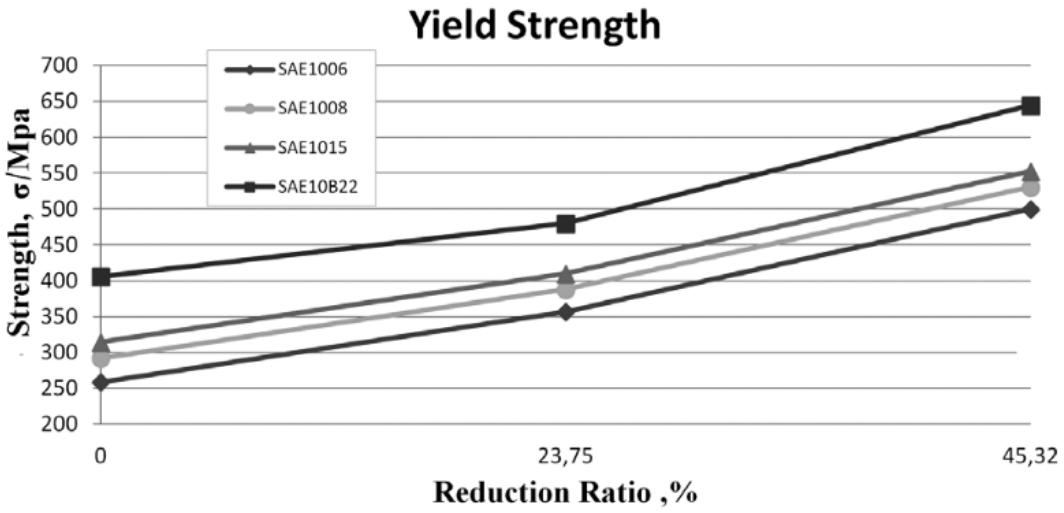

Figure 1.3. *Variation of yield strength with reduction ratio*

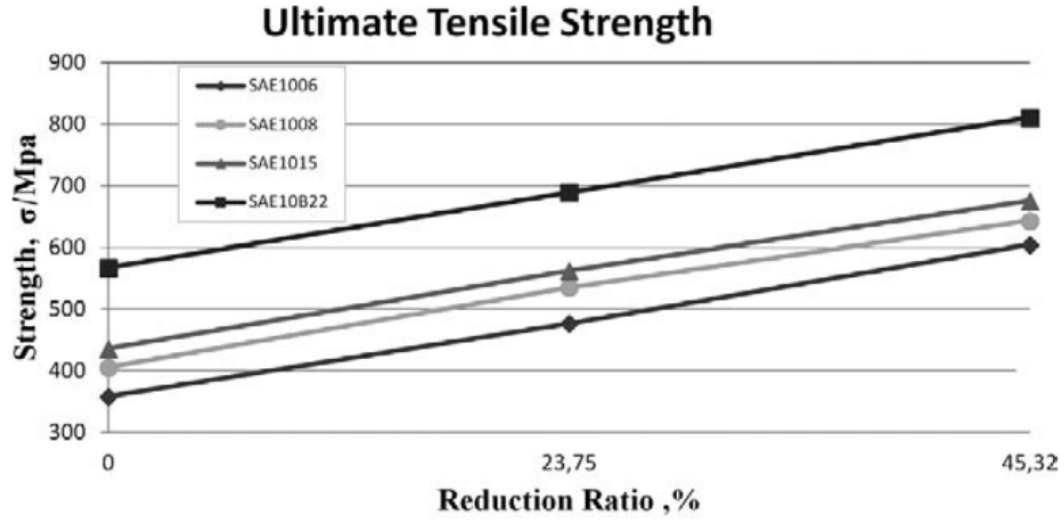

Figure 1.4. *Variation of ultimate tensile strength with reduction ratio*

Speed influence was also studied on high-carbon steel wires.
Also other mechanical properties, like torsion strength, is affected by drawing velocity and reduction ratio. Carbon content of the processed material influences wire drawing, because steels with high carbon content have worse plastic deformation characteristics than low carbon steels. Drawing parameters also affect microstructure of carbon steel wires. Zidani, Messaoudi, Baudin, Solas, Mathon [6] studied cold drawing of pearlitic steel wires intended for civil engineering applications. Drawing induces the lengthening of the pearlitic grains along the drawing axis and leads to a strong hardness increase.
Zelin's study was focused on the evolution of microstructure of pearlitic steel wires [7]. Decrease of thickness of ferrite and cementite lamellae was found, such as stretching and rotation of pearlite colonies, and their alignment with wire axis.
Phelippeau, Pommier, Tsakalakos, Clavel and Prioul studied cold drawing process of steel wires both with experiments and FEM simulations, and found that this process increased the tensile strength and decreased the elongation to failure [8]. The FEM simulation showed tensile residual stress on the surface of the wire.
Another important point is that the number of drawing steps to reduce the wire diameter influences the properties of the wire itself. Suliga [9] conducted experiments using three different approaches for the drawing process of high carbon steel wires. The reduction of the wire was always the same, the difference was only on the drawing steps.
In conclusion, it is possible to say that drawing process influences the mechanical properties, the microstructure and texture properties of steel wires.
In general, when a polycrystalline material is cold-worked, the individual grains, initially random-oriented, orient themselves in particular manner. In the wire drawing process, the deformation leads to the orientation of grains in the same direction, and the material is no longer isotropic. This means that properties of the wire in the longitudinal and in the transverse direction are different.

1.2.2 Torsion deformation

Torsion is usually used as a test to evaluate failure strength and toughness of the processed wire. But this kind of deformation has got relevant effect on metal properties. The stress-strain state that characterizes torsional deformation is complicated, and goes from a maximum at the surface to a minimum in the centre of the wire [10]. The stress state of the twisted workpiece is considered to be of pure shear. In Figure 1.5 a wire subjected to torsional deformation is shown [3].

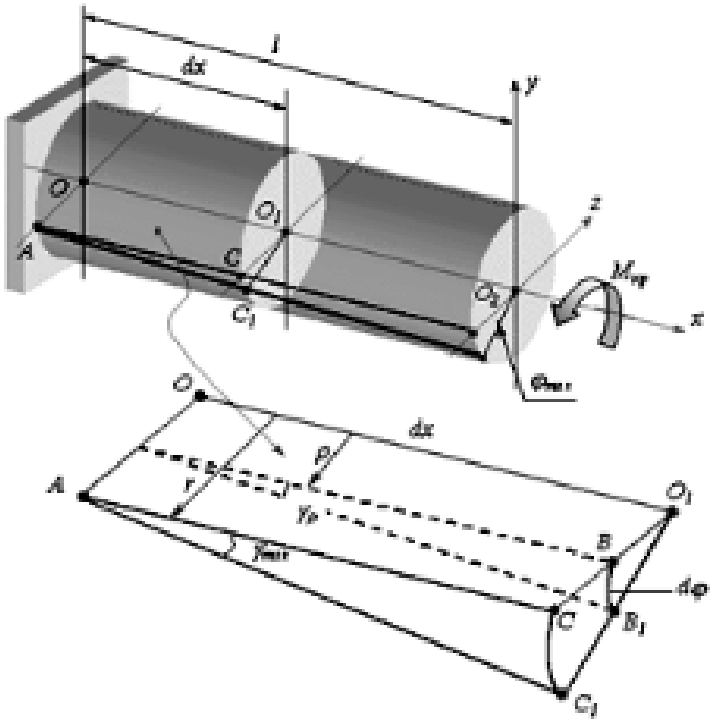

Figure 1.5. *Stress-strain scheme after torsional deformation*

Assuming to have an untwisted straight wire, with length L and circular cross-section, and that one end of the wire is fixed, if we impose an angle of twist ϕ along the length of the wire, the engineering shear γ is evaluated as follows:

$$\gamma = \frac{r \cdot \phi}{L} \tag{1.1}$$

where r varies from 0 in the axis of the wire to R, radius of the cross-section.

The maximum shear strain reaches the maximum value in the wire surface:

$$\gamma_{max} = \frac{R \cdot \phi}{L} \tag{1.2}$$

If there aren't residual stresses, plastic deformation will occur when shear strain will be equal to yield shear strain:

$$\gamma_y = \frac{\tau_y}{G} \tag{1.3}$$

The angle of twist related to this condition is:

$$\phi_y = \frac{\tau_y \cdot L}{G \cdot R} \tag{1.4}$$

Guo, Luan, and Liu investigated the effect of torsional deformation on mechanical properties of cold drawn pearlitic steel wires [11]. In their study, authors used steel wires with chemical composition of Fe-0.84-C-0.19-Si-0.72-Mn-0.04Cr in wt%. Wires initial diameter was 13.5 mm, and after eight drawing steps it became 7 mm, and these wires are used for manufacturing steel cables of suspension bridges.
Engineering stress-strain curves of processed steel wires were compared with the curve of wire without torsional deformation. It was found that both yield strength and ultimate tensile strength decrease slowly as number of revolutions increases from 2.5 to 17.5 (Figures 1.6a and 1.6b).

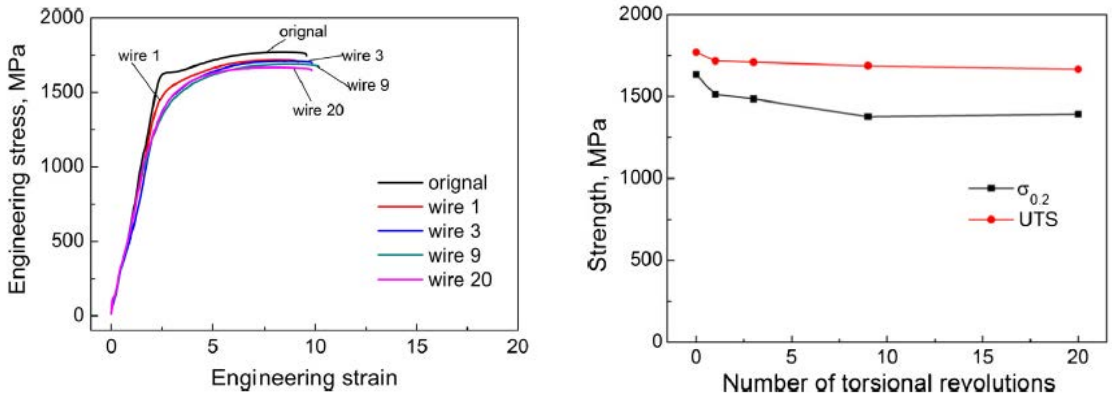

Figure 1.6. *Effect of torsional deformation on steel wires: stress-strain curve (a), variation of yield strength and UTS with torsional revolutions (b)*

Cordier-Robert, Forfert, Bolle, Fundenberger and Tidu focused their research on

pearlitic steel wire [12]. In particular, the influence of torsional deformation on cold drawn pearlitic steel wires. For torsion deformation was used a free end torsion machine. Carbon content of the steel wires was 0.77%. During torsional deformation, the mechanisms of deformation that regulate the microstructure of steel are related to the evolution of density and nature of defects (dislocations or free atoms), to lattice friction and to the ability of the lattice to reduce the internal stress created by the application of external stresses and by the interactions toward defects. As the wires are deformed in torsion, shear stress and the associated shear strain induce lattice friction.

This friction is responsible of the global and local temperature increases and helps the material to over-deform. Then, the carbon atoms diffusion by dislocation moving is possible and high enough to allow wires deformation without cracking or breaking. In this way, the torsion effect on the microstructure of pearlitic steel wires was studied.

1.2.3 Bending deformation

This kind of deformation is often used as metal processing technique, and sometimes its effect can be found in the changing of the structure but without changing shape of the product. Figure 1.7 shows the stress-strain state of an initially straight workpiece subjected to bending deformation [3].

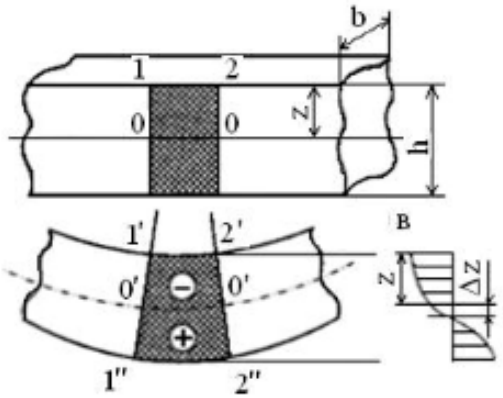

Figure 1.7. *Stress-strain scheme when workpiece is subjected to bending deformation*

In the top part of the workpiece, in the longitudinal direction, compression prevails, while in the bottom part there is tension. In the centre of the workpiece is located the neutral axis, where the longitudinal strain zero. For a bent wire, as shown in Figure 1.8,

the longitudinal strain is calculated as follows [10]:

$$\epsilon_x = -\frac{y}{R} \tag{1.5}$$

where R is called bending radius, while y is the distance from the neutral axis. The positive direction is considered toward the centre of curvature.

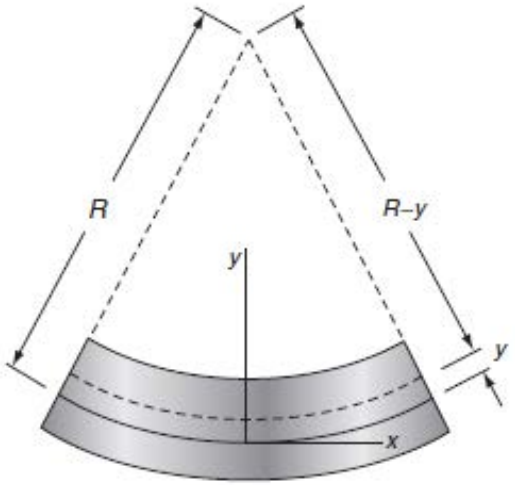

Figure 1.8. *Bent wire geometry*

Wire ropes made of steel are normally used, for example, in elevators. Many steel wires are wrapped to create strand, and many strands form the rope. Studies were conducted to investigate bending over sheave fatigue lifetimes of these steel wire ropes [13]. Specific machine was used for this purpose, and results showed that diameter of the sheave and tensile load affect bending fatigue life, in particular this quantity decreases when the tensile load increases and when sheave diameter decreases.
Steel products like wires, rods, springs require low residual stresses. In particular, researchers found that fatigue strength increases with decreasing of residual stresses, and this can be related with more favorable surface layer conditions in the presence of lower residual stresses value.
Kruzel and Suliga investigated the effect of multiple bending on the residual stresses of high-carbon steel wires [14]. It was found that, effectively, the application of bending decreased the residual stresses after wire drawing. Moreover, it was found the configuration and the number of rolls that lead to the best results from the point of view of residual stresses. Similar studies were conducted by Khromov and Kawalla, who

studied alternate bending method on wire to ensure straigthtness on the workpiece and redistribute or reduce the residual stresses in finished products [15]. Authors studied the method with computer for calculating the deflected mode of a steel wire while straightening and taking into account its real stress-strain diagram.
Bending deformation is also studied in tyre manufacturing, helical spring design, spectacles frames, and in general non-linear bending of wires, where final geometry of the wire after bending and springback is the object of the study [16].
Gillstrom and Jarl investigated mechanical descaling by reverse bending and brushing as replacement for pickling, on low carbon steel [17]. To remove the oxide layer, reverse bending is not enough, this is why also brushing, a method for cleaning the surface of the steel, is used. When the wire rod is bent over a roller, the scale is removed by the tensile and compressive deformation stresses.
Godfrey investigated bending properties of cold steel wires, with specific bend machine [18]. It was found that the bending properties of carbon steel wire after cold working increased; beyond a specific point the properties decreased.

1.3 Combined technological processes as the tendency in metal ware manufacturing

Decrease of material, energy consumption, increase of technological resourcefulness, product quality improvement as well as enhancement of its nomenclature which rise product competitiveness are the main problems in market conditions. To process and obtain new materials and alloys with broaden exploitation properties which cannot be achieved by traditional methods, in metallurgical manufacturing, is an important aim to pursue. One solution of these problems in steel downstream production is to design combined methods for metal processing. The term "combination" means fulfilment additional functions as well as basic ones by using hidden resources of the technical system. In such conditions when product manufacturing process is limited by technical and technological industrial facilities the combined and integrated processes of material processing are intensively developed. Processing methods are considered to be combined when processes of transformation, application, or re-

moval of the processed material occur as a result of behaviour two or more impacts different in their physical nature (Figure 1.9).

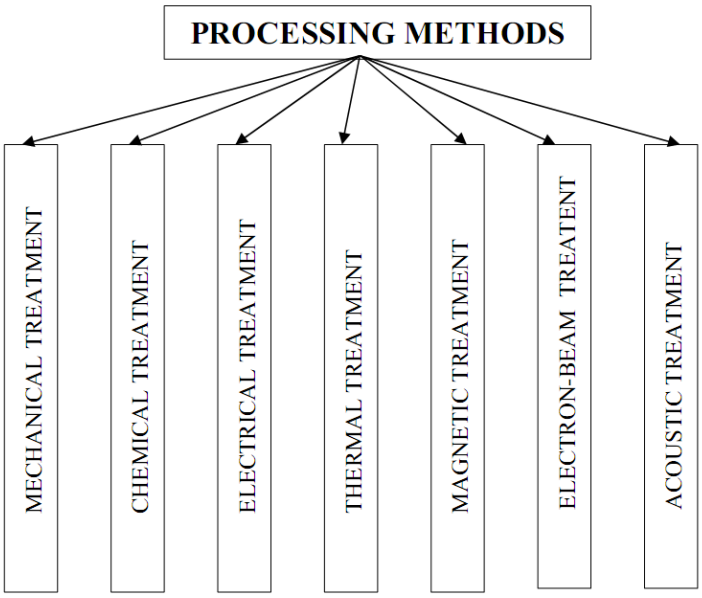

Figure 1.9. *Classification of processing methods due to kind of consumed energy*

Combined processing methods unite the impact of different physical and chemical nature as for conventional methods are based only on one route of energy transformation (Figure 1.10).

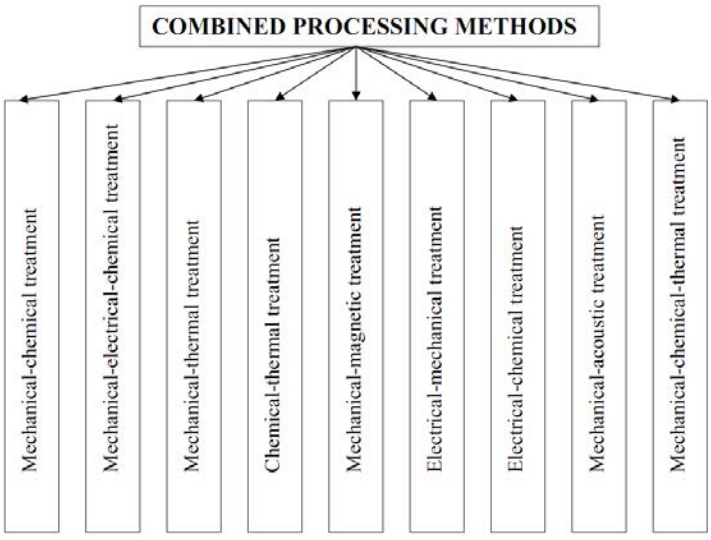

Figure 1.10. *Classification of combined processing methods due to kind of consumed energy*

Application of combined processes into industrial conditions has absolute advantages. They ensure both the productivity increase and obtaining new technical effects

during one technological processing cycle with can not be gained using conventional processing methods (Figure 1.11).

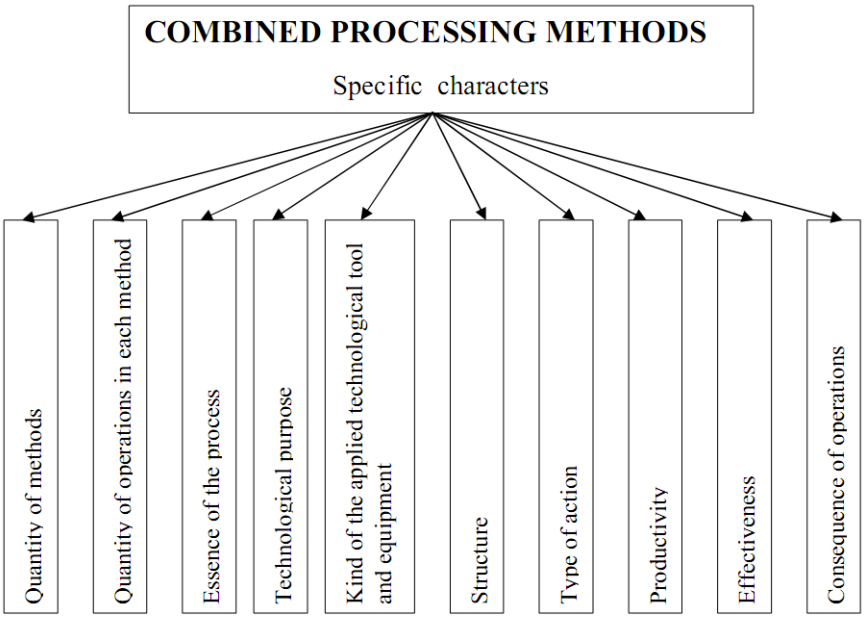

Figure 1.11. *Classification characteristics of combined processing methods*

In metallurgy combined and integrated processes are designed on the ground of four basic operations: casting, rolling, drawing and pressing (extrusion) (Figure 1.12).

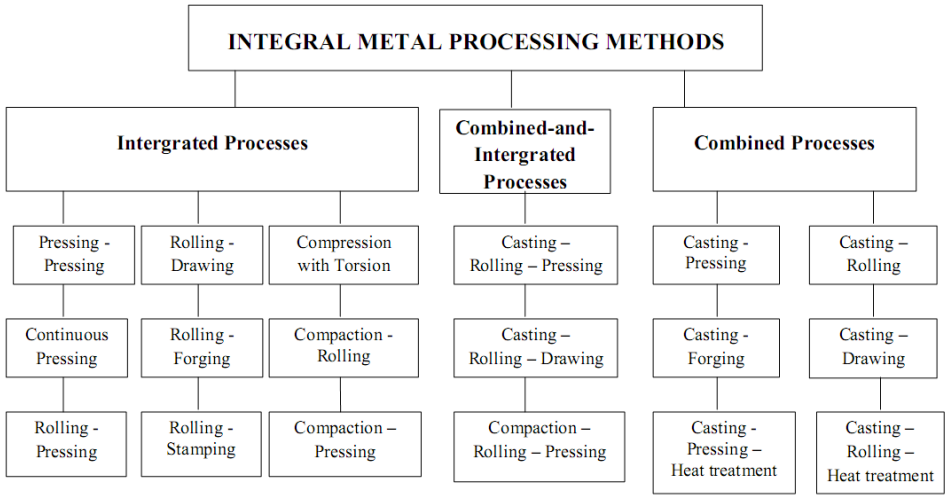

Figure 1.12. *Combined and integrated methods in metal manufacturing processes*

Main idea of combined deformation processing is the combination of different kinds of deformation. The reason why this approach is used is to improve specific

characteristics of the final product and have control on the properties of the workpiece. Every process and every single deformation has its advantages and disadvantages but the combination of them can lead to the increase of the ultimate tensile strength (and mechanical properties in general) and obtain finer microstructure.
Yanagimoto, Tokutomi, Hanazaki and Tsuji combined bending and drawing to manufacture copper alloy wire with diameter of 210 μm [19]. Copper wires are used because of their excellent electric conductivity and strong bonding to electrodes. Investigation of copper wires with small diameters was required, such as the necessity to improve their strength and flexibility. Authors investigated the mechanical properties and microstructure of the processed wires, and achieved excellent electrical and mechanical properties. Scheme of this process is shown in Figure 1.13. Thanks to this method, authors were able to control the microstructure and grain orientation.

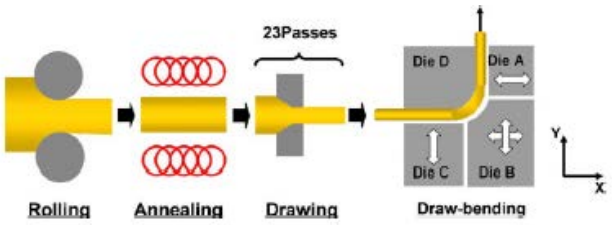

Figure 1.13. *Schematic diagram of combined bending and drawing*

Novel experimental methodologies have been implemented, for example to produce ultrafine-grain metallic microstructure [20]. To improve the ductility of ultrafine-grained materials, it was found that the use of deformation inhomogeneity is helpful. The potential of this approach is known, but the control of the workpiece properties is very difficult.
Accumulative Angular Drawing process (AAD) consists on the application of a complex strain path, where large strain accumulation is introduced to refine the microstructure of a drawn wire [21]. The main purpose of this method is the production of wire with higher strength and ductility than conventional drawing process thanks to the complex strain path history, result of various deformation modes, as shown in Figure 1.14. Also carbon steel wires have been studied using this method.

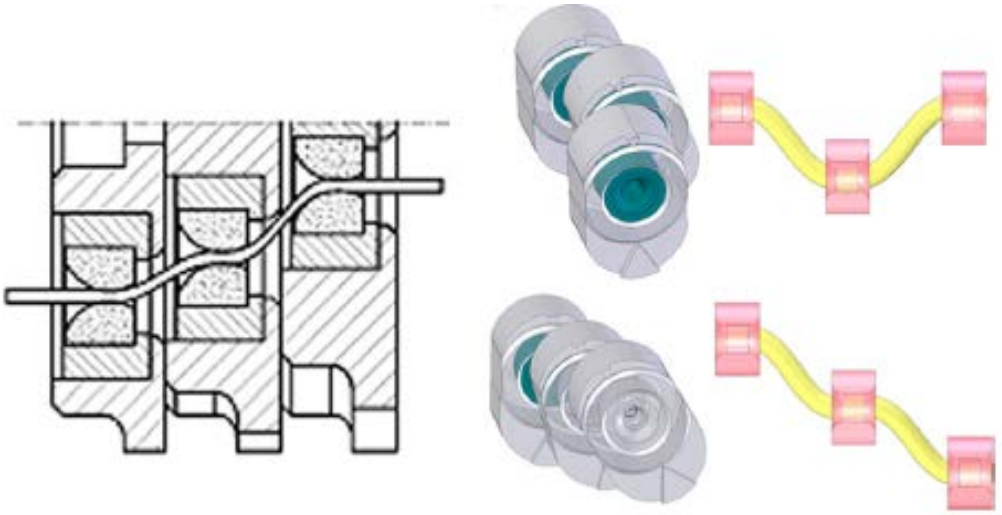

Figure 1.14. *Die assembly and positioning in Accumulative Angular Drawing*

Investigations demonstrated that non-circular drawing sequence could impose higher and relatively more homogeneous plastic deformation on the wire than the conventional drawing process, and improve workability of the workpiece [22].
Alternate drawing is another process that has been studied, and it was applied to aluminium and carbon steel wires. The aim is to increase the ductility of the drawn wire, alternating the drawing direction every step, decreasing the additional shearing strain. Comparison of results between alternate deawing and conventional drawing of wire is shown in Figure 1.15.

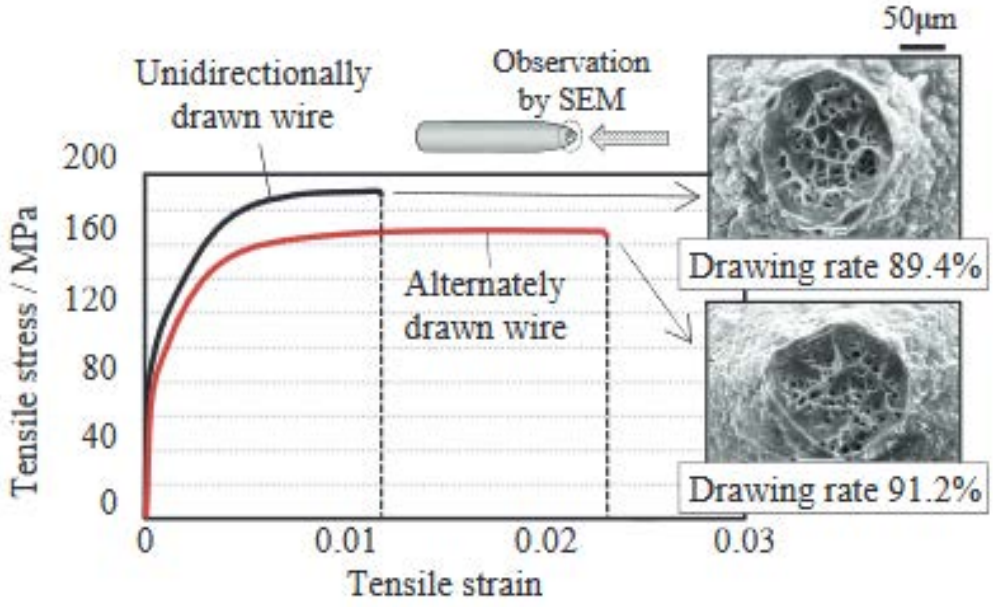

Figure 1.15. *Stress-strain curves for unidirectional and alternately drawn wire*

1.4 Continuous method of combined deformational processing by drawing with bending and torsion

1.4.1 Description of the process

Such schemes of plastic deformation as bending, torsion, tension, compression etc. are considered to be the basic schemes for metal processing methods [23]. Each of these types of deformation has specific influence on mechanical properties and microstructure of the processed metal.

To get the optimal result of plastic deformation impact on metal properties, the mechanism of plastic processing should meet certain requirements such as homogeneity of stress and strain states, possibility of precise regulation of deformation level and stress state index (hydrostatic stress) as well as obtaining both high and the ultra-high levels of deformation without significant changes in the cross section of the metal part or its damage. Simultaneous implementation of different schemes of plastic deformation is the obligatory condition for design of new combined methods. The effect of each deformation scheme on the processed metal properties should be particularly analyzed.

As drawing is the main forming operation in wire production, it was chosen as the basic one for developing the continuous method with combined deformation. It is well known that the deformation scheme during the drawing process is characterized by longitudinal and radial stresses. Dissimilar stress state scheme of metal in the deformation zone in the process of drawing creates conditions under which ductility of the treated metal is much lower than in other methods of metal processing except tensile deformation. Applying the alternating strains on deformation zone will initiate the Baushinger's effect and as a result can decrease to high extent and for several metals even exclude intermediate annealing operations. New scientific field referred to as "processes with integrated external deformation" makes it possible to enhance the technological facilities of traditional drawing processes.

Because the main deformation at drawing is the longitudinal one it is reasonable to use such schemes of deformation which make it possible to achieve high plastic deformation in the processed material. In other words it is necessary to create a

complex stress-strain state at drawing, hence, it is advisable to consider the possibility of achieving this by combining it with a twisting process which is compatible with industry-speed wire production. Under the influence of the external torsional moment, any cross-section of the workpiece keeping its flat section turns by a certain angle. This angle changes along the workpiece from zero at the fixed end to the maximum value at the free end. In this process the element of external cylindrical surface of the workpiece turns by a certain shear angle, while the cross section of diameters and the distance between them do not change. The rectangular net turns into the net consisting of parallelograms and this fact proves the presence of shear stresses in the workpiece cross section and in accordance with the reciprocity law for shearing stresses, these stresses are also present in the workpiece longitudinal section, so the stress state at the points of the torque member is the pure shear.
Laboratory setup of the process is shown in Figure 1.16a, while deformation path of the wire in Figure 1.16b [3]. The different kinds of deformations are realizable thanks to different tools.

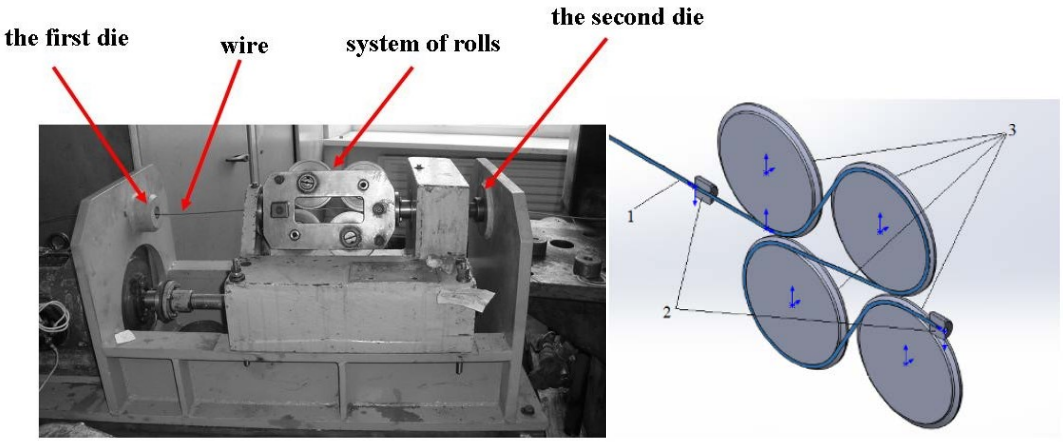

Figure 1.16. *Continuous method of combined deformational processing by drawing with bending and torsion: laboratory setup (a), deformation path (b)*

Firstly, two distant drawing dies, positioned along the same longitudinal axis. After the first die, where the prevalent stress are tensile and compression, the carbon steel wire is subjected to bending and torsion. Bending deformation is possible through the passage in a four-rolls-system, and torsional deformation is possible because the rolls system can rotate thanks to an autonomous engine. Rolls are fitted but can

rotate while the wire is moving. When the engine is switched off during the process, the wire is subjected only to drawing and bending. At the end of the process, the wire is subjected to another drawing step, through the second die. It is important to note that the equipment used in this process is also utilized in steel wire production, making this method easier to implement.
The two drawing steps, together with shear stress due to torsion and alternate bending in the rolls system, affect in a complicated way the strain-stress distribution of the metal workpiece.
One of the main advantages of the developed method is that various hardware devices and tools already applied for steel wire production can be used to implement this method thus simplifying its introduction to the current industrial equipment. Implementation of the developed continuous method by drawing with bending and torsion does not require any sophisticated tools or equipment; it can be integrated into traditional technological routes of wire production from carbon steels. With this approach the modes of traditional industrial processes of wire production do not require any significant adjustments.
The developed method also offers new opportunities for science-driven technology and its application in batch production of wire for demanding applications is possible on the operating equipment in the drawing mills of hardware plants.

1.4.2 Effects of process parameters on mechanical properties of the wire

Several studies have been conducted using combined deformational process of carbon steel wire and results have been published in various papers.
Under investigation were carbon steel wires with different carbon contents and different diameters. The aim of these studies was to analyze the effect of important process parameters like torsional rate, diameter of rolls, drawing ratios, on microstructure and mechanical properties. Moreover, comparison of carbon steel wire processed with only drawing and with combined deformations was made.
In [24] medium carbon steel wire (containing 0.5% of carbon) was chosen for the experiments, rolls with diameter 90 mm and 60 mm were used, and torsional rate was

varied 0 RPM to 150 RPM.

Mechanical properties after the process were found with tensile strength tests. Mechanical properties after combined deformational processing were compared with mechanical properties after only conventional drawing. It was found that the application of continuous method of deformational processing by drawing with bending and torsion can lead to a wide combination of strength and plastic properties. These properties can be higher or lower than the same properties after only drawing conventional process.

In Figure 1.17 one can see the relationship of ultimate tensile strength during low carbon steel wire processing [25].

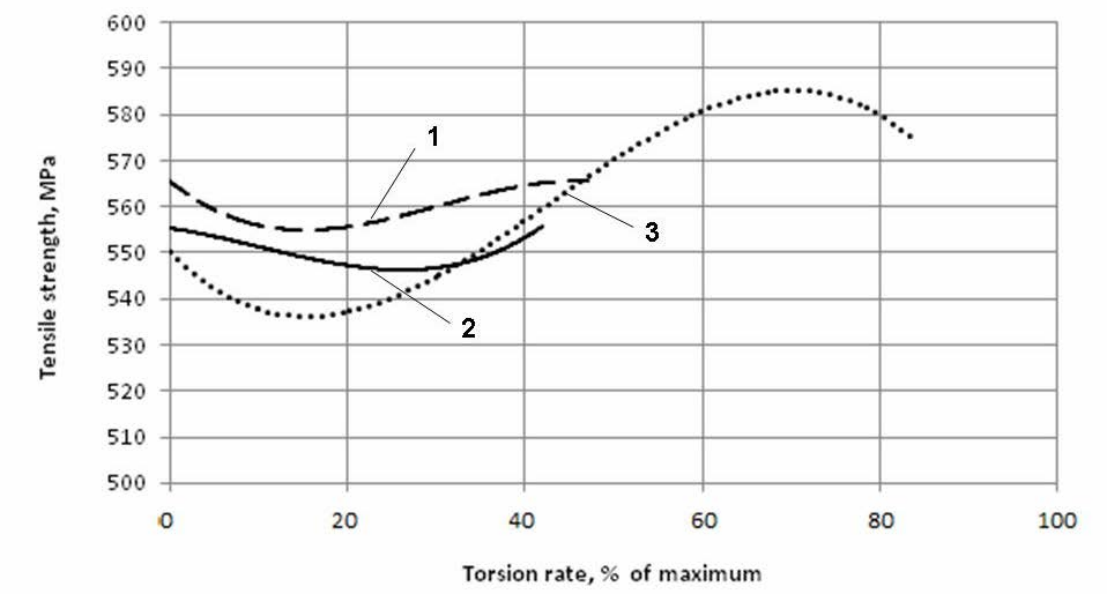

Figure 1.17. *Trend of UTS with torsion rate for low carbon steel wire, using three different drawing modes:* 1)3 → 2.75 → 2.45; 2)3 → 2.75 → 2.5; 3)3 → 2.75 → 2.6

Highest value of UTS increase was obtained with the third configuration where the deformation value in the second die was minimum, and the profile of UTS with torsion rate is sine-shaped. After continuous method of combined deformational process by drawing with bending and torsion, UTS value was 10% higher than value of UTS after conventional drawing. The same study was conducted for medium carbon steel wire, as shown in Figure 1.18.

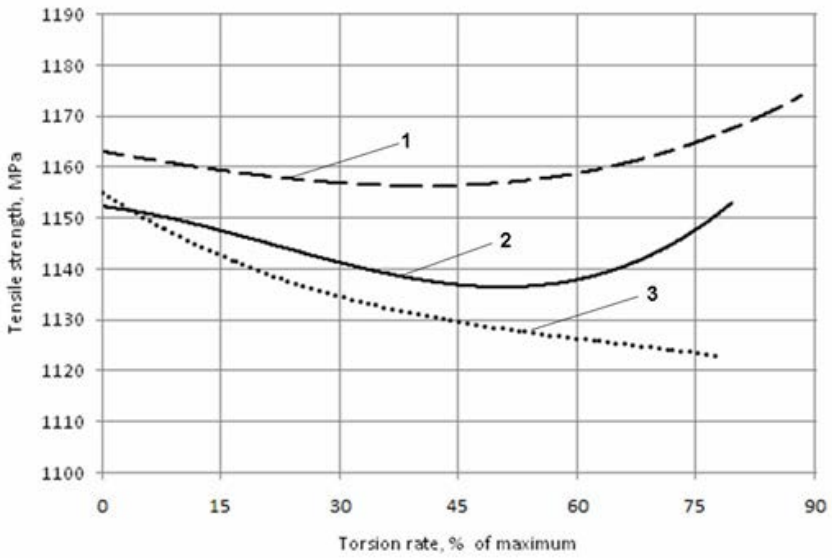

Figure 1.18. *Trend of UTS with torsion rate for medium carbon steel wire, using three different drawing modes:* 1)3 → 2.75 → 2.45;2)3 → 2.75 → 2.5;3)3 → 2.75 → 2.6

Studies showed that if the reduction in the first die is the same, higher is the reduction in the second die and higher is UTS. Both for low carbon and medium carbon steels softening takes place when the roller system rotation velocity is from 0 RPM to half of the maximum value of torsion rate. Increase of strength is provided, but is only 2%. At minimum reduction in the second die with the increase in rotation velocity of the roller system, UTS decreases up to wire breakage. Conventional yield strength of the low carbon steel changes with the same trend of UTS (Figure 1.19a and Figure 1.19b).

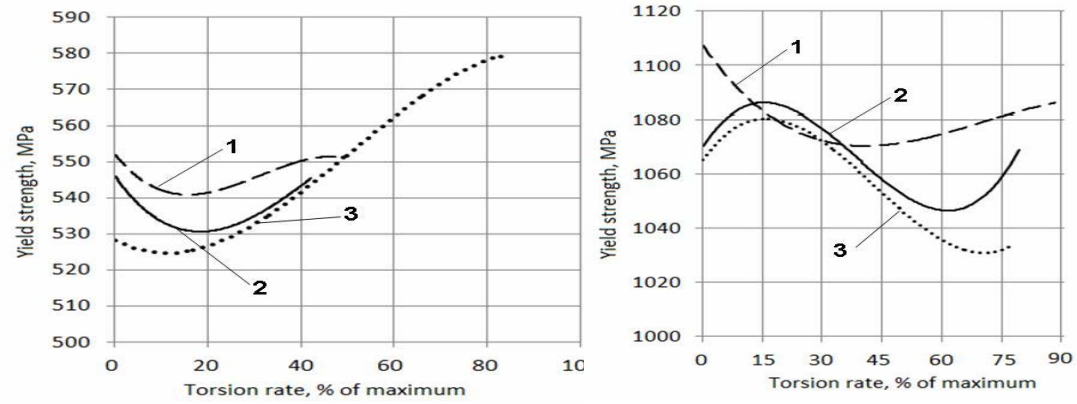

(a) **(b)**

Figure 1.19. *Relationship between conventional yield strength and torsion rate of the roller system for low-carbon steel wire (a) and medium-carbon steel wire (b) at different drawing modes:* 1)3 → 2.75 → 2.45;2)3 → 2.75 → 2.5;3)3 → 2.75 → 2.6

Depending on the rotation velocity of the roller system the value of conventional yield strength at a given reduction of cross-sectional area in the second die varies from 520 MPa to 585 MPa, which is 11.5%. Conventional yield strength of the medium carbon steel achieves its maximum value at 15% of torsion rate. However further increase of rotation velocity of the roller system causes the decrease of this value to the initial level (and even below) but this change does not exceed 5% (Figure 1.19b). When reduction in the second die increases, properties dispersion also increases and the accuracy of the trend line decreases although the degree of the curve is the same. Also, when reduction in the second die increases, the difference between peaks of the maximum and the minimum values of this characteristic of plastic properties decreases. In Figure 1.20a and Figure 1.20b one can see behavior of contraction at fracture for low carbon and medium carbon steels respectively.

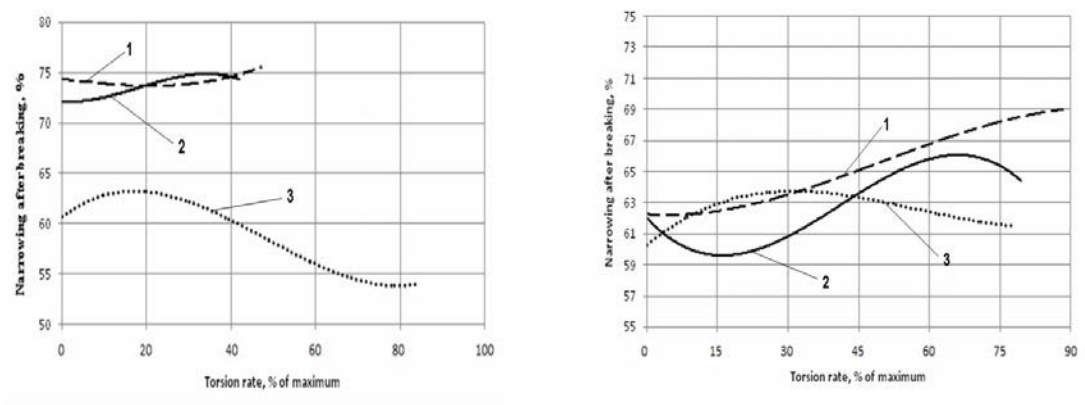

(a) **(b)**

Figure 1.20. *Relationship between contraction at fracture after low (a) and medium (b) carbon steel wire breakage and torsion rate of the roller system at different drawing modes:* 1)3 → 2.75 → 2.45; 2)3 → 2.75 → 2.5; 3)3 → 2.75 → 2.6

When the rotational velocity of the roller system is close to the maximum, the values of contraction at fracture increase for all reduction values in the second die. The biggest plasticity increase is characteristic for the drawing sequence with the biggest reduction in the second die. As it was described above, when contraction at fracture increases, UTS remains the same indicating the improvement of the wire mechanical characteristics. Also simulation of the deformation process was made using software DEFORM-3D, in order to estimate the probability of carbon steel wire fracture. No crack formation was found in the processed carbon steel wire, and the

effectiveness of the combine deformational process was verified.
Also mechanical properties using high carbon steel wire (containing 0.75% of carbon) were studied. In this case it was found again the wide range of mechanical properties that continuous method of deformational processing by drawing with bending and torsion can provide to the carbon steel wire.

1.5 Conclusion

Experiments showed that combined deformational processing by drawing with bending and torsion allows to obtain a wide range of mechanical properties for the processed carbon steel wire. This range of properties can lead to better or worse performances if compared with the conventional drawing process. It is characterized by various technological parameters that act simultaneously, and several papers demonstrated the influence of these variables on the level of mechanical properties and on the microstructure of the product. This is the reason why this process is a multivariant one.
Extension of the investigation of the process not only to study the effects of combined deformation, but also to predict the mechanical properties after the changing of one or more parameters of deformation, would give great benefits. Theoretical approach is required for this purpose, and its application would reduce the quantity of experiments, in order to study the level of mechanical properties of carbon steel wire with different carbon contents after changing deformational parameters of the combined process, and clarify the results.

Chapter 2

Dimensional Analysis

Dimensional analysis was used for the first time by Vaschy in 1882, by Riabouchinsky in 1911, and then formalized by Edgar Buckingham in 1914, with the Pi-Theorem [26]. This technique, during the last century, allowed scientists and engineers to simplify the description of physical phenomenons when a multiple number of variables affected the system. But the application of this method can also improve significantly the efficiency of experimental investigation in engineering problems and, as a result, gain more information with less amount of time and money. The continuous method of combined deformational processing by drawing with bending and torsion was described in the previous chapter. Because of this process is characterized by a great number of variables, it is a multivariant one, where also these variables can vary over a wide range of values. Due to this reason, a lot of experiments, time and money should be necessary to study the properties and the microstructure of the final products. This is why, after a brief description of dimensional analysis, this method was applied to the process as a preliminary step for further investigation and experimental activity.

2.1 Overview

Aim of dimensional analysis methods is to find dimensionless groups. These groups can be found or from the basic differential equation of the physical problem or listing all the dependent and independent variables involved in the phenomenon [27]. The first approach requires that theoretical equations are available.
The main idea of the Pi-Theorem, the fundamental theorem of dimensional analysis,

is that if a physical process depends on n quantities, it is always possible to represent this process with $n-k$ non dimensional parameters, where k is the number of fundamental dimensions. For example, in aerodynamics such kind of analysis can be used to find the acting aerodynamic force on a body, or it can reduce experiments when interest is focused on the power required to drive a fan that pumps air in a duct at low speed.
It is important to remind that despite dimensional principles are mainly used in fluid mechanics or heat transfer, this approach can be used in all science fields to plan more efficiently the experimental investigation.
The main reasons why dimensional analysis technique is used are [28]:

- Given a physical problem, group all the variables involved in it with dimensionless products called pi-groups, in order to obtain a synthetic description of the problem.

- Helpful tool for analysis and interpretation of experimental results, give a better understanding of independent variables effects on dependant ones, and reduce the number of experiments. It also helps to have great compactness of as well as an increased clarity in the ordering of the experiments.

- Obtain scaling laws: this is very important because in the first steps of engineering design is more comfortable and cheaper to test on small scale rather than test the prototypes. This aspect is still important even if nowadays computer simulations are preferred.

2.1.1 Mathematical description of the method

Any physical system can be described by physical quantities, and the system doesn't depend to the units of the measured quantities. The Pi-Theorem states that any physical system, when dimensional homogeneity is satisfied, can be described by dimensionless products of the variables that affect the system.

Dimensional homogeneity

For the principle of dimensional homogeneity, all terms of an equation that represents a physical process, must have the same dimension.
For example, we can consider a mass-spring system. The equation that describes the motion of the mass is:

$$m\frac{d^2u}{dx^2} + k(x - x_0) = 0 \tag{2.1}$$

where m is the mass, x is the space coordinate, x_0 is the coordinate of the equilibrium position, t is time and k the stiffness of the spring. Here, x and x_0 both have length dimensions, and meters have to be used for both quantities. Dimensional homogeneity states that the first and the second main terms of the equation must have the same dimensions. This principle must be satisfied in every physical equation. In general, we can say that an equation is dimensionally homogeneous when its form doesn't depend on the chosen units of measurement.

Pi-Theorem

The Pi-Theorem, or Buckingham Π-Theorem, was firstly formulated by Vaschy, but then resumed by Buckingham. The Buckingham's formal proof of the theorem is based on the expandability of the MacLaurin series of the functional relationship between the quantities involved in the process.
The most general relation involving n physical quantities of any kind, and i ratios, can be described with the following equation:

$$\boldsymbol{f_1}(Q_1, Q_2, \ldots, Q_n, r_1, r_2, \ldots, r_i) = 0 \tag{2.2}$$

[Buckingham article] where Q_j, with $j = 1 : n$, is a variable of whatever nature. It is important that in the last equation all the influencing relevant physical quantities are present, in order to get significant results. If the ratios are between geometrical quantities that don't change during the phenomenon under investigation (or already dimensionless parameters) the equation can be simplified to:

$$\boldsymbol{f_2}(Q_1, Q_2, \ldots, Q_n) = 0 \tag{2.3}$$

If all the variables of the case of study have been taken into account, the last equation gives the complete description of the system.
Let k represents the fundamental dimensions of the physical n variables (for example: Mass [M], Length [L], Time [T]). Equation can be written as:

$$\boldsymbol{f_3}(\pi_1, \pi_2, \ldots, \pi_{n-k}) = 0 \tag{2.4}$$

or, equivalently, as:

$$\pi_1 = \boldsymbol{f_4}(\pi_2, \ldots, \pi_{n-k}) = 0 \tag{2.5}$$

This equations transformation, with the creation of $n-k$ dimensionless pi-groups, is the Pi-Theorem. The important result is that the number of variables has been reduced. Then it is possible to create each pi-group as follows:
where $Q_1, Q_2, \ldots, Q_k$ are called repeating variables and they include all the k fundamental dimensions used in the method.
The dimensionless groups found with this methodology are not unique but they are independent. It is important to remember that dimensional analysis gives an output that is the functional relationship but it doesn't give the form of the function between pi-groups.
To obtain it, experimental investigation has to be made. However, it is better to study the physical system using few dimensionless groups rather than all the variables: this is the main advantage of the Pi-Theorem.
Moreover, experiments are important because after them it can be noticed if a specific variable influences or not the system.

2.1.2 Methodology to find pi-groups in dimensional analysis

When the dimensional analysis is focused on a specific dependent variable of the physical system, the following steps can be applied to find the dimensionless groups [29].

- Identification of intuitive dependent and independent variables of the physical

phenomenon, object of the study:

$$Q_1 = \boldsymbol{f}(Q_2, Q_3, \ldots, Q_n, r_1, r_2, \ldots, r_i) = 0 \tag{2.6}$$

This is a very important step, because adding too many variables would be meaningless (because of the idea, in dimensional analysis, to reduce the amount of the variables), and use only few variables wouldn't lead to the complete understanding of the phenomenon. Usually, these independent variables are related to material properties, geometry, or external effects.

- Write the dimensions of each variable, in terms of the fundamentals dimensions.
- Determination of the number of pi-groups from the variables (n) and fundamental dimensions (k). The pi-groups will be $n-k$.
- In the creation of the pi-groups, one has to solve a overdetermined system of equations. The dependent variable shouldn't appear in more than one pi-group, such as (possibly) each controllable variable. It is necessary to control that every independent variable is at least in each pi-group, and the dependent one in only one of them.
- As stated previously, before the formulation of the model it is necessary test planning and obtain experimental results to relate the pi-groups.

2.2 Dimensional analysis and experiments

The idea to apply the theory of dimensional analysis in manufacturing processes is not new. In several scientific papers it was used this approach to simplify the studies, minimizing the number of complicated and expensive experiments. Rolling and machining are the metal forming processes where this approach has been mostly used. R.J. Bhatt, H.K. Raval used a semiempirical method based on dimensional analysis to calculate the force during the flow forming process, comparing it with results obtained from simulations and analytical model [30]. The authors found that the predictability of this model was more than 90%, and the most important parameters

that affected the process have been recognized thanks to this approach. To find the relationships between the pi-groups, non linear estimation was used.
D.R. Phatak and H.B. Dhonde used dimensional analysis to predict the ultimate torsional strength of reinforced concrete beams subjected to pure torsion [31]. Starting from the theory of dimensional analysis and few experimental results, the equation was derived, and as a result it was possible to show that dimensional analysis can be used as a method to predict mechanical properties.
And metal cutting in general is one of the most used manufacturing processes. Machining processes involve a lot of operating variables, and tool wear is a very important parameter, because it affects the quality of the workpiece, productivity and cost of the operation. This is why in [32] the main purpose of the authors was to develop mathematical model to increase tool life and improve the performances of the process. Dimensional analysis together with experimental investigation of a physical phenomenon can have a lot of advantages. For example, the material and the laboratory setup of experiments can be expensive. Using dimensional analysis it is possible to:

- Reduce the amount of experiments, thanks to the reduction of independent variables.

- Find results in the range of a variable that goes beyond the range of the experiments.

- Find out that an independent variable doesn't have influence in the phenomenon under study. Or reveal the oversight of another variable.

- After organization of experiments, have more convenient and ordered data, and more compacted and clarified results presentation.

2.3 Application of dimensional analysis to continuous method of combined deformational processing by drawing with bending and torsion

According to the theory of dimensional analysis, at first the independent variables of the problem were identified. Always this analysis begins with a list of such physical parameters that are believed to be involved in the problem under study. Physical laws are not employed. This is both an advantage and disadvantage of the dimensional analysis technique, because the choice of the parameters depends only on the analyst, on knowledge and experience. If in the list are included variables that don't influence the system, or are omitted variables that influence it, the analysis will fail. The aim of every method of metal processing is to achieve a definite level of mechanical properties. One of the main properties of metal products like carbon steel wire is the Ultimate Tensile Strength (UTS). This is the reason why it is interesting find a relationship between UTS and the different parameters involved in the process.

Identification of independent, dependent and extraneous variables of the process

1. *Tools geometry*

   In the continuous method of combined deformational processing by drawing with bending and torsion the main tools are the drawing dies and the rolls system. Tests showed variation of mechanical properties, like UTS itself, with geometrical parameters like the diameter of the rolls and the diameters of the drawing dies. Use of rolls with diameters of 60 mm or 90 mm showed different results, such as experiments using different diameters of the drawing dies. This fact lead to the decision to choose the rolls diameter as the characteristic dimension of the rolls, and the diameters of the dies as the characteristic dimensions for the drawing dies.

2. *Process operating variables*

   Torsion rate of the system of rolls was selected as the most important process operating variable, on the basis of previous experimental results. Experiments with different torsion rate, keeping constant the diameters of the drawing dies

or the rolls diameters, demonstrated this fact. Drawing speed is a process parameter, but in this analysis this speed is considered as a constant.

3. *Working material*

   Density is a fundamental material property. Because of the studies were conducted using carbon steel wires with the same density, but with different carbon contents, it is reasonable to add also this last quantity as a parameter of influence. Also the selected dependent variable, UTS, is a material property itself, such as the Yield Stress (YS).

In Table 2.1 the influencing variables of the process are presented with their physical dimensions.

Table 2.1. *Influencing variables for the process with their units and dimensions*

Influencing variable	Symbol	Unit	Dimension
1st Drawing Ratio	DR_1	[-]	Dimensionless
2nd Drawing Ratio	DR_2	[-]	Dimensionless
% Carbon Content	%C	[-]	Dimensionless
Torsion rate	ω	RPM	$[T^{-1}]$
Rolls Diameter	D_{rolls}	m	[L]
Density	ρ	kg/m^3	$[ML^{-3}]$
Ultimate Tensile Strength	UTS	MPa	$[ML^{-1}T^{-2}]$
Yield Stress	YS	MPa	$[ML^{-1}T^{-2}]$

The two drawing ratios are defined as follows:

$$DR_1 = \frac{d_0^2 - d_1^2}{d_o^2} \tag{2.7}$$

$$DR_2 = \frac{d_1^2 - d_2^2}{d_1^2} \tag{2.8}$$

where d_0 is the diameter of the workpiece when it enters in the first drawing die, d_1 is the diameter when it exits from the same die, and it enters in the second drawing die, while d_2 is the final diameter of the workpiece.

Reduction of independent variables adopting the method of dimensional analysis

Before dimensional analysis, the unknown functional relationship between dependent and independent variables is the following:

$$UTS = \boldsymbol{f}(DR_1, DR_2, \omega, D_{rolls}, \%C, \rho, YS) \tag{2.9}$$

The quantities $DR_1, DR_2, \%C$ are already dimensionless, so they don't take part in the derivation of the pi-groups.
There are five dimensional variables: $UTS, \rho, \omega, D_{rolls}, YS$, so $n = 5$. The basic dimensions for this case of study are: Length [L], Mass [M], Time [T], so $k = 3$. The application of Pi-Theorem leads to $n - k = 2$, so two dimensionless products. Choosing ρ, ω and D_{rolls} as repeating variables:

$$\pi_0 = \frac{UTS}{D_{rolls}^2 \cdot \rho \cdot \omega^2} \tag{2.10}$$

$$\pi_1 = \frac{YS}{D_{rolls}^2 \cdot \rho \cdot \omega^2} \tag{2.11}$$

Reminding the dimensionless parameters in Eq. 2.3, these are the others pi-groups: $\pi_2 = DR_1$, $\pi_3 = DR_2$, $\pi_4 = \%C$.

The model is:

$$\pi_0 = \boldsymbol{h}(\pi_1, \pi_2, \pi_3, \pi_4) \tag{2.12}$$

After substitution:

$$\frac{UTS}{D_{rolls}^2 \cdot \rho \cdot \omega^2} = \boldsymbol{h}\left(\frac{YS}{D_{rolls}^2 \cdot \rho \cdot \omega^2}, DR_1, DR_2, \%C\right) \tag{2.13}$$

$$UTS = D_{rolls}^2 \cdot \rho \cdot \omega^2 \boldsymbol{h}\left(\frac{YS}{D_{rolls}^2 \cdot \rho \cdot \omega^2}, DR_1, DR_2, \%C\right) \tag{2.14}$$

Dimensional analysis lead to a reduction in the number of the variables. The five variables have been grouped into the dimensionless terms π_0, π_1. And together with π_2, π_3, π_4, they represent the physical process.

2.4 Conclusion

Aim of this chapter was to introduce the application of dimensional analysis to material processing and as an useful tool to manage experimental investigation of physical phenomenon saving time and costs. This technique was applied to find dimensionless group for the method of combined deformations with drawing, bending, and torsion. After dimensional analysis, when experimental investigation is carried out, to see the influence of one pi-group keeping the other constant, it is not necessary to vary each parameter of the group under study. There is choice to vary only one of them, or a combination of them. and over a desired range of values for the pi-group. It can be varied, for example, the most convenient parameter from a practical point of view.

Chapter 3

Numerical investigation of the continuous method of deformational processing by drawing with bending and torsion

The software DEFORM-3D is widely used for Finite Element Method (FEM) simulations and is applied to analyze various forming and heat treatment processes in metal forming and related industries. It is rather user-friendly, and it is capable of modeling complex three dimensional material flow patterns.
Wire drawing process is one of the most used metal forming processes within the industrial field, and several studies used DEFORM-3D to gain deeper knowledge about the effect of important drawing parameters, or just as simulation tool before experimental investigation to get useful information. The continuous method of combined deformational processing by drawing with bending and torsion was simulated using commercial software DEFORM-3D. Several simulations using workpiece with different carbon content and different torsion rate were made in order to study the variation of the drawing force for each configuration and obtain other useful information about strain and the damage parameter.

3.1 Pre-processing

3.1.1 Geometry and materials

The first step of the numerical study was the creation of the geometries involved in the process. At last all the parts have been unified in an assembly, saved in a proper format, and imported in software DEFORM-3D. The parts that take part in the design are the two drawing dies, two pairs of rolls, each one with the same dimensions, and the workpiece. Software SolidWorks was used to create the geometrical model of the process.
As concerns the drawing dies, the reference geometry was Forme GOST 9453-75 (Figure 3.1a). The geometry of the first drawing die of the process is shown in Figure 3.1b.

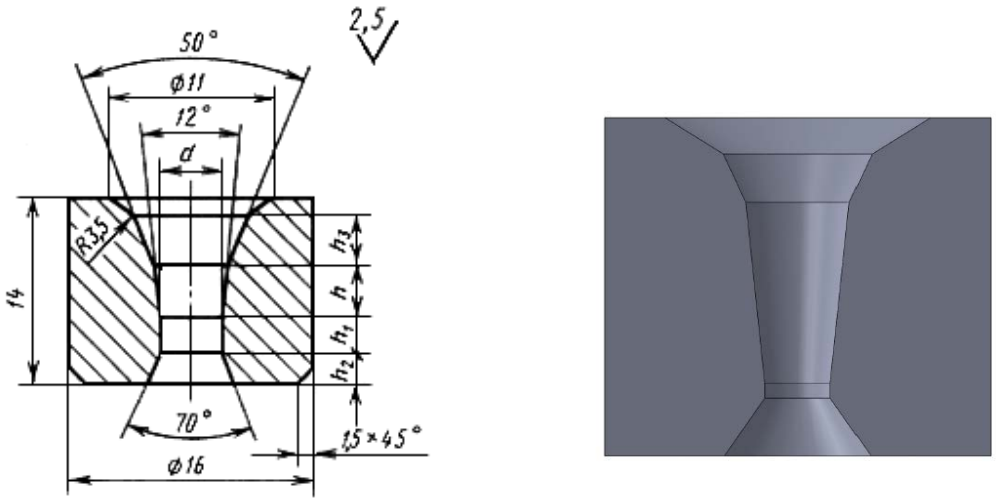

(a) **(b)**

Figure 3.1. *Geometry of the dies used for the simulation: reference geometry (a) and geometry created with SolidWorks (b)*

The rolls have a diameter of 90 mm. This tool is shown in Figure 3.2a and Figure 3.2b. Four equal rolls with a diameter of 90 mm were chosen for the simulations (Figure 3.3)

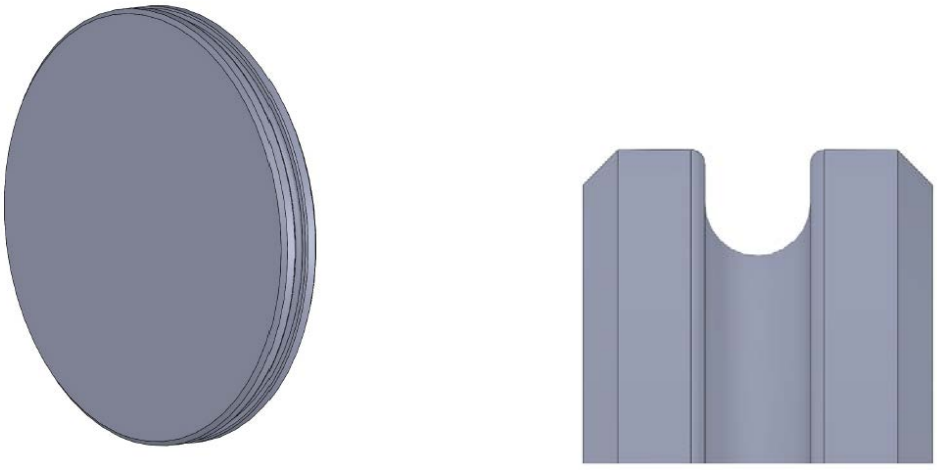

(a) **(b)**

Figure 3.2. *Roll with diameter of 90 mm: entire geometry (a) and detail (b)*

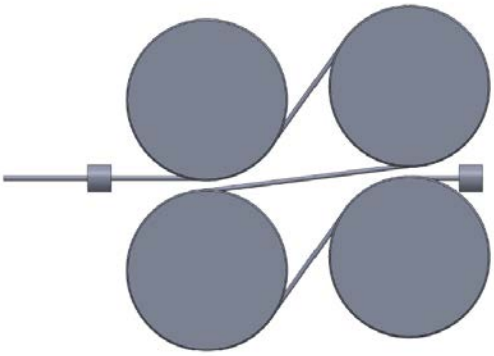

Figure 3.3. *Four-rolls configuration used for the simulations of the process*

The last single part is the workpiece (Figure 3.4). The shape begins 60 mm before the first die and ends immediately before the reduction in the second die.

(a) **(b)**

Figure 3.4. *Workpiece details: full length of the wire (a), reduction of the wire in the first drawing die (b)*

All the previous parts have been assembled into a single assembly. The idea was to simulate different configurations, using the same geometries but with two different carbon steel wires and different process parameters.
Figure 3.3 shows the assembly that was imported in software DEFORM-3D.
An additional tool was added during the setup of the simulation: a cylindrical object that pulls the wire through the dies, positioned at the end of the wire (Figure 3.5).
DEFORM-3D makes use of accurate data of material properties, in order to give better results. Useful data are for example elastic, thermal, diffusion, fracture and plastic properties of the material. In particular, the database about plastic properties contains data sets of several material flow stress, in order to give the behaviour of the material during plastic deformation [33]. Figure 3.6a and Figure 3.6b show the flow stress curve of the materials used in the simulations, that are carbon steel with 0.50 wt.%C (Figure 3.6a) and carbon steel with 0.70 wt.%C (Figure 3.6b). Such diagrams were exported from data of DEFORM-3D.

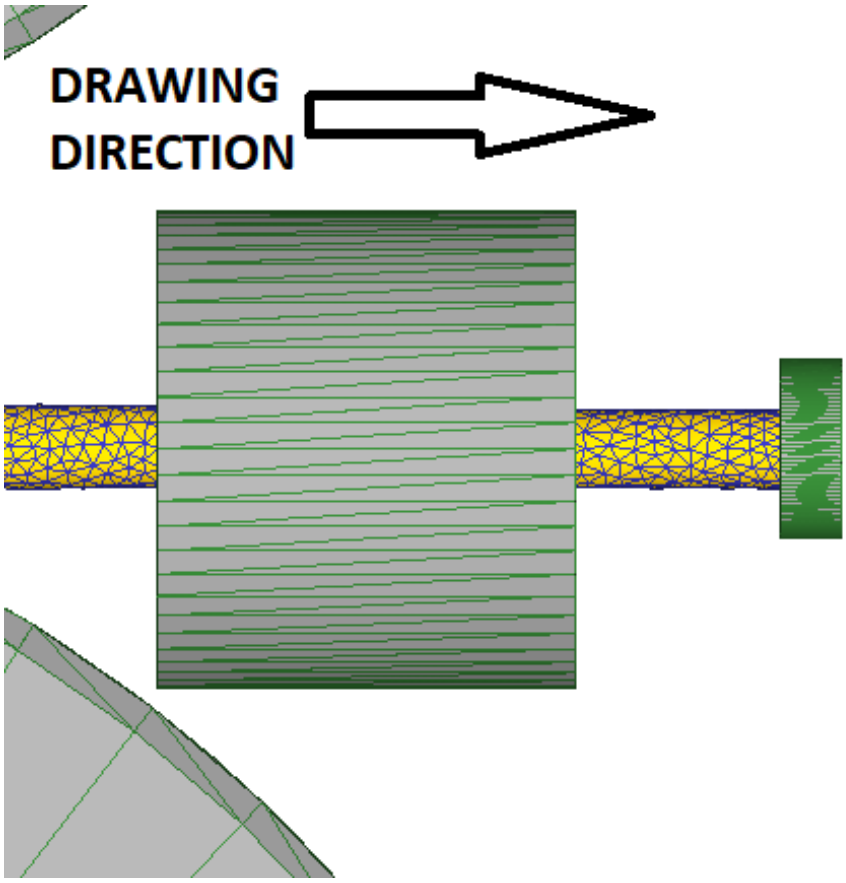

Figure 3.5. *Object used to pull the wire through the dies*

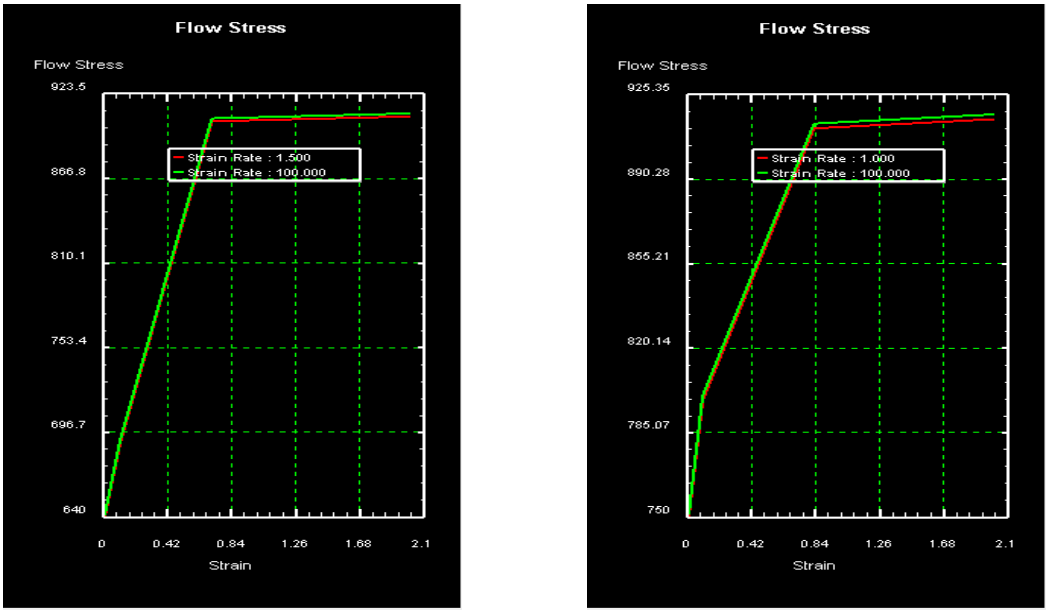

(a) *AISI-1045.COLD[70-950F(20-500C)]* **(b)** *AISI-1070.COLD[70-950F(20-500C)]*

Figure 3.6. *Flow Stress curves of the materials used for the simulations, carbon steels with 0.50%C (a) and 0.70%C (b)*

3.1.2 Mesh and input conditions

The minimum element size of the mesh, based on previous experience about this kind of simulations, was applied during the generation of the mesh. Figure 3.7 shows a detail of the mesh of the workpiece.

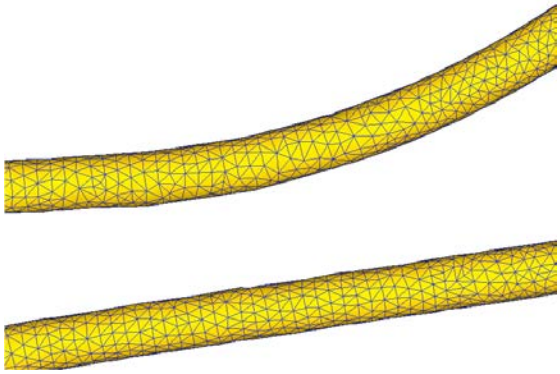

Figure 3.7. *Detail of the wire mesh*

No initial stresses or strains were set as initial conditions. Process was simulated at room temperature of 20°C. Frictions among the wire and the drawing dies was set as Coulomb friction, with a value of the friction coefficient of 0.04 [34].

All the components of the assembly, excluding the wire, have been considered rigid, so these parts does not deform, and no friction was considered between them and the wire. The wire is a plastic part, so it is the only element that deforms during the process. In the experiments, the wire is usually pulled with a velocity V_0=60 mm/s. This velocity was set as boundary condition to the object that was added to simulate the pulling action in the front end of the wire. This velocity is directed in the z direction.

In the simulations with a twisting rate different to zero, the rotation of the rolls was set, with the angular velocity as input and the axis of the drawing dies as rotation axis. Table 3.1 shows the chemical composition of the workpieces used in the simulations, while Table 3.2 shows the main wire properties. Table 3.3 summarizes the simulations and their main features. After the completion of the model building and applying the boundary condition, the case can be solved using the simulator utility.

Table 3.1. *Chemical composition of the carbon steel wires used in the simulations*

Materials	%C	%Mn	%S	%P	%Fe
AISI-1045	0.43-0.50	0.60-0.90	0.05(max)	0.04(max)	%Fe(balance)
AISI-1070	0.65-0.75	0.60-0.90	0.05(max)	0.04(max)	%Fe(balance)

Table 3.2. *Input data used in the simulations*

Wire Conditions	
Material	AISI-1045.COLD (1st regime of simulations)
	AISI-1070.COLD (2nd regime of simulations)
Object type	Plastic
Young's Modulus, E [GPa]	206.754
Poisson's Ratio [ν]	0.3
Diameter before 1st die [mm]	3.05
Diameter after 1st die [mm]	2.75
Diameter after 2nd die [mm]	2.64
Velocity of steel wire, V_0 [mm/s]	60

Table 3.3. *List of simulations with the main parameters of the process*

$n°$	Material	RD [cm]	1st DR, %	2nd DR, %	Torsion rate [RPM]
1	AISI-1045	90	18.70	7.84	0
2	AISI-1070	90	18.70	7.84	0
3	AISI-1045	90	18.70	7.84	50
4	AISI-1070	90	18.70	7.84	50
5	AISI-1045	90	18.70	7.84	100
6	AISI-1070	90	18.70	7.84	100
7	AISI-1045	90	18.70	7.84	150
8	AISI-1070	90	18.70	7.84	150
9	AISI-1045	90	18.70	7.84	200
10	AISI-1070	90	18.70	7.84	200

3.2 Results and discussion

3.2.1 Drawing force of the continuous method of deformational processing

Data about drawing force obtained from the simulations were analyzed using MATLAB.

Process of drawing using rotating dies was studied in various papers, especially in [34], where also a DEFORM-3D analysis was conducted. But the theoretical basis of the idea of rotating die in drawing process and its benefits was formulated decades ago. The main concept of this theory is that with the assumption of taking constant the size of friction force, but not the direction, this leads to a decrease in the drawing stress. Also the numerical simulations of drawing with rotating die showed that the drawing force decreases due to the rotation of the dies [35]. In the process of combined deformation with drawing, bending and torsion, the rotation occurs not cause of the movement of the drawing dies, but cause of the rotating movement of the system of rolls, so also of the wire.

The simulations verified this phenomenon and the results about drawing force are shown below. In particular, in Figure 3.8 and Figure 3.9 the mean value of drawing force found from the simulations is plotted with the torsion rate. It is interesting to note that after a specific point the drawing force doesn't decrease as much as after with lower torsion rates.

Simulations made with a coarse mesh, without roll-system, just with the sequence

of drawing dies showed a mean value of drawing force of almost 1000 N for the medium-carbon steel wire and 1200 N for the high-carbon steel wire.

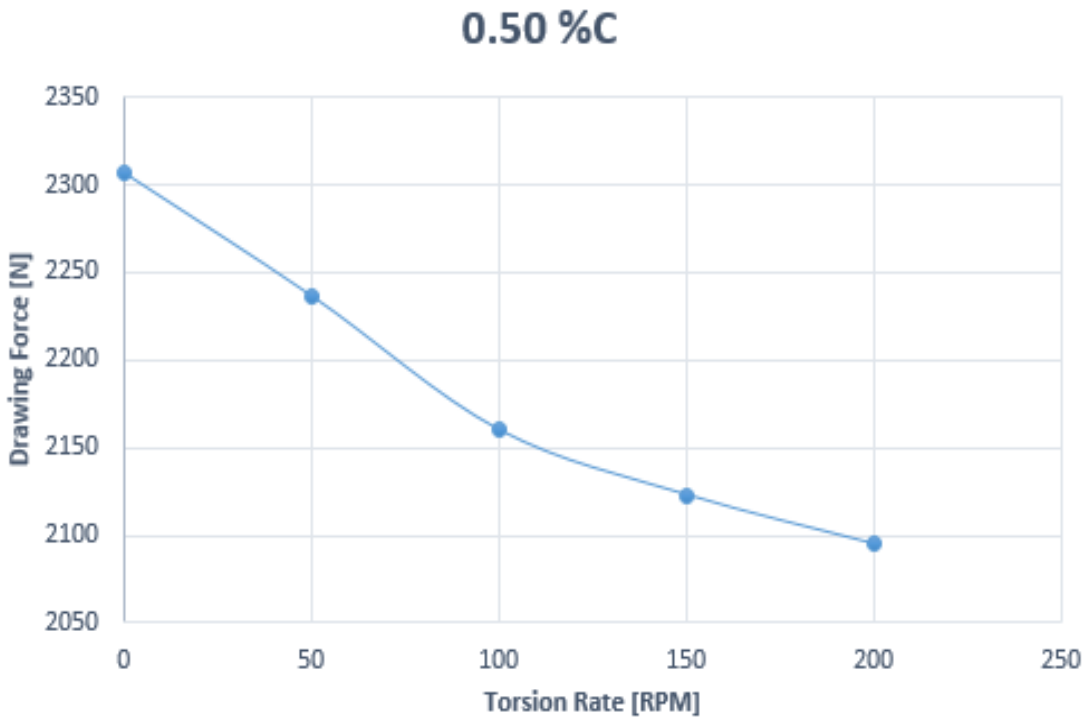

Figure 3.8. *Trend of drawing force with torsion rate (0.50 %C)*

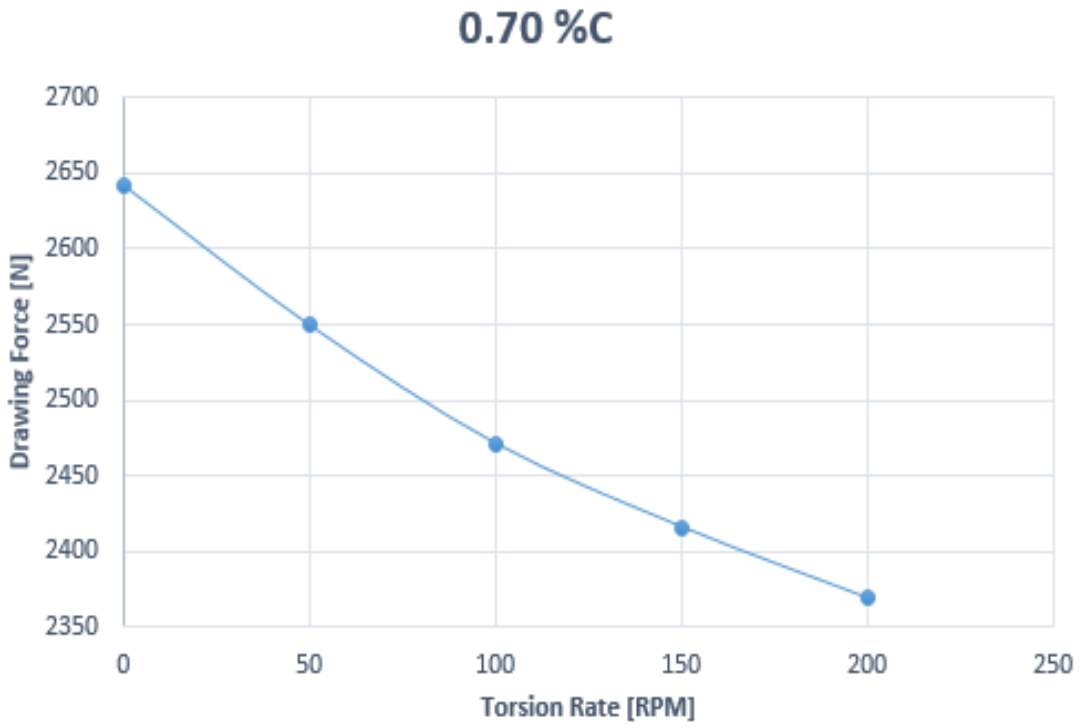

Figure 3.9. *Trend of drawing force with torsion rate (0.70 %C)*

3.2.2 Stress and strain in the continuous method of deformational processing

After results about drawing force in the previous section, stress and strain distributions will be presented below.

Stress and strain in the drawing die

During conventional drawing each elementary volume is subjected to tension in the longitudinal direction (i.e. σ_z), and compression in x and y direction (i.e. σ_x and σ_z). In Figure 3.10 it is shown the scheme of conventional drawing and the main stresses that affect an elementary volume in the material. σ_r and σ_θ in the scheme can be replace with σ_x and σ_y in the simulations, while σ_l is the same of σ_z.

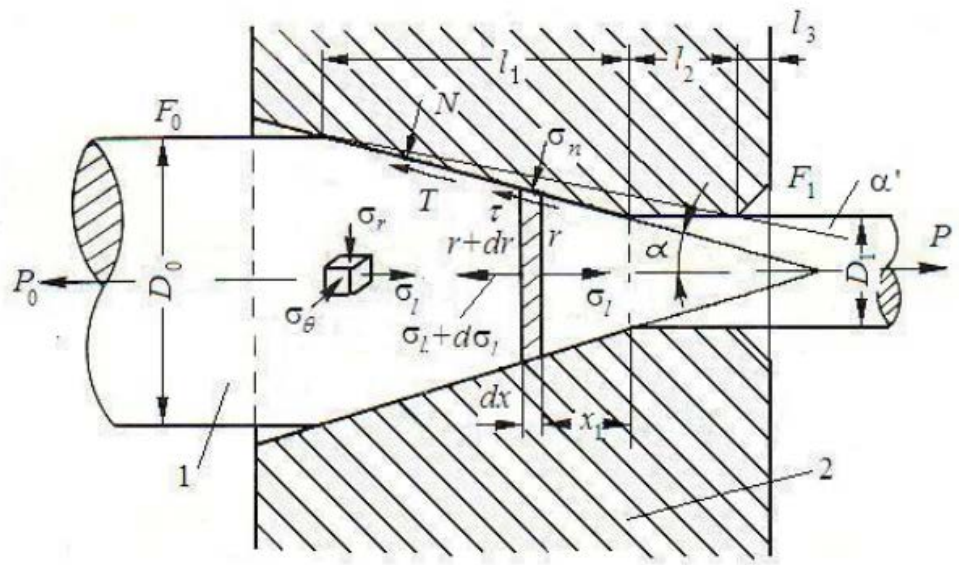

Figure 3.10. *General drawing scheme with elementary volume subjected to tensile and compressive stress [36]*

Effective strain and stress distribution along the diameter of the cross-section the wire after the reduction in the first drawing die are shown in Figure 3.11a and 3.11b. The results are relative to the simulation of medium-carbon steel wire with torsion rate of 50 RPM. Figures 3.12a and 3.12b show the same results but for high-carbon

steel wire. Effective strain and stress are based on Von Mises criterion [37]:

$$\sigma_{eff} = \sqrt{\frac{(\sigma_x - \sigma_y)^2 + (\sigma_y - \sigma_z)^2 + (\sigma_z - \sigma_x)^2}{2} + 3(\sigma_{xy}^2 + \sigma_{yz}^2 + \sigma_{zx}^2)} \tag{3.1}$$

$$\epsilon_{eff} = \sqrt{\frac{2}{3}[\epsilon_x^2 + \epsilon_y^2 + \epsilon_z^2 + 2(\epsilon_{xy}^2 + \epsilon_{yz}^2 + \epsilon_{zx}^2)]} \tag{3.2}$$

These quantities can be also expressed in terms of principal stresses:

$$\sigma_{eff} = \sqrt{\frac{(\sigma_1 - \sigma_2)^2 + (\sigma_2 - \sigma_3)^2 + (\sigma_3 - \sigma_1)^2}{2}} \tag{3.3}$$

such as for the effective strain:

$$\epsilon_{eff} = \frac{\sqrt{2}}{3}\sqrt{(\epsilon_1 - \epsilon_2)^2 + (\epsilon_2 - \epsilon_3)^2 + (\epsilon_3 - \epsilon_1)^2} \tag{3.4}$$

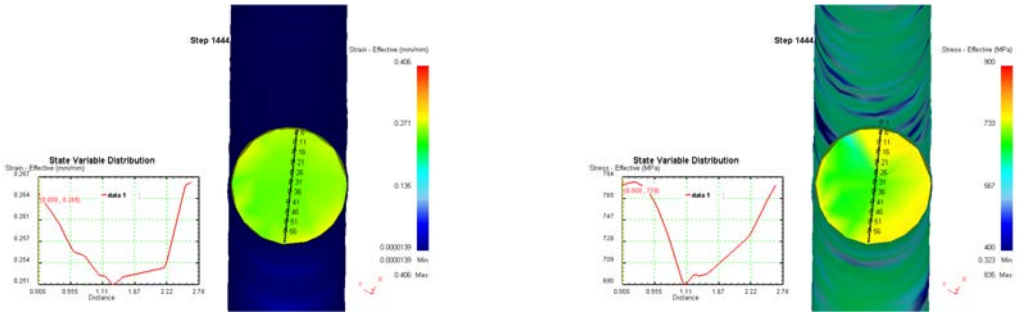

(a) **(b)**

Figure 3.11. *Strain (a) and stress (b) effective in the cross-section immediately after the drawing cone of the first drawing die (0.50%C)*

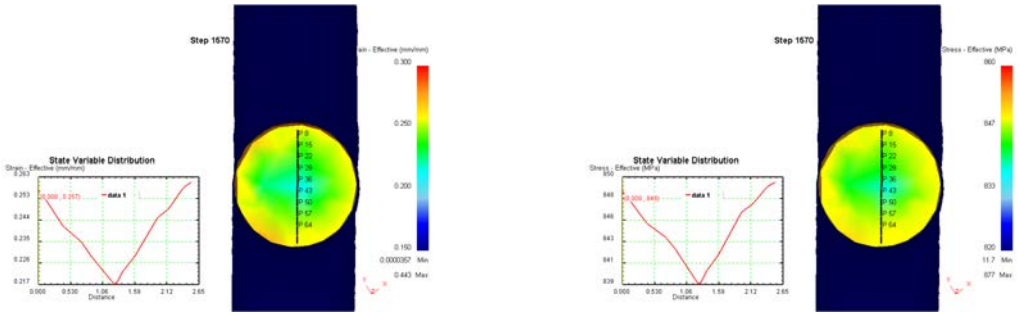

(a) **(b)**

Figure 3.12. *Strain (a) and stress (b) effective in the cross-section immediately after the drawing cone of the first drawing die (0.70%C)*

Because of the cross section of the wire studied in the simulations is circular it is, for symmetry, $\sigma_x = \sigma_y$.

Figures 3.13, 3.14, 3.15 and 3.16 show the distribution of strain intensity along the longitudinal section of the wire axis, for the first drawing die (3.13a, 3.14a, 3.15a, 3.16a) and for the second die (3.13b, 3.14b, 3.15b, 3.16b).

In conventional drawing the deformation zone is confined in the drawing cone of the die. In the continuous method of combined deformational processing by drawing with bending and torsion, it is noted an elongation of the deformation zone for all the simulations taken in exam.

Effective strain distribution along the longitudinal section of the surface of the wire is shown in the figures below. Values of strain effective are higher in the surface of the wire than values in the core.

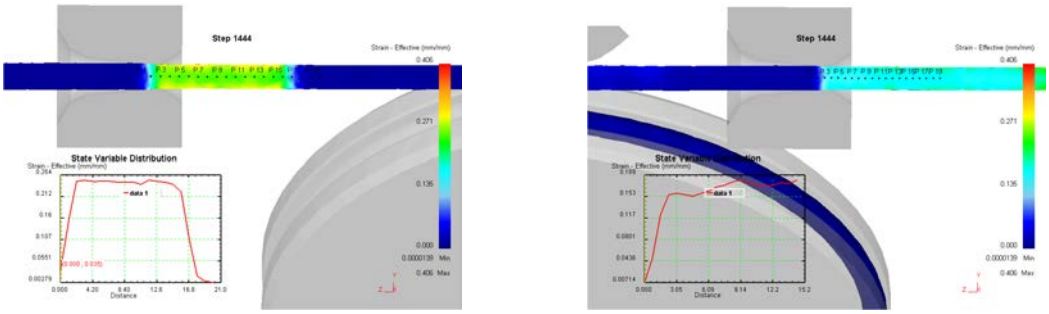

(a) **(b)**

Figure 3.13. *Effective strain distribution along the axis of the wire, after the first die (a) and second die (b) (0.50%C)*

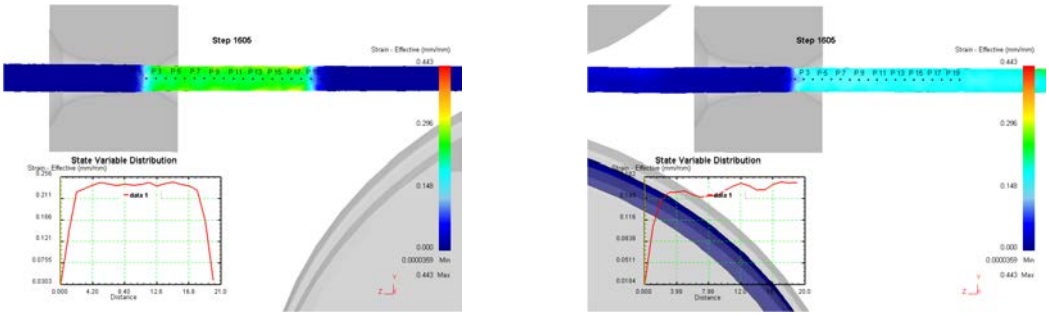

(a) **(b)**

Figure 3.14. *Effective strain distribution along the axis of the wire, after the first die (a) and second die (b) (0.70%C)*

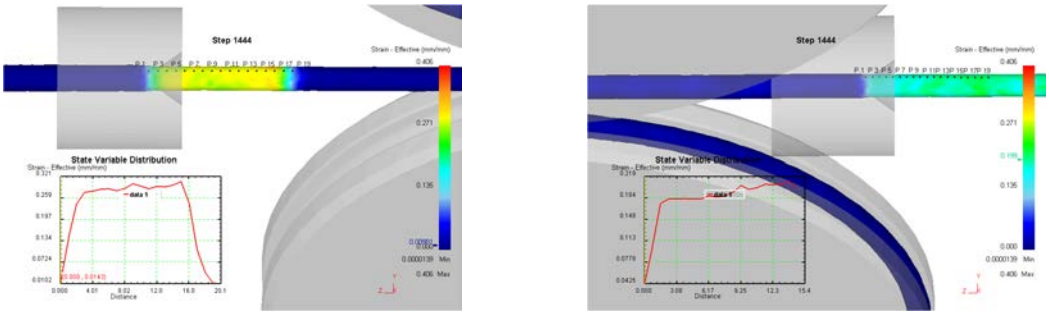

(a) **(b)**

Figure 3.15. *Effective strain distribution along the surface of the wire, after the first die (a) and second die (b) (0.50%)*

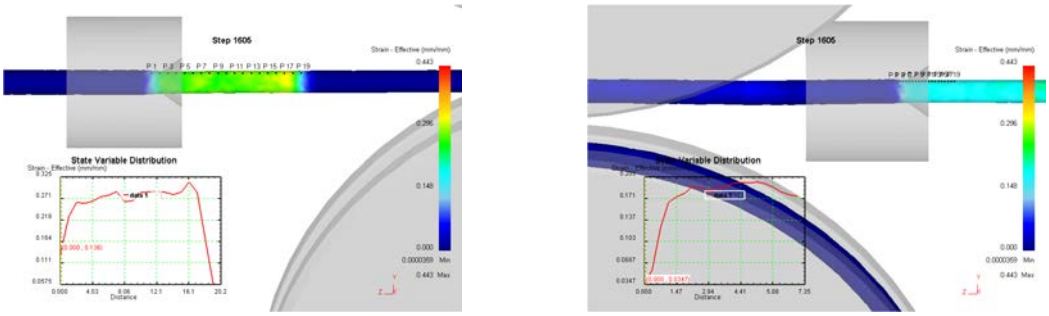

(a) **(b)**

Figure 3.16. *Effective strain distribution along the surface of the wire, after the first die (a) and second die (b) (0.70%C)*

Values of strains along the longitudinal section on the wire axis are reported in Table 3.4. Values of strains are not much different between one simulation and another. But it can be noted that value of strain increase, especially from the condition of the process without torsion rate and with torsion rate.

Table 3.4. *Mean values of strains for all simulations corresponding to the first drawing die*

Torsion rate [RPM]	%C	ϵ_x [-]	ϵ_y [-]	ϵ_z [-]	ϵ_{eff} [-]
0	0.50	-0.0987	-0.0991	0.215	0.245
50	0.50	-0.102	-0.105	0.224	0.249
100	0.50	-0.104	-0.101	0.217	0.251
150	0.50	-0.105	-0.106	0.223	0.251
200	0.50	-0.103	-0.104	0.223	0.252
0	0.70	-0.1	-0.1	0.209	0.242
50	0.70	-0.104	-0.103	0.221	0.245
100	0.70	-0.106	-0.103	0.219	0.25
150	0.70	-0.105	-0.107	0.221	0.251
200	0.70	-0.106	-0.106	0.221	0.251

Bending in continuous method of deformational processing

Bending deformation was studied in terms of longitudinal stress distribution σ_z in definite cross-sections along the deformation path. Stress behaviour is not the same of pure bending but it is bending in tensile conditions. The cross-sections where stress distribution was visualized along the diameter are shown in Figure 3.17, and the simulations are the ones without torsion rate, for both the carbon steel wires (Figure 3.18 and Figure 3.19).

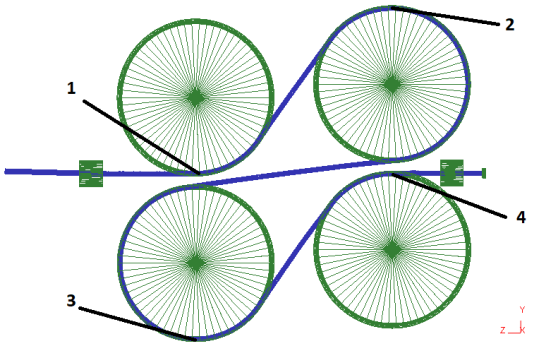

Figure 3.17. *Cross-sections for the analysis of bending deformation*

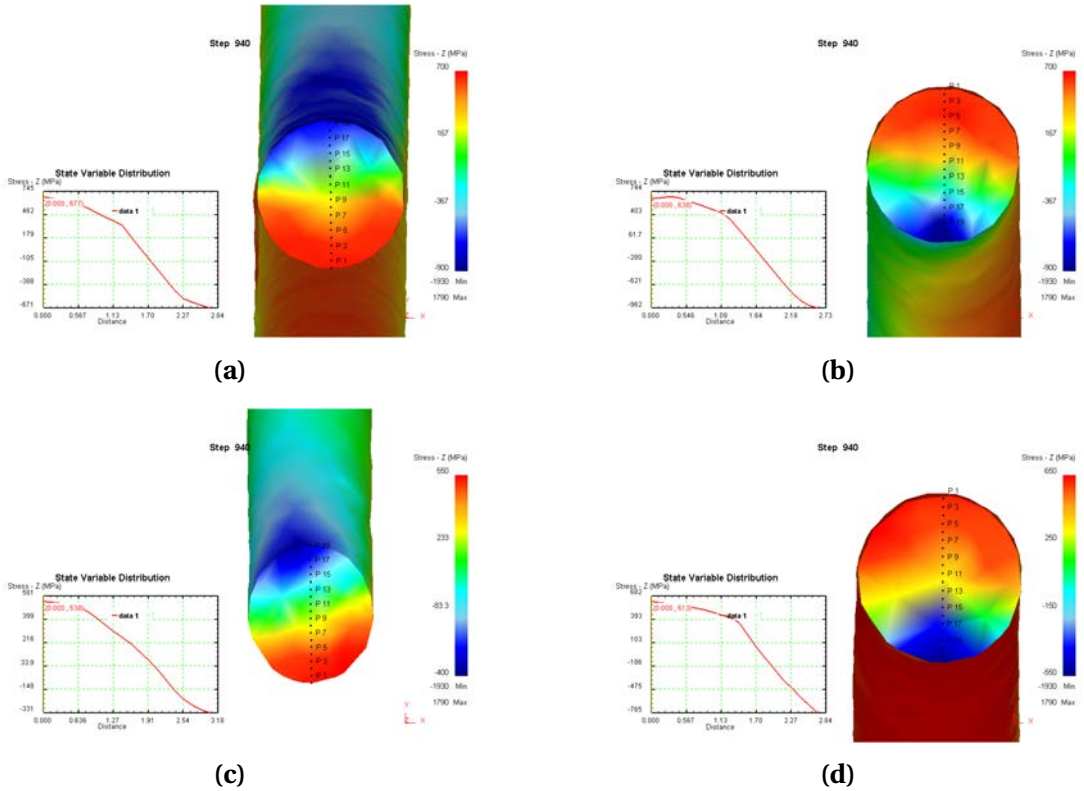

Figure 3.18. *Stress distribution along the diameter in different cross-section of the bending deformation path (0.50%C): a) first roll, b) second roll, c) third roll, d) fourth roll*

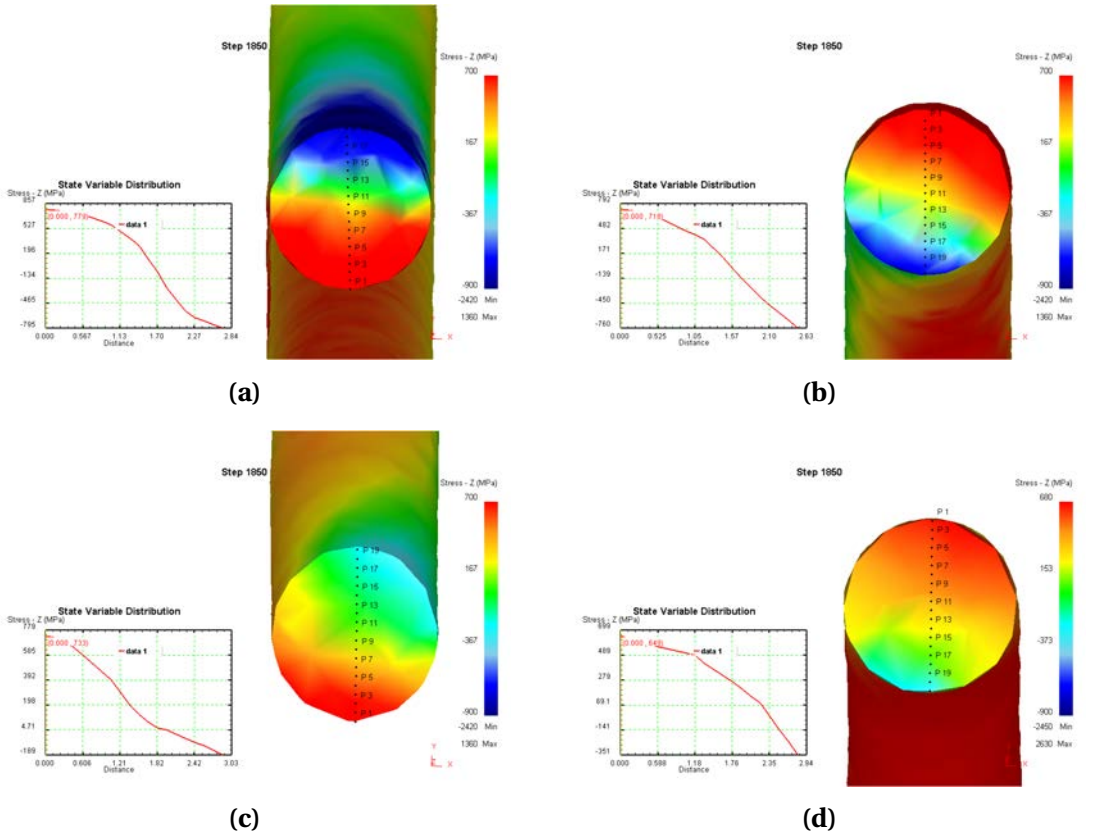

Figure 3.19. *Stress distribution along the diameter in different cross-section of the bending deformation path (0.70%C): a) first roll, b) second roll, c) third roll, d) fourth roll*

In particular, the z-stress distribution along the diameter of the cross-section is plotted: it reveals the tension and compression stress of the wire due to the process in the selected points.

As can be seen in Figure 3.18 and Figure 3.19, the combination of bending with tension leads to high tensile and compressive stresses in the cross-sections of the wire in the rolls-system: compressive stress prevails in the contact zone between the wire and the rolls, while tensile stress prevails in the opposite side of the wire.

3.2.3 Damage parameter in the continuous method of deformational processing

Several failure criteria can be used to predict cracking due to critical tensile stresses when metals are subjected to plastic deformation.

Cockcroft and Latham failure criterion is one of the most used.

This criterion takes into account the critical damage parameter C_1, defined by the

following equation [37]:

$$\int_0^{\epsilon_f} \sigma^* \, d\bar{\epsilon} = C_1 \tag{3.5}$$

On the left of the equation there is the maximum energy of deformation per unit of volume, and σ^* is the maximum principal stress in the material.
In accordance to the Cockcroft and Latham failure criterion, when damage parameter reaches the critical value given by the critical damage parameter C_1, cracking occurs. It is important to note that there are two main factors that are related to C_1: the maximum principal stress when it is tensile, and the effective strain of the material.
Deform 3D FEM software allows user to calculate the damage parameter, based on the default damage model which uses the Cockcroft-Latham criterion. This model is chosen because it is demonstrated to give good indications relatively some kinds of tensile ductile fracture like cracking after stretching, for example chevron crackings (and not good for example for fractures in compression) [33].
Using Cockcroft-Latham criterion is also possible to quantify workability or in this case, the drawability of the metal product, which quantifies how much it can be plastically deformed before fracture.
This fracture criterion was applied, using DEFORM 3D, to the simulations of the continuous method of combined deformational processing by drawing with bending and torsion, and the results are shown in Figure 3.20 and Figure 3.21, relatively to the simulation of medium-carbon steel wire (Figure 3.20) and high-carbon steel wire (Figure 3.21) with a torsion rate of the four-rolls system of 200 RPM.

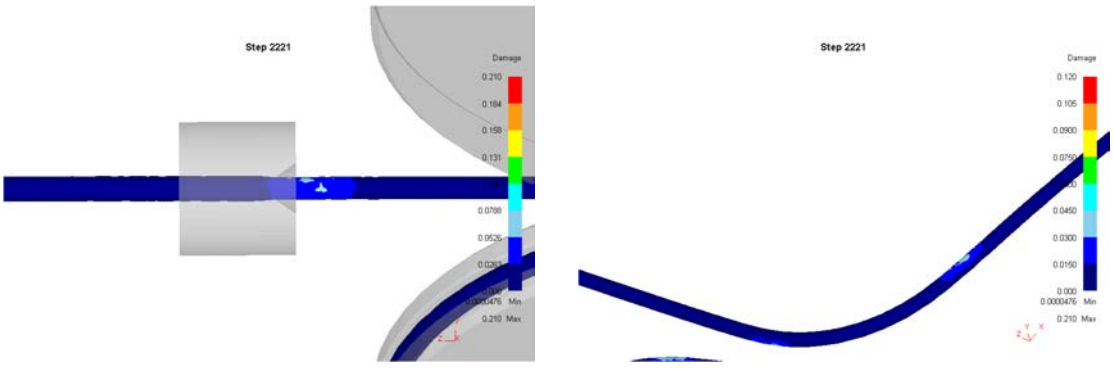

(a) **(b)**

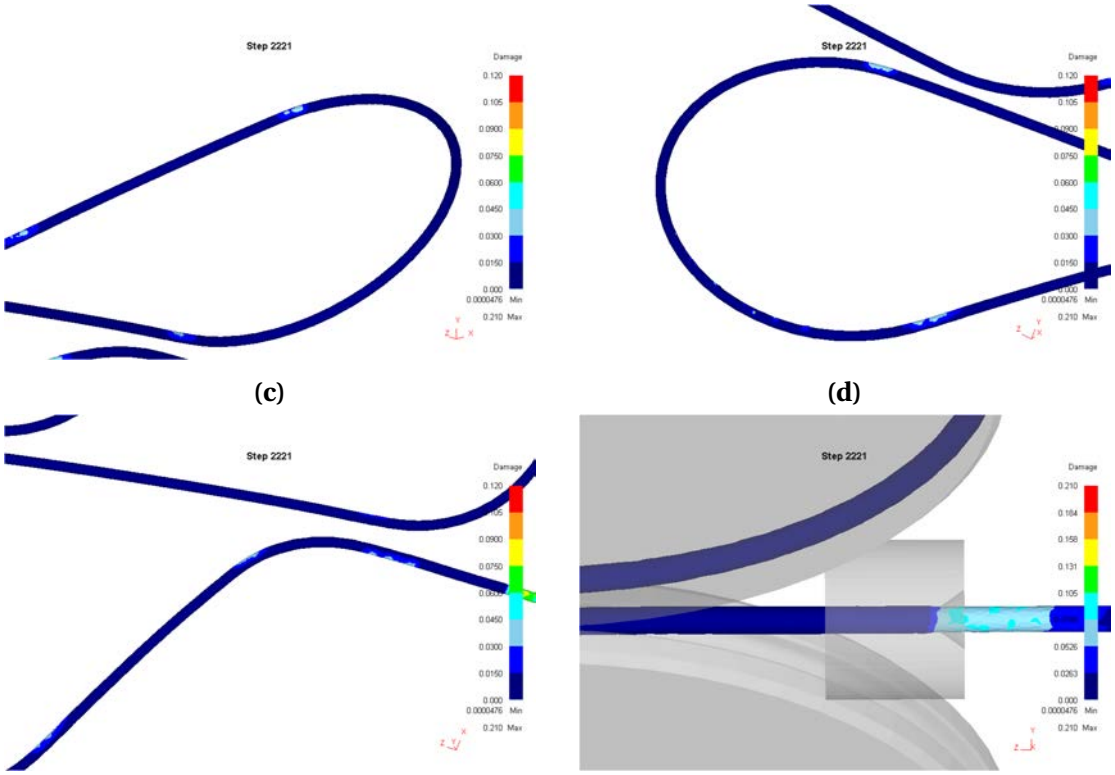

(c) (d)

(e) (f)

Figure 3.20. *Damage parameter along the deformation path: a) in the first die; b) on the first roll; c) on the second roll; d) on the third roll; e) on the fourth roll; f) in the second die (0.50%C)*

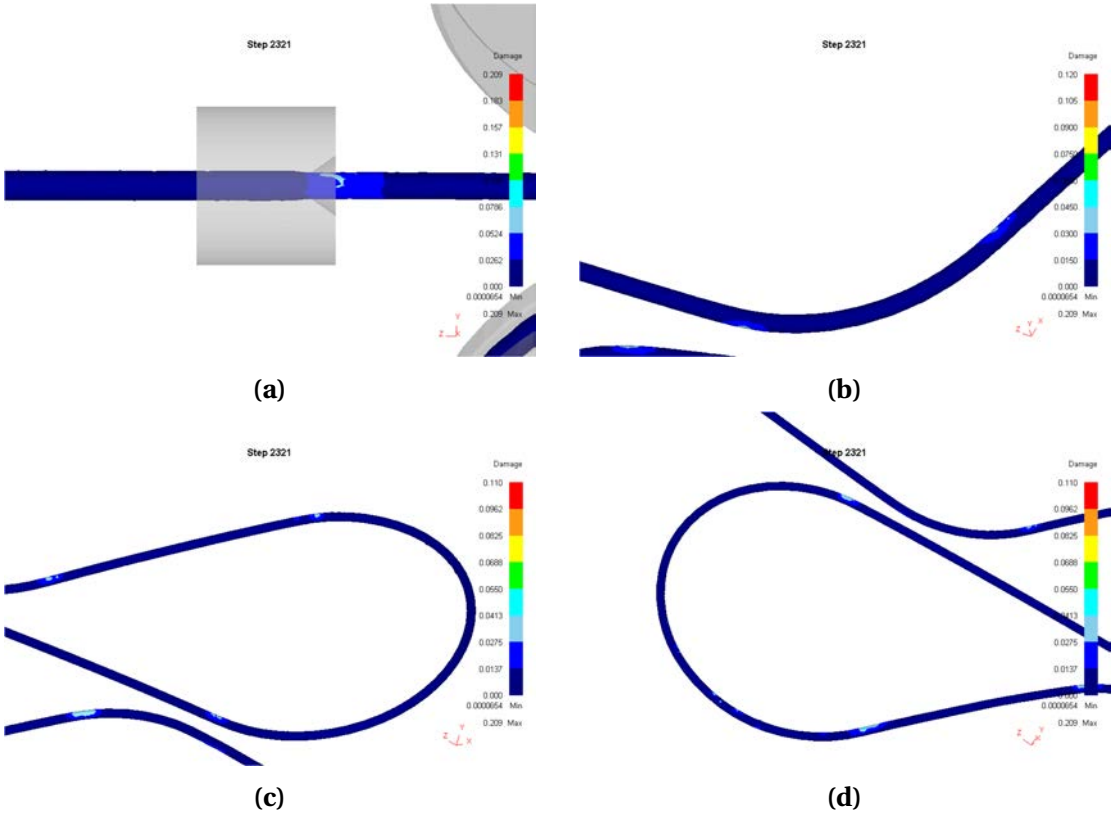

(a) (b)

(c) (d)

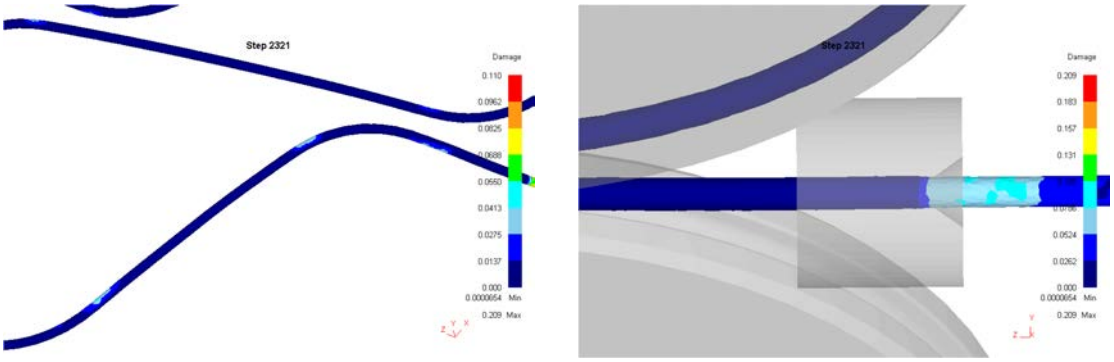

(e) **(f)**

Figure 3.21. *Damage parameter along the deformation path: a) in the first die; b) on the first roll; c) on the second roll; d) on the third roll; e) on the fourth roll; f) in the second die (0.70%C)*

The results of all the simulations showed that there aren't areas with high concentrations of hydrostatic pressure and damage parameter. It is observed an increase of the damage parameter calculated with the Cockcroft-Latham criterion from the first die to the second die, after the four-rolls block.
It can be stated that no cracks formation was found along the deformation path in all the simulations.
Table 3.5 shows the values of damage parameter for each regime of torsion rate relatively to each content of carbon in steel wire.
Values were computed displaying the damage parameter in the cross-section immediately after the parallel land of the second drawing die, and displaying the values of damage parameter along the diameter of the cross-section.
The values shown in the table are the maximum values, which occur in the centre of the wire cross-section.

Table 3.5. *Values of damage parameter for torsion rate regime and carbon content of steel wire*

	0 RPM	50 RPM	100 RPM	150 RPM	200 RPM
0.50%C	0.15	0.146	0.135	0.146	0.146
0.70%C	0.142	0.144	0.135	0.145	0.142

Values of damage parameter are always higher in the simulations with medium carbon steel (0.50%C), rather than high carbon steel (0.70%), and it can be seen that the minimum values of the damage parameter occur in the simulations using a

torsion rate of 100 RPM.

3.2.4 Hydrostatic stress in the continuous method of deformational processing

The hydrostatic stress, or mean stress, is defined by:

$$\sigma_m = \frac{\sigma_x + \sigma_y + \sigma_z}{3} \tag{3.6}$$

Figure 3.22, Figure 3.23, Figure 3.24, and Figure 3.25 are referred to the simulation without torsion rate and both carbon steel wires.

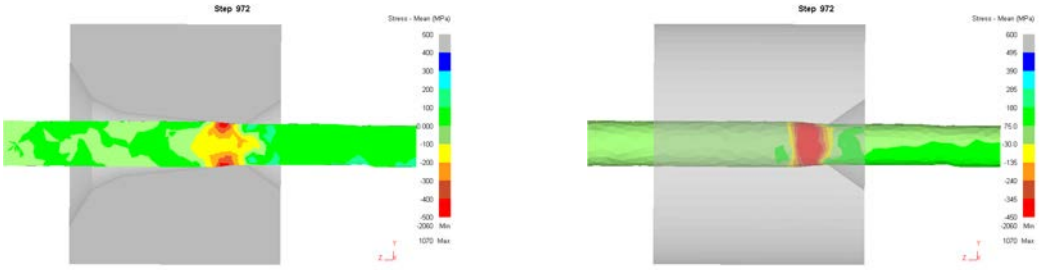

(a) **(b)**

Figure 3.22. *Hydrostatic stress along the longitudinal section of the wire axis (a) and at the surface (b) (first drawing die, 0.50%C)*

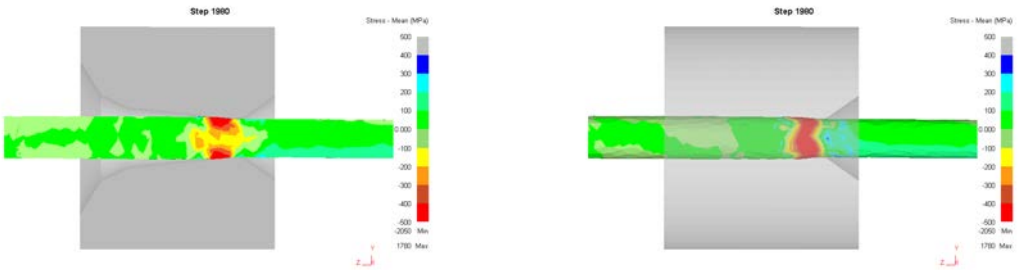

(a) **(b)**

Figure 3.23. *Hydrostatic stress along the longitudinal section of the wire axis (a) and at the surface (b) (first drawing die, 0.70%C)*

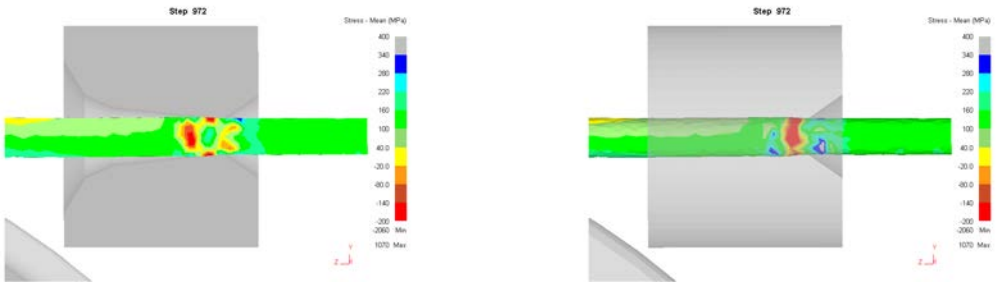

(a) **(b)**

Figure 3.24. *Hydrostatic stress along the longitudinal section of the wire axis (a) and at the surface (b) (second drawing die, 0.50%C)*

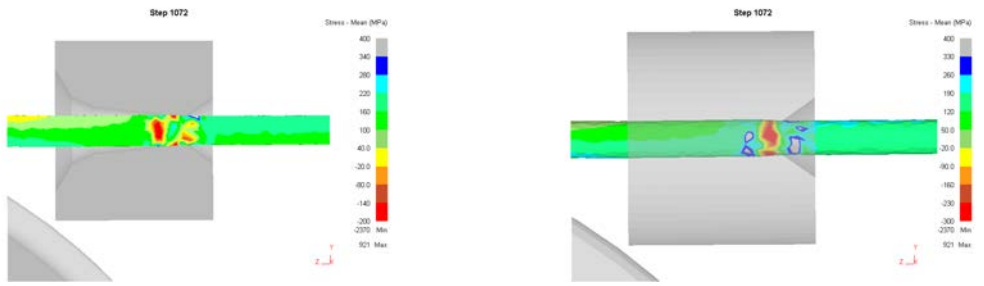

(a) **(b)**

Figure 3.25. *Hydrostatic stress along the longitudinal section of the wire axis (a) and at the surface (b) (second drawing die, 0.70%C)*

It was found that the hydrostatic stress is higher in the surface of the wire than the core. Figure 3.26, Figure 3.27, Figure 3.28 and Figure 3.29 show the distribution of the mean stress along the longitudinal axis (z-axis) when the wire is subjected to plastic deformation in the first and second drawing die, both for the core and the surface.

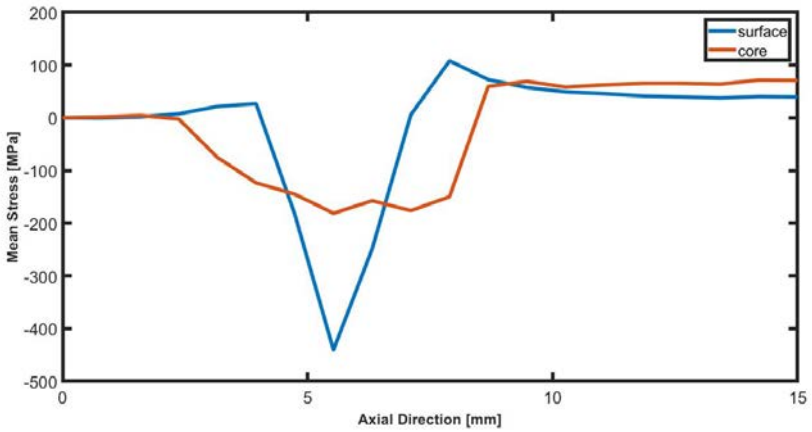

Figure 3.26. *Distribution of hydrostatic stress along the longitudinal direction in the core of the wire and in the surface of the wire (first drawing die, 0.50%C)*

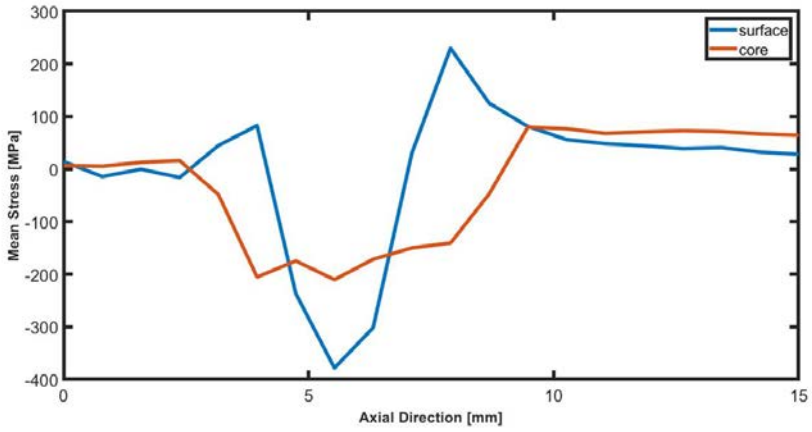

Figure 3.27. *Distribution of hydrostatic stress along the longitudinal direction in the core of the wire and in the surface of the wire (first drawing die, 0.70%C)*

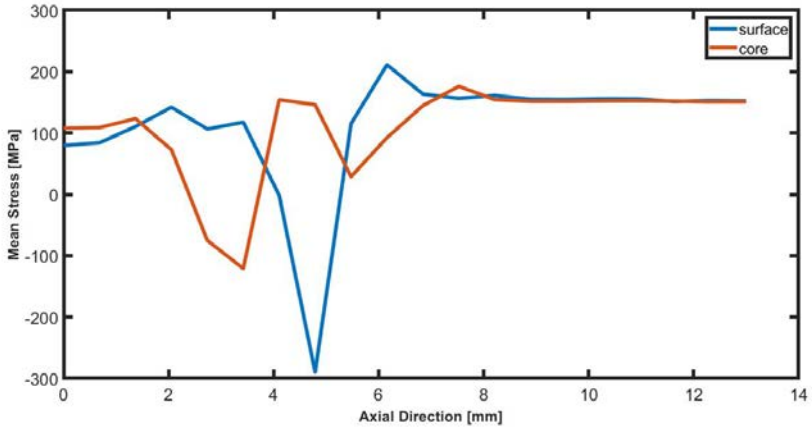

Figure 3.28. *Distribution of hydrostatic stress along the longitudinal direction in the core of the wire and in the surface of the wire (second drawing die, 0.50%C)*

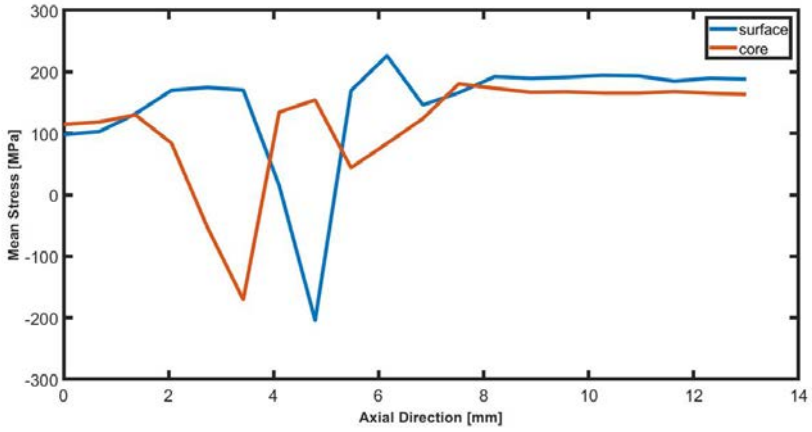

Figure 3.29. *Distribution of hydrostatic stress along the longitudinal direction in the core of the wire and in the surface of the wire (second drawing die, 0.70%C)*

Before the first drawing die, mean stress is almost zero. In the drawing zone, the highest values of compressive stress occur. As stated before, the lowest values occur in the surface of the wire. After the die, tensile stress takes place in the bearing zone, resulting in residual tensile stress at the exit of the die. For the second drawing die, the behaviour is similar .

Chapter 4

Experimental investigation of carbon steel wire mechanical properties and microstructure after continuous method of deformational processing

After results obtained from simulations, experimental investigation has been carried out in the laboratory of Nosov Magnitogorsk State Technical University. Experiments are necessary to obtain those important results which are impossible to study with numerical investigation, such as about UTS and yield strength. Anyway, the combination of results from numerical investigation, together with experimental one, can give a great understanding to the process itself.

Carbon steel wires with carbon contents 0.50% (0.5 %C - 0.2 %Si - till 0.6 %Mn - till 0.25 %Cu - till 0.08 %As - till 0.25 %Ni - till 0.040 %S - till 0.035 %P - till 0.25 %Cr - in wt.%) and 0.70% (Fe-0.75 %C-0.2 %Si-0.6 %Mn-till 0.25 % Ni-till 0.035 %S-till 0.0035 %P-till 0.25 %Cr-till 0.2 %Cu in wt.%) and with initial diameter of 3 mm have been processed by continuous method of combined deformational processing by drawing with bending and torsion. Results concern mechanical properties, microstructure, and thermogravimetric analysis. These results are presented in this chapter. In the last section an application of theory of technological inheritance is introduced.

Table 4.1 shows different regimes for experimental activity. In particular, regime 1 is

referred to carbon steel wires in the initial state that have not been processed with the continuous method of combined deformational processing.

Table 4.1. *Different regimes during experimental investigation of carbon steel wires*

№ regime	Drawing	Bending	Torsion
	Drawing route	Diameter of rolls, mm	RPM
1	----	-----	------
2	3,00 → 2,75 → 2,64	------	------
3		90	50
4			100
5			150
6			200

4.1 Mechanical properties after combined deformational processing

4.1.1 Tensile test: description

The most common method used for the determination of mechanical properties is tensile test. Preparation of the wire test specimen is the first step for this purpose. Assuming l_0 the initial length of a wire and A_0 its cross-sectional area, during tensile test a wire specimen (Figure 4.1) is progressively subjected to a constant rate of elongation. The length l_0 (called gage length) in Figure 4.1 is contained in the reduced section of the specimen. Specimen is pulled by a force P, and l is the elongation in a specific step of the test. Values of F and $(l - l_0)$ are stored during test. During tensile test, one end of the sample is fixed, the other is gripped by a moving, screw-driven crosshead. A load cell monitors the pulling force, while an extensometer is applied to the gage length to measure extension and rate of extension.
Wire specimen are usually too thin for the application of the extensometer [10].

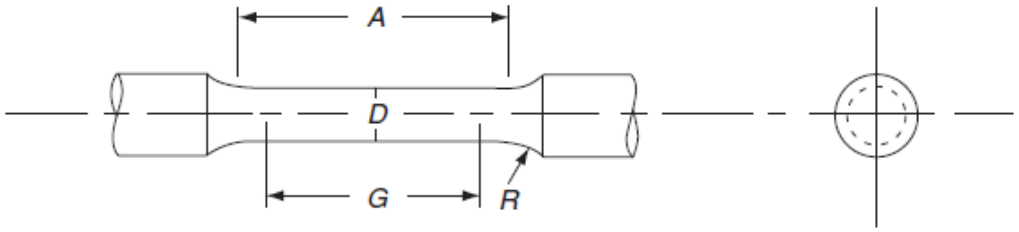

Figure 4.1. *Scheme of tensile test design ASTM Standard E8/E8M-08, specific for wire tensile testing*

Figure 4.2 shows a generic stress-strain readout [2]. The use of engineering stress and strain instead of force and elongation is for generalize the behaviour, becoming independent to the size of the specimen. Considering A_0 the initial cross-sectional area of the gage section, the engineering stress, in tension test, is defined by the following equation:

$$\sigma = \frac{P}{A_0} \tag{4.1}$$

On the other hand, engineering strain is defined in the following way:

$$\epsilon = \frac{l - l_0}{l_0} \tag{4.2}$$

and l is the instantaneous length of the specimen.

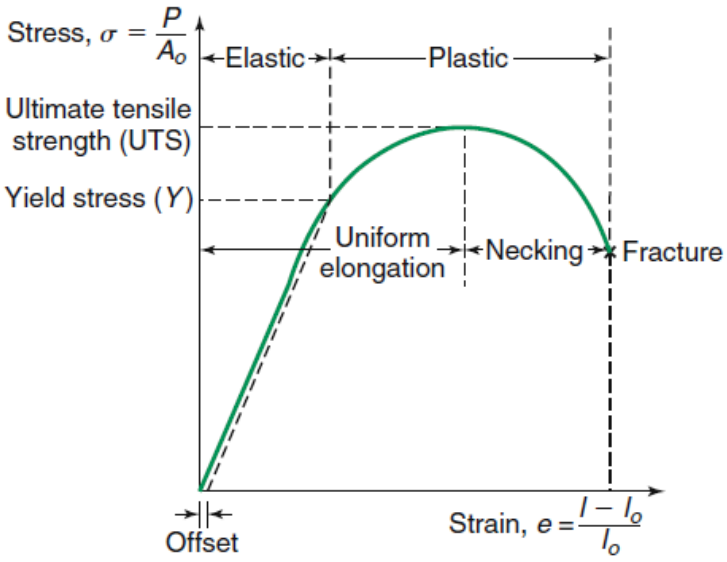

Figure 4.2. *General engineering stress-strain curve obtained after tensile test*

Specimens are generally extended until they break. During the first part of the test, force is nearly proportional to the elongation (Hooke's law). If the test is stopped in this region, the specimen will "spring back" to its original dimensions. This first region, where elongation is proportional to force, is called linear elastic region, and the ratio between stress and strain is the Young's modulus:

$$E = \frac{\sigma}{\epsilon} \tag{4.3}$$

In the second part specimen begins to be subjected to permanent elongation. If test is stopped here, a certain part of the elongation is recovered, with the specimen unloading along a line parallel to the slope of the line of uniform elongation. The recovered elongation is, again, elastic deformation. The permanent (or non-recoverable elongation) is described as plastic deformation. This deformation occurs after the point of yield stress. Sometimes it is not easy to determine the exact position, on the stress-strain curve, of the yield point because the slope of the curve begins to decrease slowly above the proportional limit. Therefore, yield stress is usually defined by drawing a line with the same slope as the linear elastic curve, but that is offset by a strain of 0.002, or 0.2% elongation. The yield stress is then defined as the stress where this offset line intersects the stressâstrain curve. Increasing load after yield point, cross-sectional area decreases uniformly and permanently along the gage length, and a maximum in the engineering stress-strain curve is reached. The level of stress that corresponds to this point of maximum is the tensile strength, or UTS of the material under exam. Increasing load after this point, specimen begins to neck and its cross-sectional area doesn't decrease uniformly anymore. Elongation after UTS concentrates in the neck, until fracture, and engineering stress at this point is called breaking or fracture stress.

4.1.2 Results and discussion

In Figure 4.3 it is shown the relationship between ultimate tensile strength and torsion rate during carbon steel wire processing (medium-carbon steel wire with 0.50% carbon content and high-carbon steel wire with 0.70% carbon content). Results presented in this section concern UTS, yield strength, elongation and ratio between yield

strength - UTS.

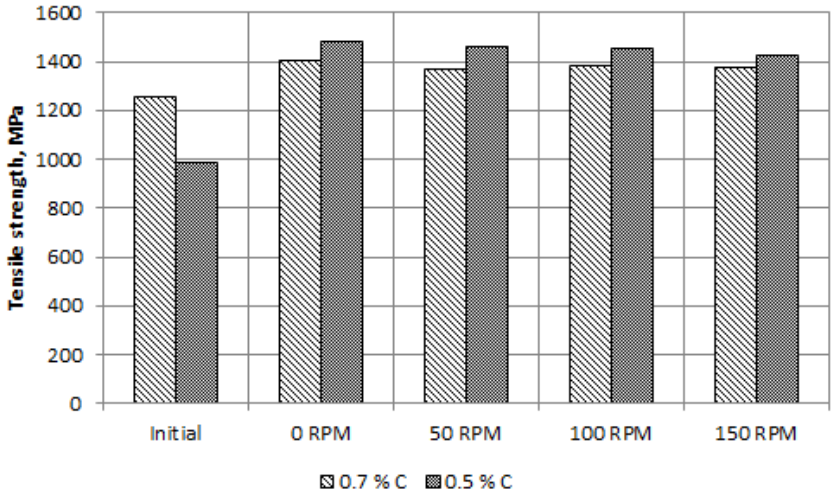

Figure 4.3. *Relationship between UTS of high-carbon wire (0.70 %C) and medium-carbon wire (0.50 %C) and rotation velocity of the four-rolls system*

Initial state of the wires is referred to a diameter of 3 mm, and not processed with continuous method of combined deformational processing by drawing with bending and torsion.

Considering high-carbon wire, in the initial state tensile strength was 1255 MPa, after the continuous method of combined deformational processing by drawing with bending, the strength reached the highest value, almost 1400 MPa. In the cases of torsional deformation application, UTS is lower. It is interesting to note another peak for the value of UTS with a torsion rate of 100 RPM.

As concerns medium-carbon wire, in the initial state UTS is lower than high-carbon wire in the same conditions. But after the combined deformational processing the UTS is greatly improved, with the highest value in the process condition without torsion rate (1483 MPa).

For both cases, a general decrease for UTS increasing torsion rate can be noticed. Application of theory of technological inheritance for product quality prediction using tensile strength results is presented at the end of this chapter.

As concerns yield strength, another behaviour was found, especially for high-carbon wire (Figure 4.4):

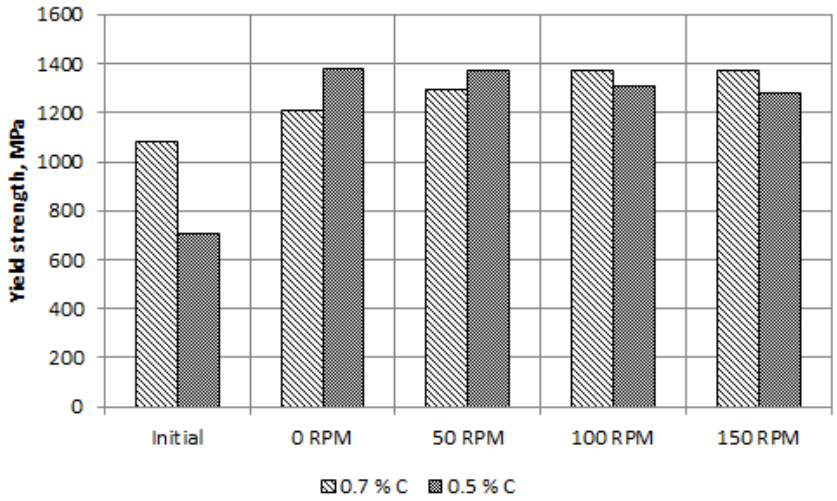

Figure 4.4. *Relationship between yield strength of high-carbon wire (0.70 %C) and medium-carbon wire (0.50 %C) and rotation velocity of the four-rolls system*

As regards high-carbon wire, the value of conventional yield strength for the case under study is dependent on the rotation of the roller system, and varies from a minimum of 1210 MPa to a maximum value (relatively to the torsion rate of 150 RPM) of 1373 MPa. The trend of yield strength is different from UTS, because increasing torsion rate this quantity increases. On the other hand, for medium-carbon wire the maximum value of yield strength is 1378 MPa and it decreases, increasing torsion rate. Results about elongation at break of the different specimen, in relation to the torsion rate and for high-carbon wire are reported in Figure 4.5.

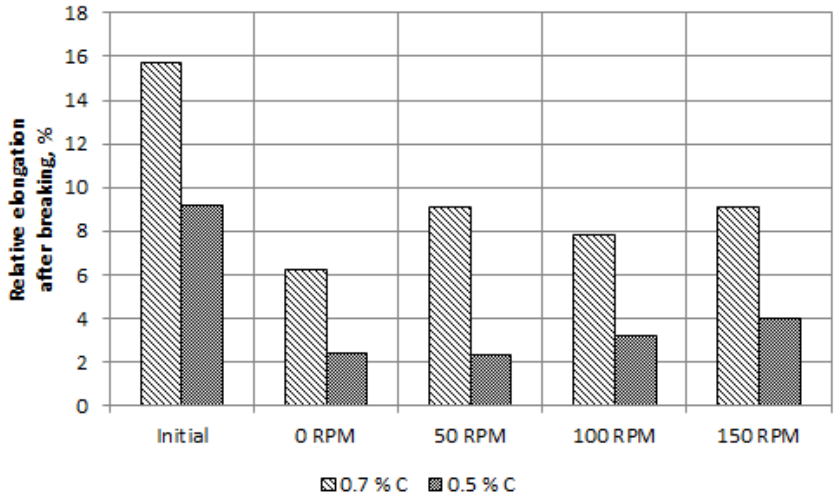

Figure 4.5. *Relationship between elongation of high-carbon wire (0.70 %C) and medium-carbon wire (0.50 %C) and rotation velocity of the four-rolls system*

For both carbon steel wires, it can be noted that a relevant increase of this quantity occurs when torsion is applied to the process.
Another parameter that has been calculated is the ratio between yield strength and UTS, the so called Y/T ratio (Figure 4.6).

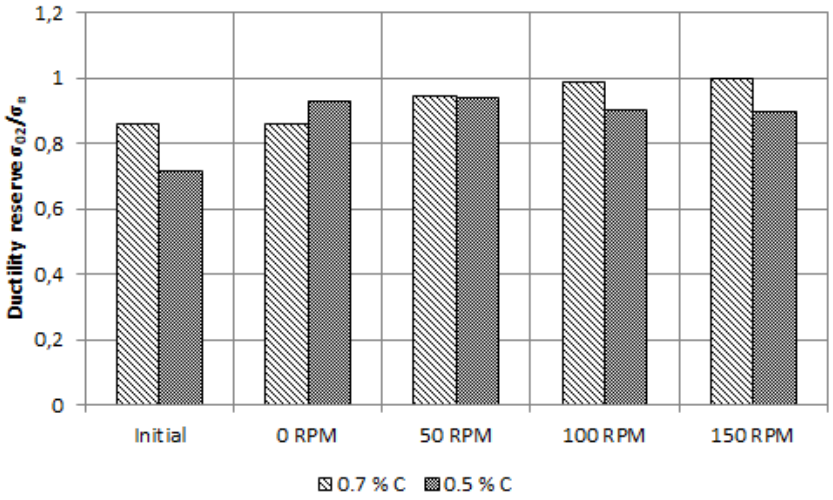

Figure 4.6. *Relationship ratio yield strength-UTS of high-carbon wire (0.70 %C) and medium-carbon wire (0.50 %C) and rotation velocity of the four-rolls system*

This parameter is an indication of the level of stress the steel will sustain beyond its yield point to reach UTS. A low Y/T ratio has been considered as providing a high capacity for plastic deformation and a safe margin against fracture. Results for medium-carbon wire relatively to this parameter show that it decreases, increasing torsion rate. For high-carbon wire the behaviour is the opposite.

4.2 Microstructure after combined deformational processing

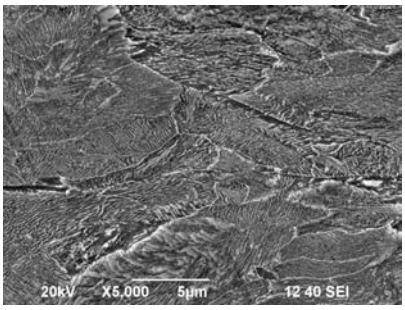

(a)

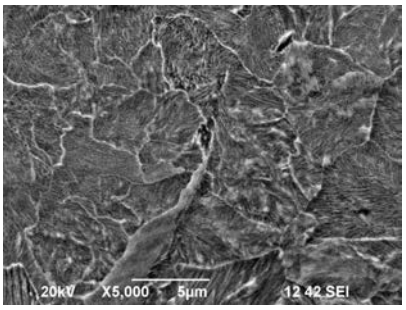

(b)

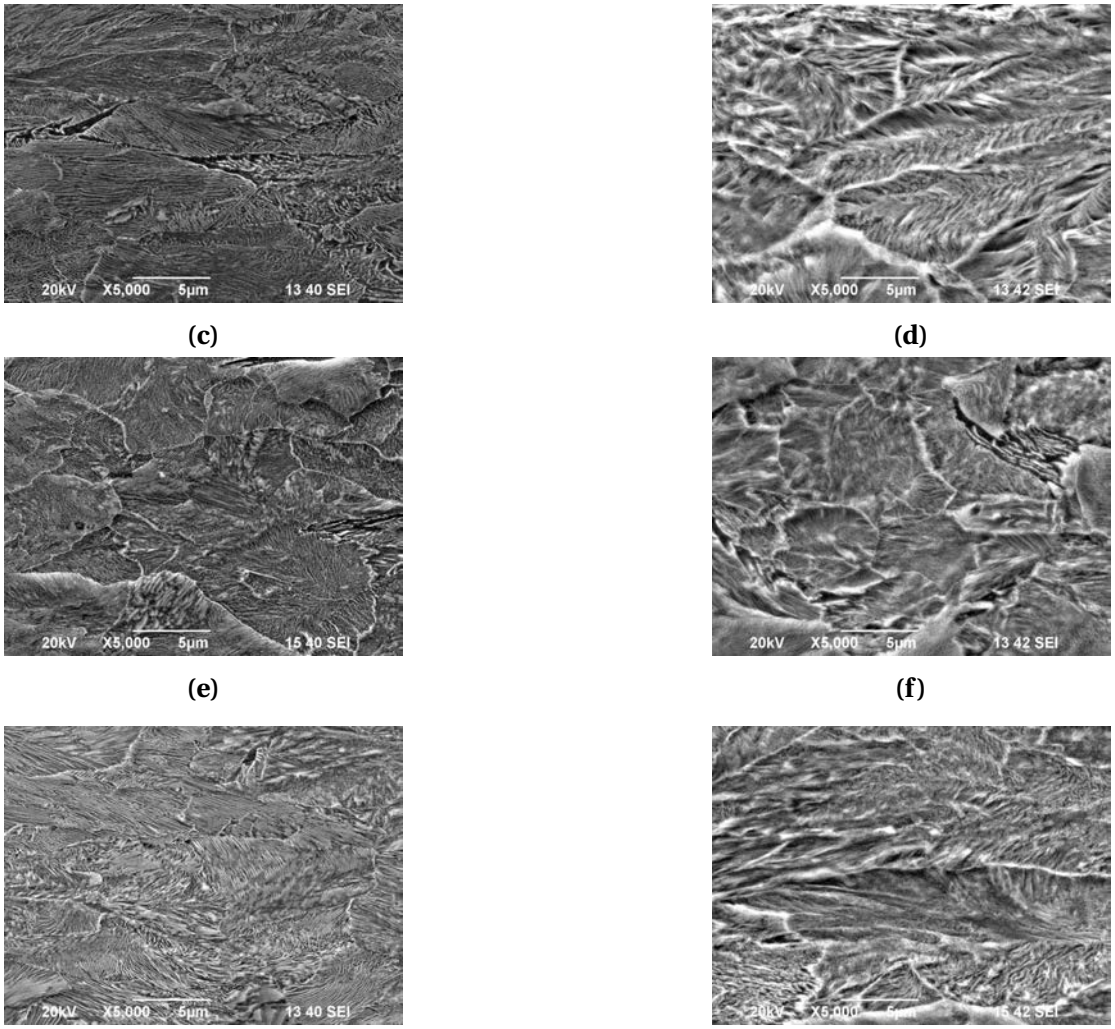

Figure 4.7. *Medium (a,c,e,g) and high (b,d,f,h) carbon steel wire, with carbon content respectively of 0.50 %C wt. and 0.70 %C wt. after different types of deformation processing: as received state (a,b), after drawing with bending (c,d), after drawing with bending and torsion with torsion rate of 50 RPM (e,f) and after drawing with bending and torsion with torsion rate of 150 RPM (g,h)*

Scanning electron-microscope analysis of the wire was done on the electron microscope JEOL JSM-6490 LV in conditions of Nano Steel Research Studies Institute of Nosov Magnitogorsk State Technical University. Samples for metallographic examination were prepared from the deformed wire by polishing and etching.
Microstructure of medium carbon steel wire with 0.50 %C in as received state consists of ferrite-carbide mixture and low quantity of structural free ferrite which locates along the grain boundaries. Microstructure of high carbon steel wire with 0.70 %C is fully pearlitic with low amount of ferrite which is observed as small separate areas

around the boundaries of pearlite colonies.

In carbon steel wire from both steels the texture formation is observed after drawing which is typical to this kind of deformational processing. Grains elongate along the main line of tensile deformation at drawing. In that pearlite colonies where cementite plates orientation coinsides with deformation axis the decrease of interlamelar space is observed due to the ferrite plates thinning. Evidently it can be explained that at chosen deformation degree at drawing density of dislocations in the ferrite interspaces is not so high and plastic flow is in progress there. In that colonies where cementite plates are oriented perpendicular to the deformation axis the clearing bands are observed. These are spaces where plastic deformation locates. Besides processes of plates crashing start.

When combined deformational processing on carbon steel wire is applied one can observe the same character of microstructure evolution for both grades of steel. After combined deformation by drawing with alternative bending the pearlite colonies elongate to more extent and rotate along the deformation axis. In pearlite colonies which are oriented along the drawing axis lamellar structure of pearlite continues to exist. Inside the pearlite colony parallel structure is observed and carbide phase has plate form. The length of the majority of carbide plates can be compared with the dimension of the whole pearlite colony. In that colonies which orientation does not coinside with the deformation axis the interlamelar distance is slightly larger as compared with the same distance in the colonies oriented parallel to the deformation axis. During combined deformation there is an incentive to reorientation under outer loading in these areas wherein carbide phase morphology changes, cementite plates start to bend and crash. Plate form of the carbide phase step by step changes into the curvative one.

After imposing on the carbon steel wire torsion deformation 150 RPM as the result one can achieve the combined deformational processing by drawing with alternate bending and torsion the same tendency in microstructure changing can be denoted as at drawing with bending. But elongation and rotation of the pearlite colonies along the deformation axis is more effective. Proportion of the areas with highly curvative and crashed cementite plates drastically increases. After combined deformational processing with drawing with alternative bending and torsion the plate structure of

pearlite is broken. The substructure with mixed dislocation-carbide boundaries and some increase in dislocation density which is observed in the crashed form of the pearlite structure after steel cold deformation leads to the resistance of dislocation movement and hence to the increase in strength properties of the processed carbon steel wire.

4.3 TGA after combined deformational processing

In the majority of investigations devoted to the metals deformation mechanisms the dislocation-disclination mechanism is considered to be the main one. Dislocations are the most studied kinds of microstructure defects. Dislocations while moving inside the crystallite lattice meet with other dislocations.
Stationary areas form at their interaction and in order to remove them it is necessary to apply more amount of energy. Besides, on their route other kinds of obstacles can appear such as submicroscopic particles on the sliding plains, different phase inclusions, alloying additions, etc. Both grains and connections of intergrain matter are destroyed at plastic deformation and formed fragments complicate plastic deformation and block dislocation movement. As a result of all these processes metal strengthens at plastic deformation.
Relatively not so much time ago investigations about studies of the role of point defects in metals and alloys structure formation processes during plastic deformation appeared. It is the high concentration of point defects which makes contribution to expedite fragmentation when microstructure with low-angle boundaries is formed with its further transformation to grain structure with high-angle boundaries. During plastic deformation defects of structure interact with each other which results in their displacement, annihilation, and appearing of new defects. Part of the energy spent to plastic deformation is stored by structure defects and can be evolved in the form of heat while their movement to draughts or their annihilation at annealing of the deformed samples. For measurement of this energy differential scanning methods of high accuracy are used. Preliminary history of deformation as well as initial grain size have great effect on the amount of the stored energy.

4.3.1 Materials and methods

Table 4.1 shows different regimes at which carbon steel wires were subjected during continuous method of deformational processing by drawing with bending and torsion. A method showing good results is a thermal gravimetric analysis (TG), applied together with differential thermal analysis (DTA) and differential scanning calorimetry (DSC), and particularly recommended as reflecting to the fullest extent all the processes occurred during specimen heating and cooling, and ensuring good comparability of results. The laboratory study was performed using the STA Jupiter 449 F3 simultaneous thermal analyzer. It ensures both a differential scanning calorimetric and a thermal gravimetric analysis of a specimen at the same measurement, providing a possibility to compare results of TG and DSC directly and eliminate effects of material non-uniformity, specimen preparation and measuring conditions. DSC has been used to fix a temperature difference, which is in proportion to a difference in a heat flow between a reference (an empty crucible for STA) and a sample in another crucible from the same material. TG has been used to measure changes in the specimen weight, depending on temperature at specific controlled conditions. To carry out experiments, we have cut disc specimens, 2.64 mm in diameter and 1 mm high, ground the surface with an abrasive paper SiC 1200 grit, and degreased with acetone. Weight of the specimens amounted to 130-150 mg. Measurements were performed in corundum crucibles. Before analyzing, the device was calibrated with reference to melting temperatures of pure metals. A temperature measurement error did not exceed ± 0.1°C. Thermal curves of the specimens were recorded at a speed of 20°C/min in a flow of argon (protective gas - 10 cm^3/min, working gas - 20 cm^3/min) within a temperature range of 25°C. Before measuring the specimen in an argon flow, a specimen holder of DSC together with the crucibles was pre-heated to 100°C, in an air flow - to 1200°C. When the specimen was installed and the crucible was put on the specimen holder, the furnace was tightly closed and heated as stated in the above. TG and DSC curves were automatically fixed. Data obtained were processed by Netzsch Proteus Analysis software. Peaks of heat release were registered on the calorimetric curves. Temperatures of peaks were identified by tangent method. Amount of released energy was estimated as the square under the calorimetric peak. In order

to convince that heat release was irreversible after heating the sample was cooled to ambient temperature and reheated in the same range of temperature with the same rate. After reheating no heat release peaks were not identified which prove the heat released during the first cycle is the measure of heat stored during carbon steel wire deformation processing. The error of calorimetric measurements is not higher than 2.5%.

4.3.2 Results and discussion

One wide exothermic peak in the temperature range 120°C with maximum at 148°C is observed on curves of the dependence of heat flow on temperature (DSC-curves) both for wire in as received state and after drawing (Figure 4.8 and Figure 4.9).

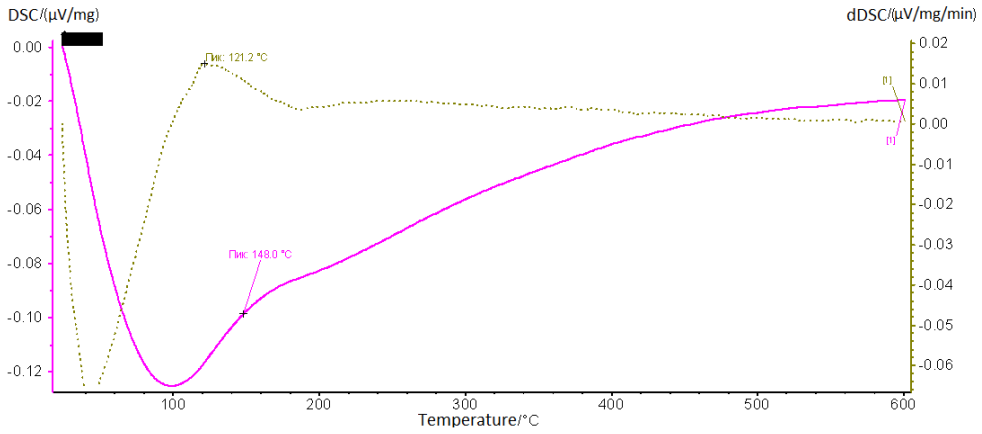

Figure 4.8. *Thermogram of carbon steel wire in as received state with 3.0 mm in diameter (regime 1)*

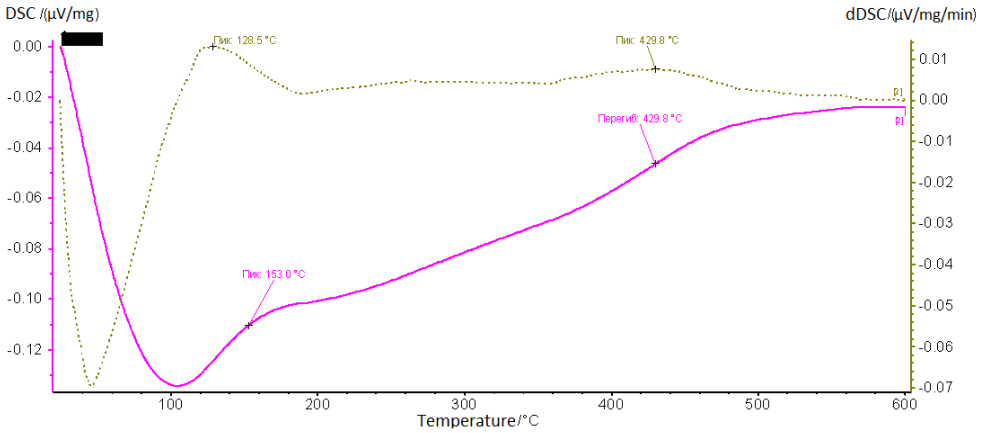

Figure 4.9. *Thermogram of carbon steel wire with 2.64 mm in diameter after drawing (regime 2)*

Discontinuity of the curve is registered at temperature 430°C only for carbon steel wire with 2.64 mm in diameter after drawing. It is confidently fixed as exothermal effect on dDSC-curve in the temperature range 350°C (Figure 4.9). Peaks which are similar to the peak of the sample after drawing are observed on calorimetric curves dDSC of the samples after combined deformational processing of carbon steel wire (Figure 4.10). It is obvious that all curves have similar view but with increasing torsion rate temperature of the peak translocates to the area of higher values from 430°C to 470°C. It makes it possible to assume that combined deformational processing by drawing with bending and torsion leads to changes in carbide phase which results in cementite (Fe_3C) crystalline lattice distortion. This conclusion matches well with results obtained by other researchers who proved that transfer of cementite phase with deformed crystalline lattice $(Fe_3C)_{def}$ to the equilibrium state (Fe_3C) occurs at temperature approximately 500°C. Absence of discontinuity on the curve for carbon steel wire in as received state also proves this fact.

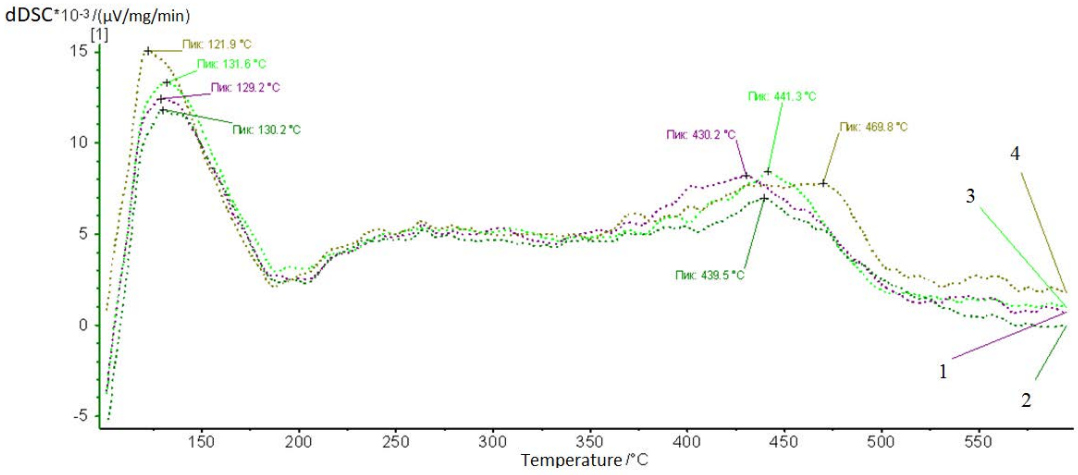

Figure 4.10. *dDSC-curves of carbon steel wire after different kinds of deformational processing: 1 - Regime n.3 ; 2 - Regime n.4 ; 3 - Regime n.5 ; 4 - Regime n.6*

Interpretation of differential calorimetric scanning data is rather complicated task especially when several thermal anomalies are observed on the curve. It is necessary to use other methods of analysis in order to get more data about steel behavior under such deformational conditions using special methods of analysis. That is why we can explain the obtained results taking into consideration the investigations of carbon steel behavior under severe plastic deformation conducted by other researchers. On

the first step of pearlite carbon steel cold plastic deformation the increase of defects density of both -Fe and cementite Fe_3C phase crystalline structure occurs. Further deformation leads to dislocations density increase in -Fe with probable transfer to nanostructured form. At the same time with defects accumulation the cementite phase Fe_3C crystalline lattice transforms from equilibrium nondeformed state to the state with distorted crystalline lattice, i.e. $(Fe_3C)_{def}$ phase. Hence, the observed peak in the temperature range 120°C is the result of rearrangement and annihilation both of linear and point defects in phase -Fe and cementite Fe_3C. Temperature of the peak practically does not change with deformation degree increase but peak square which is the measure of stored deformation energy increases from 0.11 to 0.175 J/g. It is necessary to mention that this peak was fixed on the DSC-curve of the wire sample in as received state without deformational processing (Figure 4.8). It can be explained that in as received state carbon steel wire has already got definite level of internal energy dealt with the existence defects in the structure. But in this case the level of the stored energy is very low and is equal to 0.03 J/g. Change of peak square with torsion deformation degree increase (Figure 4.11) is connected with variation of internal stresses level which raises with dislocation density increase. Evidently with higher torsion rate limits dislocation movement and enables the dislocation storage which explains the high amount of stored energy.

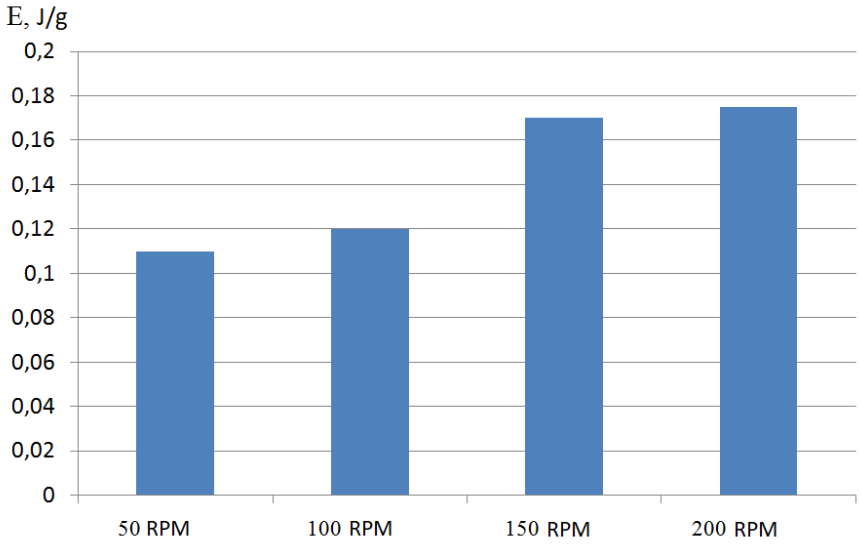

Figure 4.11. *Dependence of deformation stored energy on torsion rate*

The value of stored energy at torsion rate 200 RPM does not differ from the value

of stored energy at 150 RPM to high extent. This indicates that carbon steel wire microstructure reached its maximum concerning dislocation density in grains. That is why increasing of torsion rate over 200 RPM will not lead to further grain size reduction and microstructure changes. It matches well with previous results which showed that the most effective regime for combined deformational processing by drawing with bending and torsion is the regime with torsion rate of 75-80% RPM. At this level of torsion rate carbon steel wire mechanical properties reach their maximum values. At torsion rate more than 85% level of carbon steel wire mechanical properties decreases hence it is unreasonable to increase the value of torsion deformation degree.

4.4 Product quality prediction and application to continuous method of combined deformational processing

Processing factors affect mechanical properties and quality of metal products. Developed models and algorithms help manufacturers in the selection of the best solutions for the implementation of the manufacturing process when there are external factors, like customer demands, to guarantee high quality level of the finished metal product. One approach to predict quality of the products is technological inheritance. The main idea of technological inheritance theory is the transfer of metal products quality characteristics from the upstream processing stage to the downstream processing stages when several processing factors are involved. This idea can be used to control the product quality in metalware manufacturing.

4.4.1 Forecast of mechanical properties in manufacturing processes

The problem to forecast of the mechanical properties in manufacturing processes is of primary importance. The approach described in this section can be used to both direct and inverse problem. Direct problem is when level of mechanical properties is known and technological modes of the process are preset, and forecast of the mechanical properties after processing is investigated. On the other hand, inverse problem

consists in the investigation of the initial level of mechanical properties in order to get a specific set of these properties. Continuous method of combined deformational processing by drawing with bending and torsion, such as every manufacturing process, can be represented by the scheme in Figure 4.12 [24].

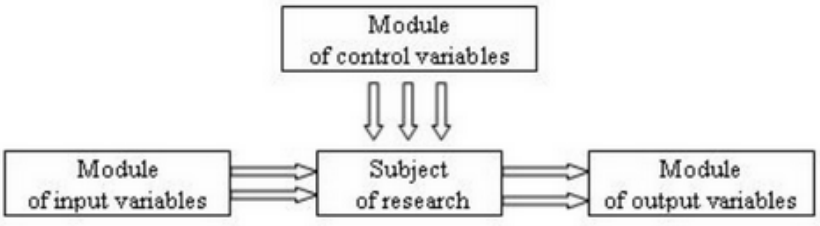

Figure 4.12. *Functional block diagram of the manufacturing process*

For example, mechanical properties are input parameters and after the influence of reduction in drawing dies and torsion rate, block of output variables is generated. Figure 4.13 shows a more developed scheme specifically for the continuous method of combined deformational processing by drawing with bending and torsion.

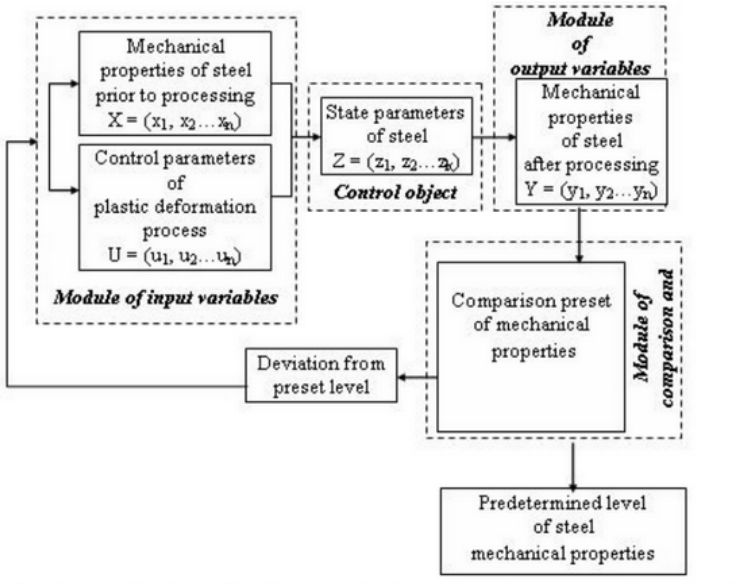

Figure 4.13. *Algorithm for the prediction of carbon steel wire microstructure and mechanical properties changing at combined deformation processing*

In particular, one block in the module of input variables contains the mechanical properties of the carbon steel wire in its received state, while the other block the control parameters like torsion rate, reductions in drawing dies, drawing speed. Control object includes state variables characterizing parameters of the microstructure of

the processed steel. Mechanical properties of the carbon steel wire after the process like UTS and yield stress are contained in the block of output variables. One module compares the mechanical properties after the process with the target properties, in order to understand these properties are the same that are required in the oprative conditions or if need further processing of the wire. Target functions are set and chosen to improve the efficiency of the process.

4.4.2 Techological inheritance to predict product quality

A sequence of microscopic and macroscopic transformations occurs in manufacturing processes of metalware products, starting from the initial structure. It is important to formalize the behaviour of mechanical properties in the manufacturing processes. Technological inheritance theory is a theoretical approach to formalize this behaviour, while inheritance factor is the mathematical operator used to quantify these changings in mechanical properties, in particular the direction of variation and the degree of transfer from one processing cycle to the next one.
Changings in rates of deformation affect strength and plastic properties of the processed carbon steel. This property of steel structure and properties forming can be expressed using the mathematical operator taking into account the transformation character of mechanical properties of steel, according to the processing cycle, by the use of the inheritance coefficient:

$$\beta_{i,j} = \frac{K_{i,j}}{K_{i,j-1}} - 1 \tag{4.4}$$

$K_{i,j}$ and $K_{i,j-1}$ are the values of the i^{th} factor of mechanical properties of the nanostructured steel after the j^{th} and $(j-1)^{th}$ processing cycle, respectively. When $\beta_{i,j} = 0$ the value of the i^{th} factor of mechanical properties after the j^{th} cycle of plastic deformation corresponds to the initial value $K_{i,j} = K_{i,(j-1)}$. It can be seen the full inheritance of the property. When $\beta_{i,j} < 0$ the trend has been to inheritance with decreasing of the numerical value of some mechanical properties $K_{i,j} < K_{i,(j-1)}$, and when $\beta_{i,j} > 0$ the trend has been to its increase $K_{i,j} > K_{i,(j-1)}$. The limit value of the inheritance coefficient is $\beta_{i,j} = -1$, when $K_{i,j}$.
In Figure 4.14 scheme with quality indices and technological operations in industry

are presented [38].

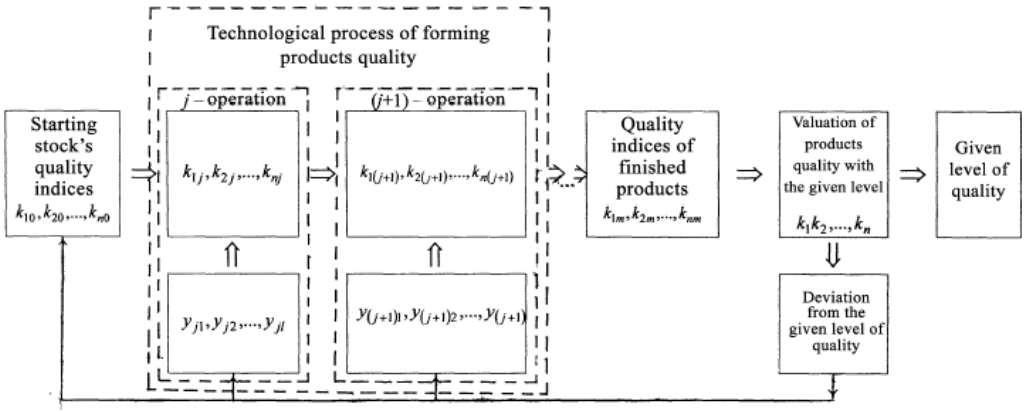

Figure 4.14. *Product quality indices in industry technology, where index "j" denote the technological operation*

Technological inheritance theory was applied to the results of the experiments presented in Chapter 4.

Figure 4.15 is a representation of the results about inheritance coefficients, calculated using Equation 4.4. Coefficient of technological inheritance is calculated for values of tensile strength [39]. Figure 4.16 gives detail of the values of the coefficient for 50, 100 and 150 RPM.

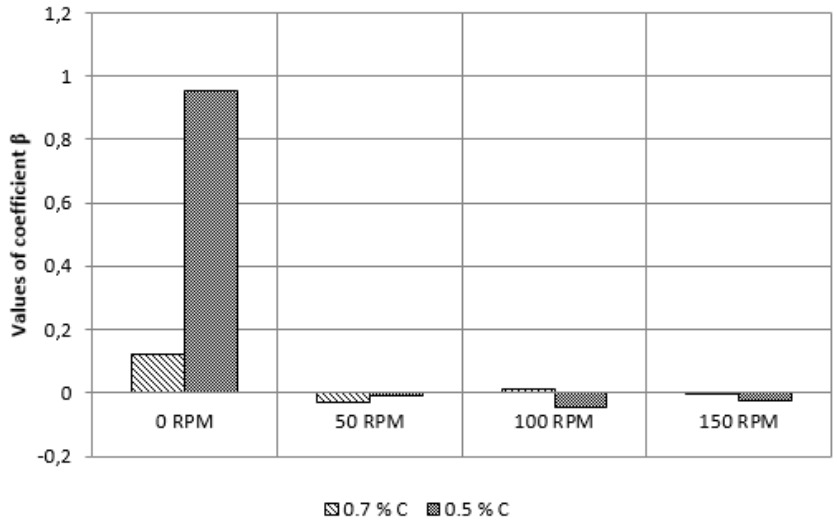

Figure 4.15. *Values of the coefficient of technological inheritance for wire mechanical properties for both carbon contents (0.50% and 0.70%) after continuous method of combined deformational processing*

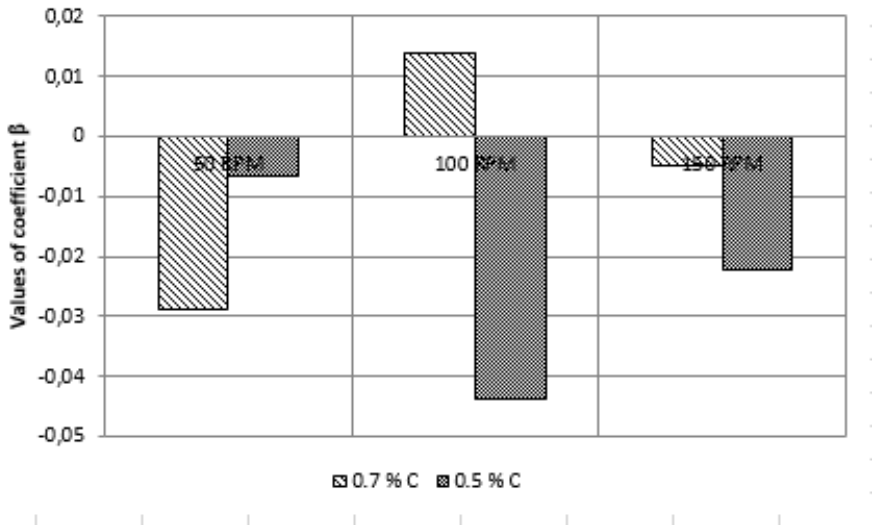

Figure 4.16. *Detail of the values of the coefficient of technological inheritance for wire mechanical properties for both carbon contents (0.50% and 0.70%) after continuous method of combined deformational processing (50, 100, 150 RPM)*

Values of coefficient of technological inheritance referred to experiments conducted with high-carbon steel wire after continuous method of combined deformational processing by drawing with bending and torsion show that for a torsion rate of 100 RPM $\beta > 0$. Under such conditions, the process is efficient in terms of improving the mechanical properties. For the other conditions, the process is inhefficient.
On the other hand, for medium-carbon wire, coefficient β after the continuous method of deformational processing is always negative, and this implies inhefficiency of the process. Values of β calculated relatively to 0 RPM are referred to the initial conditions of the carbon wire, before processing. This explains why for 0 RPM values of coeffient of technological inheritance are higher and positive.

Chapter 5

Steel in aerospace: description and applications

Materials science is one of the most important aspect in aerospace engineering, where high-performance materials are required. The impact of the chosen material for a specific component is crucial for each step, from preliminary design to manufacturing, from operative life to disposal, and this is true both for vehicles that work in the atmosphere and out of it.

5.1 Metals in aerospace: an overview

Aerospace engineers can choose among a large amount of materials, and nowadays the availabilty of materials for aircraft construction is rather wide. For the airframe and engine it is possible to choose among different kinds of metals, plastics, ceramics, composites and natural substances. New materials are in constant development.
But in the aerospace field, a specific combination of properties is required to materials, and many of them can not be considered from the engineers. The main properties are lightweight, stiffness, damage tolerance, durability. This explains why only a small percentage of materials can be considered suitable for aerospace purposes, from the components of the aircrafts to the spacecrafts. Together with the properties cited before, also the cost and manufacturing processes are key factors for aerospace materials, and the use of renewable materials and environmentally friendly processes are becoming more important nowadays and will be important in the future.

Aluminium and titanium alloys, steel and composites are the most important materials used for aerospace structures. Copper is used for electrical wiring, semiconductors are used for electronics and other materials are also used, but not in such large quantities as the previous ones, and sometimes only for specific applications.
It is important to highlight that not only one material is able to provide the needed properties, but combination of different materials, in order to achieve balance between performance, cost and other features.
The use of aluminium, titanium, steel and composites is a common feature for civil and military aircraft, and their amount is the 80%−90% of the total weight of the structural mass of the aircrafts. Figure 5.1 shows the types and amounts of structural materials in Airbus 340-330 [40].

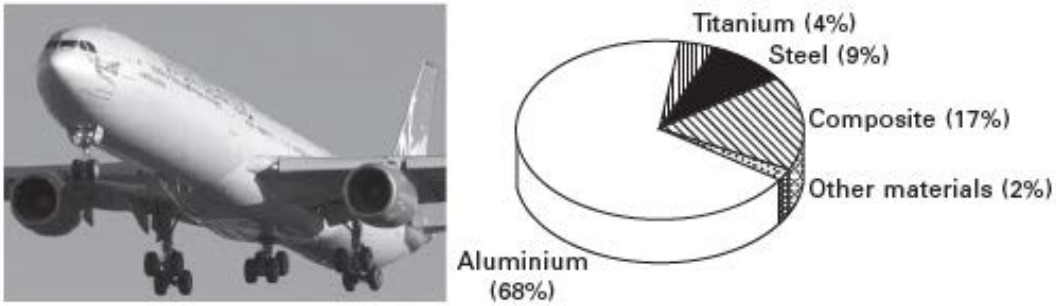

Figure 5.1. *Different structural materials used in Airbus 340-330*

For the wings, fuselage and other structures high-strength aluminium alloy is the most used material, especially before year 2000. Low cost, light weight, easy to manufacture, good strength, stiffness and fracture tougness are the main reason why aluminium was chosen.
Ti6Al4V is the titanium alloy used for aircraft structures and engines. Properties of titanium are better than aluminium, but it is more expensive. This is why it is more used for military aircraft. In the engine, titanium-based components are fan blades, low-pressure compressor parts, and plug and nozzle assemblies in the exhaust section.
Major structures of aircrafts are also made of carbon fibre composite. Properties of these materials are better than aluminium alloys because they are stronger and lighter, but are more expensive and more susceptible to impact damage.
Figure 5.2 gives an approximate grading of the common aerospace materials for several key factors and properties for airframes and engines.

Property	Aluminium	Titanium	Magnesium	High-strength steel	Nickel superalloy	Carbon fibre composite
Cost	Cheap	Expensive	Medium	Medium	Expensive	Expensive
Weight (density)	Light	Medium	Very light	Heavy	Heavy	Very light
Stiffness (elastic modulus)	Low/medium	Medium	Low	Very high	Medium	High
Strength (yield stress)	Medium	Medium/high	Low	Very high	Medium	High
Fracture toughness	Medium	High	Low/medium	Low/medium	Medium	Low
Fatigue	Low/medium	High	Low	Medium/high	Medium	High
Corrosion resistance	Medium	High	Low	Low/medium	High	Very high
High-temperature creep strength	Low	Medium	Low	High	Very high	Low
Ease of recycling	High	Medium	Medium	High	Medium	Very low

Figure 5.2. *Aerospace materials and main design key factors*

5.2 Application of steel in aerospace

As concerns structural engineering, steel is the most used metal in this application. If compared with many other materials, metals and composites, steel is cheaper and stroger. This is why such material is often chosen also for vehicular applications. But if we consider the application of steel for aircraft structures, its use is small (5/10% in weight). Usually the components in aircrafts made of steel are safety critical structural parts. This can be explained because high strength is the most important parameter for these parts. Yield strengths that can be found for steels used in aircrafts have values above 1500/2000 MPa. For comparison, yield strength of high strength aluminium is between 500 and 650 MPa. Together with high strength, mechanical properties of steel don't change significantly at high temperatures, they have high fatigue resistance and high elastic modulus. Especially for aircrafts which are heavily loaded, these properties of steel are particularly suitable. The reason why steel is not the most used material in aircrafts is weight: its density is ρ= 7.7g/cm^3, higher than titanium (1.5 times) and higher than aluminium (2.5 times). Also corrosion is an important problem when talking about steels, which can lead to surface pitting and other damages. Another kind of damage is hydrogen embrittlement, caused by hydrogen absortion. This absortion can lead to cracking even if with low concentration of hydrogen. This fracture occurs at a level of stress below yield strength.

Among components of aircrafts made of steel, the most important are the undercarriage landing gear, the wing-root attachments and the engine pylons. These parts are shown in Figure 5.3. The main advantages of using steel in landing gear is high strength and stiffness, and fatigue resistance. This last in particular is the mechanical property that ensures to withstand high impact loads in landing phase and support aircraft weight during taxiing and takeoff phases. About load-bearing section of the

landing gear and wing-root attachments, thanks to the high mechanical properties of steel, these components can be very small. This means minimum space for their storage in the aircraft. For wing root attachments, again steel is used thanks to its high strength and toughness and fatigue resistance.

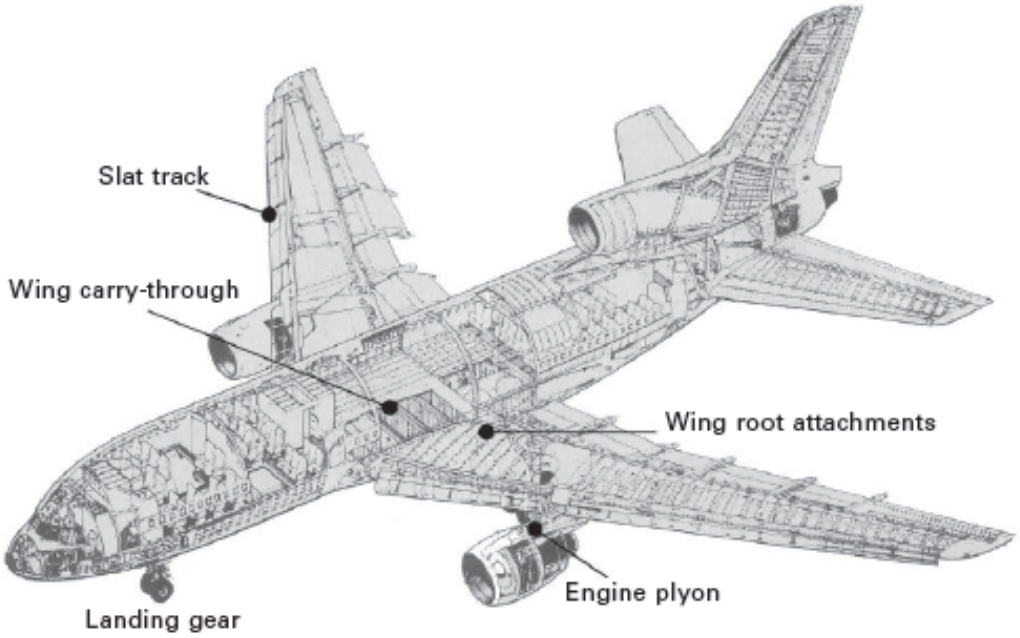

Figure 5.3. *Steel components in civilian aircrafts*

High-tensile, pearlitic high-carbon steel wires (drawn 0.8 wt.%C) were also used to tow targets behind aircrafts, in conditions of speed up to 740 km/h and altitude up to 10000 m. After several failures of this application, four kinds of failure characteristics were found. Dynamic tests were made for the investigation, subjecting wire to dynamic loading. Dynamic shock loading transimitted from the target during unsteady flight conditions was the major cause of failure. It was concluded that a suitable shock absorber was needed to be fitted at the constant-tensioning device of the winch system (Figure 5.4) [41].

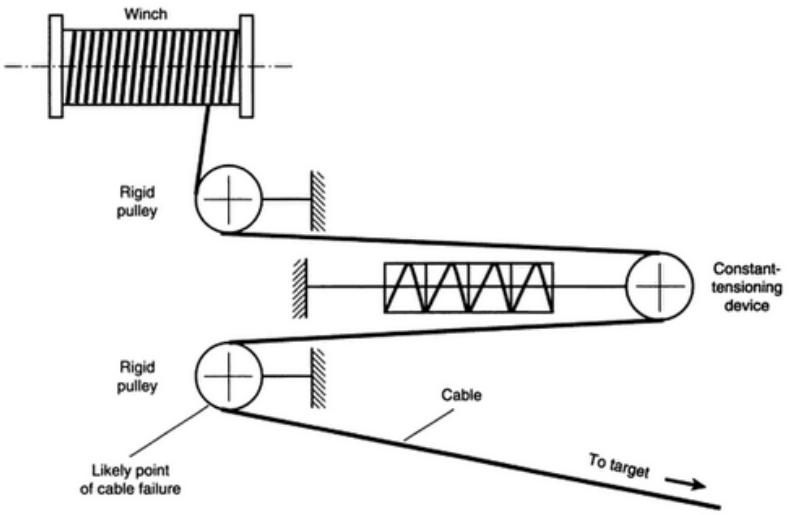

Figure 5.4. *Constant tensioning device of the winch system*

The static load absorber of the system was unsuitable for the application to the aircraft winch. Failure occured at one of the rigid pulleys of Figure 5.4.

5.3 Steel for composite materials for aerospace application

Composites materials are multiphase materials, artificially made and consist on the combination of two or more individual materials. One phase, the matrix, is continuous, the other phase is dispersed, is discontinuous and surrounded by the matrix. The main aim of these kind of materials is to obtain a more desirable combination of properties, for example low density and high strength.
Matrix can be metal, ceramic or polymer, the dispersed phase can be made of particles, fibers or other structures. Metal Matrix composites are well-known in aerospace, automotive and structural applications. Composites with metallic matrix are fabricated by reinforcing different types of metallic matrices such as aluminium, magnesium, titanium, copper and so on. Typical reinforcements for metallic matrix composites are ceramic particles or fibres, carbon fibres and metallic fibres. Different processing techniques are used for metal matrix composites such as liquid metal (electroplating and electroforming, stir casting, pressure infiltration, squeeze casting, spray deposition and reactive processing) and powder metallurgy [42]. Various features of metallic

matrix composites are:

- High transverse strength and stiffness
- High ductility and fracture toughness
- High temperature resistance
- High electrical and thermal conductivities
- Radiation protection

In fiber-reinforced composites very strong fibers in tension are used, providing significant strength improvement to the composite. The fibers used for this kind of composites are whiskers, fibers or wires. Classification of the different kinds of fibers is shown in Figure 5.5 [43].

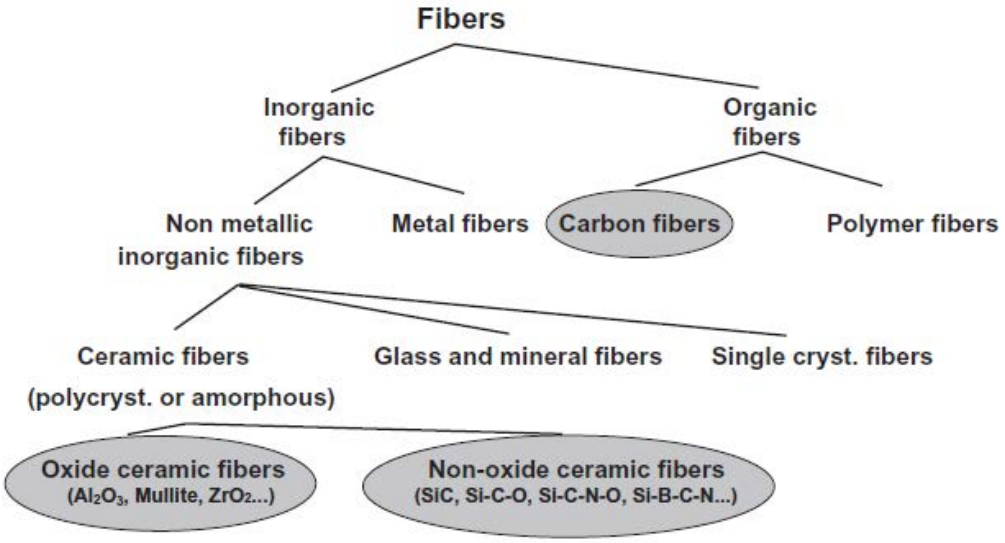

Figure 5.5. *Different kinds of fibers for composite materials*

Historically, steel-wire reinforced copper, were among the first continuous-fiber reinforced composites studied as a model system. Piehler made composites that consisted on steel fibers (0.8 %C carbon steel wires) embedded in a silver matrix. Full-length fibers, either 7 or 19 per cross section, plated with varying thicknesses of silver, were packed together in a hexagonal stacking pattern inside a silver tube and consolidated by a combined mechanical working and heat treating procedure. Cratchley embedded stainless steel fibers in an aluminum matrix by a hot pressing

process. The stainless steel contained 18 percent chromium, 9 percent nickel, and 0.6 percent titanium. Such materials could be used as engineering materials. Stainless steel reinforcement in aluminium matrix is used for automotive applications and also military airplanes. The strongest metallic fibers that has been made is a steel wire that has a strength of about 600 000 pounds per square inch (4136 MPa) [43].
Fiber Reinforced Polymeric (FRP) composites are becoming most popular materials in aerospace and other industries where high strength to weight ratio is the requirement. These structures are chiefly manufactured using the hand lay-up or carpet sweeper infusion techniques [44]. Studies were conducted on bidirectional Glass Fiber Reinforced Polymer (GFRP)/0.3mm diameter steel wire embedded laminates. Results showed increase of the energy absorption, ultimate yield strength and stiffness of the laminates.

5.4 Application of carbon steel wires to electric solar wind sail

Between the spacecrafts subsystems, the aim of propulsion subsystem is to change the motion of the spacecraft from its natural keplerian motion. Δv and payload mass fraction are important parameters in space propulsion. The payload mass fraction is the payload mass divided by the total initial mass (payload mass plus initial propulsion system mass) of the spacecraft. The Δv is the time integral, computed over the working time of the propulsion system, of the non-gravitational acceleration provided by the propulsion system. Electric and chemical propulsion are the most used. In the former, higher the Δv and lower is the payload mass fraction (with exponential decrease). For the latter limitation is on the values of Δv, normally not sufficiently high to reach targets in reasonable time. Other solutions are based on natural phenomenons that occur in space. For example the electric solar wind sail (E-sail) is an advanced concept for spacecraft propulsion [45]. It is based on momentum transfer from the solar wind plasma stream, intercepted by long and charged tethers. The electrostatic field created by the tethers deflects trajectories of solar wind protons so that their flow-aligned momentum component decreases. The flow-aligned mo-

mentum lost by the protons is transferred to the charged tether by a Coulomb force (the charged tether is pulled by the plasma charge separation electric field) and then transmitted to the spacecraft as thrust. This concept is attractive for applications because no propellant is needed for travelling over long distances. The E-sail's operating principle is different from other propellantless propulsion technologies such as the solar photon sail and the solar wind magnetic sail. The former is based on momentum transfer from sunlight (solar photons) while the latter is based on a large loop-shaped superconductive wire whose magnetic field deflects solar wind protons from their originally straight trajectories.

This new approach comprises multiple elongated electric wires that are extended in the radial direction from the airframe of the spaceship, thanks to an auxiliary jet power system: the system rotates the airframe, centrifugal force is developed extending the wires. Figure 5.6 shows the airframe with the multiple electric wires [46].

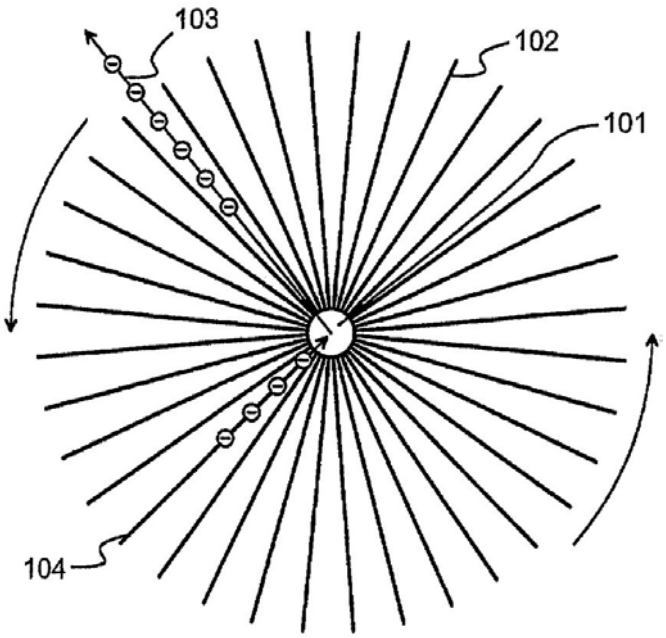

Figure 5.6. *Multiple elongated electric wires (102), spaceship airframe (101), electron flow from the airframe (103) and to the airframe (104)*

An electric potential generator is installed in the airframe. For example it is an electron gun connected to wires with controlled electric connection. Electrons flow from the wires to the airframe, and wires get positive potential relative to plasma that surrounds the spaceship. The interaction with the sun wind protons generate thrust. A navigation system device control the voltage at wires with the electric connection,

so that it is possible to control the magnitude and direction of thrust.
Deployment configuration is shown in Figure 5.7. Initially, wires are stored in reels, and reels are located near the airframe of the spacecraft. Thanks to rotation of the main body, centrifugal force makes it possible that wires unwind themselves. Small and lightweight mass are needed at the end of the wires, in order to avoid the tendency of the wires to curl up slightly when the deployment phase takes place. When the spacecraft Is set to rotation, the wires unwind themselves assisted by the centrifugal force.

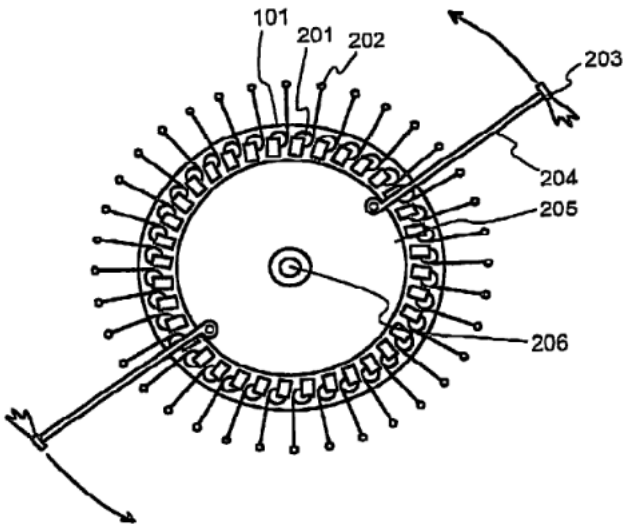

Figure 5.7. *Deployment scheme of the wires in the propulsion device: airframe (101), small mass (202)*

Single thin monofilament wire with a length of 100 meters, could survive in outer space only for some months. After this period, they will be severed by a micrometer. Wires that are part of the electric sail need have a construction that has better chances to survive, so monofilament are not a good solution. Various solutions have been suggested to overcome this problem: braids, multifilament wires, cables, ropes and tethers can be used. The operating principle as such would not exclude even rigid rod or beam-like constructions. The problem is that it would be extremely difficult to construct an ultra-light-weight deployable structure of the required dimensions from rigid pieces. The high positive potential and electric conductivity of the wire means that if and when it consists of a number of separate filaments or component strings, these are all in the same potential and repel each other. Thus the filaments or

component strings are naturally kept apart, which reduces the risk that a micrometer would cut all of them simultaneously. High tensile strength, low density and good electrical conductivity are important features for the material of the wire. For example, good material choices include steel alloys and other metals that have high tensile strength. But also the wire material can be a composite, like a carbon fiber or aramid fiber core with a surface metallization or other electrically conductive coating, or a metal core wire with fiber coating. The wire should be as thin as possible, to save mass and space in the spacecraft before electric sail deployment and to keep the gathered electron current constituted by the solar wind elections as low as possible. The electron current is approximately proportional to the outer surface area of the wires. Length of the wires depends on many factors: total number of wires, spacecraft mass, desired magnitude of propulsion, orbit radius, etc. Tensile strength of the wire material is the most important parameter to take into account, talking about the maximum length of the wire, because each piece of wire must stand the centripetal force (plus a safety marginal) that the remaining portion of wire between that segment and the distant end will cause. It is naturally possible to use wires that have non-constant cross-section, so that the tensile strength of the wire would be a decreasing function of the distance from the main body of the spacecraft towards the distant end of the wire. Carbon steel wires obtained after continuous method of combined deformational processing by drawing with bending and torsion, thanks to their mechanical and electrical properties, could be considered for this new propulsion device.

Conclusion

The main object of this work of thesis was the continuous method of combined deformational processing by drawing with bending and torsion, and drawing as the main operation. This process and its setup are defended by patents of the Russian Federation. Continuous methods for metal processing like these are promising in order to follow the main tendency in metallurgy, where the creation of new technological systems without a great amount of processes, wastes and manual management, is required. Tension, compression, bending and twisting are the main deformations during metal deformational processing in general. The effect of these deformations results in changings of mechanical properties in different ways. The process analyzed in this thesis showed that mechanical properties like UTS can vary in a very wide range, as shown in several experiments conducted at Nosov Magnitogorsk State Technical University on carbon steel wires with different carbon contents. This concepts were subject of Chapter 1. Moreover, the method is characterized by several tools and many variables are involved in the process: torsion rate of the four-rolls system, reduction in the two drawing dies, rolls diameter, carbon content of the wire. After the introductory chapter, theoretical part was developed in Chapter 2. In particular, basic principles of dimensional analysis have been applied to find some dimensionless groups that could improve the planning of experiments of the continuous method of deformational processing. Such application of dimensional analysis for planning experiments has not been used much in the past, especially in manufacturing processes. But such technique can lead to great advantages in terms of: improvement of the efficiency of the experimental activity, decrease of costs, time and waste of materials. Chapter 3 was focused on the numerical simulations of the process. Geometrical model, including the carbon steel wire, the rolls system and the drawing dies was designed using SolidWorks, while software DEFORM-3D was used for the

FEM simulations. Carbon steel wires with two different carbon contents were investigated, 0.50%C and 0.70%C, and five different torsion rates of the four-rolls system have been applied: 0 RPM, 50 RPM, 100 RPM, 150 RPM, 200 RPM. Relevant results were obtained about drawing force and damage parameter. In particular, drawing force was observed to decrease, increasing the torsion rate of the four-rolls system, such as was observed for process of drawing using rotating dies. Damage parameter analysis is necessary in order to avoid crack formation in the wire. After numerical simulations of the process, experimental investigation was needed to obtain results about mechanical properties and microstructure of the processed wires. Also TG (Thermogravimetric) and DSC (Differential Scanning Calorimeter) analyses were conducted. Theory of technological inheritance was applied to the results about mechanical properties, in particular to the results of tensile strengths. Last chapter was devoted to the application of steel in aerospace, in particular steel components in aircrafts. Carbon steel wires are used also as fibers in composite materials, using a metal matrix. At the end, one possible application of carbon steel wires on electric solar wind sail was studied, in particular to the E-Sail, a new propulsion device that consists of multiple elongated electric wires extended radially out of an airframe. In particular, this solution could be interesting from the point of view of the high mechanical properties that are possible to be obtained from the continuous method of combined deformational processing by drawing with bending and torsion and the well known good electric properties of steel wires.

Bibliography

[1] Cardarelli, F. (2000). *Materials handbook* (3rd ed.). Springer, pp.128-135.

[2] Kalpakjian, S., S.R. Schmid (2010). *Manufacturing Engineering and Technology* (6th ed.). Pearson, pp.373-375.

[3] Polyakova, M., I. Calliari, A. Gulin (2016). *Effect of Microstructure and Mechanical Properties Formation of Medium Carbon Steel Wire through Continuous Combined Deformation*. Key Engineering Materials 716:201-207.

[4] Polyakova, M., M.V. Chukin, K. Brunelli, Y.Y. Efimova, E.M. Golubchik (2018). *Study of texture and microstructure formation in medium carbon steel wire submitted to combined deformation by drawing with bending and twisting*. Materials Physics and Mechanics 36(1):60-66.

[5] Cetinarslan, C.S., A. Guzey (2013). *Tensile properties of cold-drawn low-carbon steel wires under different process parameters*. Materiali in Tehnologije 47(2):245-252.

[6] Zidani, M., S. Messaoudi, T. Baudin, D. Solas, M.H. Mathon (2010). *Tensile properties of cold-drawn low-carbon steel wires under different process parameters*. International Journal of Material Forming 3(1):7-11.

[7] Zelin, M. (2002). *Microstructure evolution in pearlitic steels during wire drawing*. Acta Materialia 50(17):4431-4447.

[8] Phelippeau, A., S.N. Pommier, T.Tsakalakos, M. Clavel, C. Prioul (2006). *Cold drawn steel wires - Processing, residual stresses and ductility - Part I: Metallography and finite element analyses*. Fatigue & Fracture of Engineering Materials & Structures 29(3):201-207.

[9] Suliga, M. (2012). *The Theoretical and Experimental Analyses of the Influence of Single Draft on Properties of Rope Wires*. Archives of Metallurgy and Materials 57(4):1021-1030.

[10] Wright, R.N. (2012). *Wire Technology: Process Engineering and Metallurgy* (2nd ed.). Elsevier, pp.273-277.

[11] Guo, N., B. Luan, Q. Liu (2013). *Influence of pre-torsion deformation on microstructures and properties of cold drawing pearlitic steel wires*. Materials and Design 50:285-292.

[12] Cordier-Robert, C., B. Forfert, B. Bolle, J.J. Fundenberger, A. Tidu (2008). *Influence of torsion deformation on microstructure of cold-drawn pearlitic steel wire*. Journal of Materials Science 43(4):1241-1248.

[13] Onur, Y.A., C.I Erdem (2012). *Experimental and theoretical investigation of bending over sheave fatigue life of stranded steel wire rope*. Indian Journal of Engineering and Materials Sciences 19(3):189-195.

[14] Kruzel, R., M. Suliga (2013). *The effect of multiple bending of wire on the residual stresses of high carbon steel wires*. Metalurgija-Sisak then Zagreb-52(1):93-95.

[15] Khromov, I., R. Kawalla (2012). *Simulation of a Steel Wire Straightening Taking into Account Nonlinear Hardening of Material*. Engineering, Technology and Applied Science Research 2:320-324.

[16] Baragetti, S. (2006). *A Theoretical Study on Nonlinear Bending of Wires*. Meccanica 41(4):443-458.

[17] Gillstrom, P., M. Jarl (2006). *Mechanical descaling of wire rod using reverse bending and brushing*. Journal of Materials Processing Technology 172(3):332-340.

[18] Godfrey, H.J. (1941). *The fatigue and bending properties of cold drawn steel wire*. Trans. American Society of Metals, Vol.29, p.133.

[19] Yanagimoto, J., J. Tokutomi, K. Hanazaki, N. Tsuji (2011). *Continuous bending-drawing process to manufacture the ultrafine copper wire with excellent electrical*

and mechanical properties. CIRP Annals - Manufacturing Technology 60(1):279-282.

[20] Abdul-Latif, A., G.F. Dirras, S. Ramtani, A. Hocini (2009). *A new concept for producing ultrafine-grained metallic structures via an intermediate strain rate: Experiments and modeling*. International Journal of Mechanical Sciences 51(11-12):797-806.

[21] Muszka, K. (2013). *The effects of deformation and microstructure inhomogeneities in the Accumulative Angular Drawing (AAD)*. Materials Science and Engineering A 574:68-74.

[22] Joo, H.S., S.K. Hwang, H. M. Baek, Y.T.Im, I.H. Son, C.M. Bae (2015). *The effects of deformation and microstructure inhomogeneities in the Accumulative Angular Drawing (AAD)*. Journal of Materials Processing Technology, Volume 216, pp.348-356.

[23] Polyakova, M., A. Gulin, E. Golubchik (2017). *Effect of combined tensile, bending and torsion deformation on medium carbon steel wire*. MATEC Web of Conferences 128(912):05007.

[24] Polyakova, M., A. Gulin, E. Golubchik (2018). *Assessment of Structure Integrity and Mechanical Properties of Carbon Steel Wire in Combined Deformation Processing*. Key Engineering Materials, Volume 769, pp.277-283.

[25] Golubchik, E., M. Polyakova, A. Gulin (2014). *ADAPTIVE APPROACH TO QUALITY MANAGEMENT IN COMBINED METHODS OF MATERIALS PROCESSING*. Applied Mechanics and Materials, Volume 656, pp.497-506.

[26] Magnani, L., T. Bertolotti (2017). *Springer Handbook of Model-Based Science*. Springer, pp.406-407.

[27] Doebelin, E.O. (1995). *Engineering Experimentation: Planning, Execution, Reporting*. McGraw-Hill, pp.323-338.

[28] Gibbings, J.C. (2011). *Dimensional Analysis*. Springer.

[29] Zohuri, B. (2016). *Dimensional Analysis Beyond the Pi Theorem*. Springer.

[30] Bhatt, R., H.K. Raval (2017). *Semi empirical modeling of flow forming process*. International Journal of Modern Manufacturing Technologies, Volume IX.

[31] Phatak, D.R., H. Dhonde (2003). *Dimensional Analysis of Reinforced Concrete Beams Subjected to Pure Torsion*. Journal of Structural Engineering 129(11).

[32] Kadu, R.S., G.K. Awari, C.N. Sakhale, J.P. Modak (2014). *Formulation of Mathematical Model for the Investigation of Tool Wears in Boring Machining Operation on Cast Iron Using Carbide and CBN Tools*. Procedia Materials Science, Volume 6, pp.1710-1724.

[33] *DEFORM 3D User's Manual*.

[34] Tzou, G.Y., U.C. Chai, C.M. Hsu, H.Y. Hsu (2017). *FEM simulation analysis of wire rod drawing process using the rotating die under Coulomb friction*. MATEC Web of Conferences 123:00033.

[35] Gillemot, L. (1975). *STUDY ON INDUSTRIAL APPLICATION OF WIRE DRAWING WITH ROTATING DIE*. Periodica Polytechnica: Mechanical engineering. Mashinostroenie, Volumes 18-19.

[36] Rudskoi, A.I., V.A. Lunev, O.P. Sciaboldo. *Manual of the course, Peter the Great St.Petersburg Polytechnic University*

[37] Valberg, H.S. (2010). *Applied Metal Forming (INCLUDING FEM ANALYSIS)*. Cambridge University Press.

[38] Korchunov, A., M. Polyakova, A. Gulin, D. Konstantinov (2014). *Technological Inherited Connections in Continuous Method of Deformational Nanostructuring*. Applied Mechanics and Materials, Volume 555, pp.401-405.

[39] Gulin, A., A. Korchunov, M. Polyakova (2012). *DEVELOPMENT AND EFFICIENCY ESTIMATION OF THE METHOD OF CONTINUOUS DEFORMATION NANOSTRUCTURING OF HIGH-CARBON STEEL WIRE*. Conference Paper: Nanocon 2012, Brno, Czech Republic.

[40] Mouritz, A.P. (2012). *Introduction to aerospace materials*. Woodhead Publishing.

[41] Esaklul, K.A. (1994). *Handbook of Case Histories in Failure Analysis*. ASM International, Volume 2.

[42] Rana, S., R. Fangueiro (2016). *Advanced Composite Materials for Aerospace Engineering: Processing, Properties and Applications*. Woodhead Publishing, pp.8-9.

[43] Weeton, J.W., R.A. Signorelli (1965). *Fiber-Metal Composite Materials*. Twelfth Sagamore Army Materials Research Conference, U.S. Army Materials Research Agency, Roquette Lake, New York.

[44] Periyardhasan, R., A. Devaraju (1994). *Mechanical Characterization of Steel Wire Embeded GFRP Composites*. materialstoday: PROCEEDINGS, Volume 5, Issue 6, Part 2, pp.14339-14344.

[45] Janhunen, P., P. Toivanen, J. Envall, S. Merikallio, G. Montesanti, J.G. del Amo, U. Kvell, M. Noorma, S. Latt (2014). *Electric solar wind sail applications overview*. arXiv:1404.5815

[46] Janhunen, P., inventor. *ELECTRIC SAIL FOR PRODUCING SPACECRAFT PROPULSION*. US 7,641,151 B2, Jan. 5, 2011.